



National Library  
of Canada

Bibliothèque nationale  
du Canada

Canadian Theses Service

Services des thèses canadiennes

Ottawa, Canada  
K1A 0N4

## CANADIAN THESES

## THÈSES CANADIENNES

### NOTICE

The quality of this microfiche is heavily dependent upon the quality of the original thesis submitted for microfilming. Every effort has been made to ensure the highest quality of reproduction possible.

If pages are missing, contact the university which granted the degree.

Some pages may have indistinct print especially if the original pages were typed with a poor typewriter ribbon or if the university sent us an inferior photocopy.

Previously copyrighted materials (journal articles, published tests, etc.) are not filmed.

Reproduction in full or in part of this film is governed by the Canadian Copyright Act, R.S.C. 1970, c. C-30.

THIS DISSERTATION  
HAS BEEN MICROFILMED  
EXACTLY AS RECEIVED

### AVIS

La qualité de cette microfiche dépend grandement de la qualité de la thèse soumise au microfilmage. Nous avons tout fait pour assurer une qualité supérieure de reproduction.

S'il manque des pages, veuillez communiquer avec l'université qui a conféré le grade.

La qualité d'impression de certaines pages peut laisser à désirer, surtout si les pages originales ont été dactylographiées à l'aide d'un ruban usé ou si l'université nous a fait parvenir une photocopie de qualité inférieure.

Les documents qui font déjà l'objet d'un droit d'auteur (articles de revue, examens publiés, etc.) ne sont pas microfilmés.

La reproduction, même partielle, de ce microfilm est soumise à la Loi canadienne sur le droit d'auteur, SRC 1970, c. C-30.

LA THÈSE A ÉTÉ  
MICROFILMÉE TELLE QUE  
NOUS L'AVONS REÇUE

Canada

THE UNIVERSITY OF ALBERTA

EMBRYO SAC DEVELOPMENT IN SOYBEAN: MEGASPOROGENESIS THROUGH  
EARLY EMBRYOGENESIS AND THE FUNCTIONAL ANATOMY OF NUTRITION.

by



MICHAEL WARREN FOLSOM

A THESIS

SUBMITTED TO THE FACULTY OF GRADUATE STUDIES AND RESEARCH  
IN PARTIAL FULFILMENT OF THE REQUIREMENTS FOR THE DEGREE  
OF DOCTOR OF PHILOSOPHY

IN

STRUCTURAL BOTANY

DEPARTMENT OF BOTANY

EDMONTON, ALBERTA

Fall 1986

Permission has been granted to the National Library of Canada to microfilm this thesis and to lend or sell copies of the film.

The author (copyright owner) has reserved other publication rights, and neither the thesis nor extensive extracts from it may be printed or otherwise reproduced without his/her written permission.

L'autorisation a été accordée à la Bibliothèque nationale du Canada de microfilmer cette thèse et de prêter ou de vendre des exemplaires du film.

L'auteur (titulaire du droit d'auteur) se réserve les autres droits de publication; ni la thèse ni de longs extraits de celle-ci ne doivent être imprimés ou autrement reproduits sans son autorisation écrite.

ISBN 0-315-32467-8

THE UNIVERSITY OF ALBERTA

RELEASE FORM

NAME OF AUTHOR MICHAEL WARREN FOLSOM

TITLE OF THESIS EMBRYO SAC DEVELOPMENT IN SOYBEAN:  
MEGASPOROGENESIS THROUGH EARLY EMBRYOGENESIS  
AND THE FUNCTIONAL ANATOMY OF NUTRITION.

DEGREE FOR WHICH THESIS WAS PRESENTED DOCTOR OF PHILOSOPHY

YEAR THIS DEGREE GRANTED Fall, 1986

Permission is hereby granted to THE UNIVERSITY OF ALBERTA LIBRARY  
to reproduce single copies of this thesis and to lend or sell such copies for private,  
scholarly or scientific research purposes only.

The author reserves other publication rights, and neither the thesis nor extensive  
extracts from it may be printed or otherwise reproduced without the author's written  
permission.

(SIGNED)

PERMANENT ADDRESS:

..... 417 W. Barbour St. ....  
..... Eufaula, Alabama 36027-2005 .....  
..... U. S. A. ....

DATED September 17, 1986

"Lately it occurs to me,  
what a long  
strange trip its been."

words by Robert Hunter

from *Truckin*

The Grateful Dead, 1971.

THE UNIVERSITY OF ALBERTA  
FACULTY OF GRADUATE STUDIES AND RESEARCH

The undersigned certify that they have read, and recommend to the Faculty of Graduate Studies and Research, for acceptance, a thesis entitled EMBRYO SAC DEVELOPMENT IN SOYBEAN: MEGASPOROGENESIS THROUGH EARLY EMBRYOGENESIS AND THE FUNCTIONAL ANATOMY OF NUTRITION, submitted by MICHAEL WARREN FOLSOM in partial fulfilment of the requirements for the degree of DOCTOR OF PHILOSOPHY.

*David W. Cas*

Supervisor

*Paul R. Garbom*  
*Ruth A. Stacey*  
*B. A. Hume*

*William A. Jones*

External Examiner

Date September 17, 1986

## ABSTRACT

The processes of megasporogenesis, megagametogenesis, fertilization and early embryogenesis in soybean, *Glycine max* (L.) Merr. cv. Gnome were examined using light, fluorescence and electron microscopy. The megasporocyte of soybean is large and undergoes meiosis to produce 4 linear megaspores. The chalazal megaspore undergoes 3 mitotic divisions to form an 8-nucleate, 7-celled embryo sac.

During megasporogenesis a distinct cellular region, the inner nucellus, develops around the expanded megasporocyte and persists until destruction by embryo sac expansion. The inner nucellus is composed of densely-staining thick-walled cells which enclose expanded megasporocytes, megaspores, 2- and 4-nucleate embryo sacs and the chalazal region of cellular megagametophytes. Ultrastructural observations suggest that an elevated level of ribosomes is responsible for increased inner nucellar cell density.

Prior to the third mitotic division and cellularization a rearrangement of the relative positions of the 4 nuclei occurs. After cellularization, egg and antipodal apparatus cells are enclosed in thick walls that lack distinct middle lamellae. Expansion of egg apparatus cells results in stretching, thinning and segmentation of their walls until the beaded structure of the mature wall is formed. Central cell wall ingrowths and large multigrain amyloplasts form only after cellularization has occurred. As embryo sac development proceeds the large central cell vacuole is segmented into smaller vacuoles. Ultimately the multigrain amyloplasts appear to fill the central cell. Other vacuoles develop, fuse with protein bodies and expand forming a network throughout the central cell.

Fertilization occurs by pollen tube penetration and discharge into a synergid. Course of the pollen tube indicates that it grows through the center of the common synergid wall and turns to enter one synergid chalazal to the filiform apparatus.

After nuclear fusion zygotic shrinkage occurs, resulting in a 38% decrease in cell length. This reduction in zygote size is accompanied by fragmentation of the large micropylar vacuole. The first division of the zygote results in a 2-celled embryo with the basal cell being more vacuolate. Numerous plasmodesmata occur in the wall separating the 2 cells of the

proembryo with only a few being found in the wall between the cells of the proembryo and the central cell.

Some suggestions about metabolic flow provided by the presence of transfer cells in various regions of the ovule. It is proposed that these transfer cells, along with nucellar cells, are all involved in augmenting metabolite transport and that their orderly appearance in different areas of the ovule signifies changes in the nutritional environment of the developing soybean embryo sac, embryo and endosperm. As these transfer cells are closely associated with the embryo sac wall it is proposed that the embryo sac wall is a common apoplast functioning as both a sink for metabolites from the nucellus and source for all solutes taken up by embryo sac cells.



### Acknowledgments

I wish to thank Dr. D. D. Cass for serving as my major professor and providing support and advice during the course of my research. I also wish to thank Drs. R. A. Stockey, P. R. Gorham and B. Heming for serving on my committee and providing advice during my tenure at the University of Alberta. Special thanks are expressed to Dr. W. A. Jensen for serving as my external examiner.

Thanks are expressed to B. Boogaard for help with translation of manuscripts. I wish to thank Dr. G. W. Scott, Director of the Surgical-Medical Research Institute, Mrs. E. Schwalt and Mr. G. Higgs for their help with the TEM. I also wish to gratefully acknowledge the gift of Gnome soybean seeds by Drs. R. J. Martin and R. L. Cooper both of The Ohio Agricultural Research and Development Center. Support for this research was provided by grants to D. D. Cass from NSERC (A-6103) and the University of Alberta CRF (55-48646).

## Table of Contents

Chapter	Page
I. Introduction .....	1
II. Material and methods .....	3
III. Results .....	8
Megasporogenesis through cellularization: .....	8
The development of the cells of the egg apparatus: .....	47
Developmental changes of the central cell: .....	71
The antipodals: .....	85
The embryo sac after pollen tube discharge: .....	85
Early embryogenesis: .....	93
Development of transfer cells in the ovule after fertilization: .....	100
IV. Discussion .....	108
Megasporogenesis: .....	108
Megagametogenesis: .....	111
Expansion of the egg apparatus: .....	123
Development of the central cell: .....	127
The antipodals: .....	131
The central cell and egg apparatus after pollen tube entry: .....	132
Involvement of transfer cells in embryo nutrition: .....	135
Embryo sac wall as a common apoplast in soybean: .....	138
V. Literature cited .....	140

## LIST OF FIGURES

FIGURE	PAGE
Fig. 1. Light micrograph of a young soybean ovule showing nucellus, megasporocyte and integuments. ....	10.
Fig. 2. Electron micrograph of a soybean ovule showing the nucellus, megaspore and one of the integuments. ....	10.
Fig. 3. Electron micrograph showing nucleus with diffuse chromatin. ....	10.
Fig. 4. Electron micrograph showing plasmodesmata connecting the soybean megasporocyte to surrounding nucellar cells. ....	10.
Fig. 5. Electron micrograph showing mitochondria, plastids and vacuoles in the megasporocyte. ....	12.
Fig. 6. Electron micrograph showing a soybean megasporocyte after callose deposition. ...	12.
Fig. 7. Fluorescent micrograph showing callose in the megasporocyte wall. ....	12.
Fig. 8. Fluorescent micrograph showing callose in the megasporocyte wall. ....	12.
Fig. 9. Electron micrograph of an expanded megasporocyte and inner nucellar cells. ....	14.
Fig. 10. Electron micrograph of an expanded megasporocyte showing pinocytosis. ....	14.
Fig. 11. Electron micrograph showing a collection of vacuoles in the expanded megasporocyte micropylar end. ....	14.
Fig. 12. Electron micrograph showing a collection of vacuoles in the chalazal end of the expanded megasporocyte. ....	14.
Fig. 13. Electron micrograph of inner, outer and transitional nucellar cells. ....	17.
Fig. 14. Electron micrograph of inner and outer nucellar cells. ....	17.
Fig. 15. Electron micrograph of the middle lamella between nucellar cell types. ....	17.

Fig. 16. Electron micrograph of inner, outer and transitional nucellar cells. ....	17.
Fig. 17. Fluorescent micrograph showing a callose walls separating 2 megaspores. ....	19.
Fig. 18. Fluorescent micrograph showing location of cellulose. ....	19.
Fig. 19. Light micrograph shows callosic wall along with darkly staining inner nucellar cells. ....	19.
Fig. 20. Electron micrograph of a megaspore showing micropylar callosic wall and nucleus. ....	21.
Fig. 21. Electron micrograph showing 2 vacuolate megaspores. ....	21.
Fig. 22. Electron micrograph of the chalazal, functional megaspore. ....	21.
Fig. 23. Electron micrograph of a megaspore's cytoplasm. ....	21.
Fig. 24. Electron micrograph of a callosic wall. ....	23.
Fig. 25. Light micrograph of an expanded functional megaspore and remains of degenerated megaspores. ....	23.
Fig. 26. Electron micrograph showing the osmiophilic remains of the 3 micropylar megaspores. ....	23.
Fig. 27. Fluorescent micrograph showing the callosic wall lining the micropylar extent of the megaspore. ....	23.
Fig. 28. Fluorescent micrograph showing cellulose in the micropylar wall of the functional megaspore. ....	23.
Fig. 29. Electron micrograph showing a 1-nucleate embryo sac. ....	26.
Fig. 30. Electron micrograph showing a condensed myelin-like body associated with a vacuole. ....	26.
Fig. 31. Electron micrograph showing Golgi bodies producing vesicles. ....	26.
Fig. 32. Electron micrograph showing a protein and myelin-like body fused with a	

vacuole. ....	26.
Fig. 33. Light micrograph of a metaphase plate during the first mitotic division of megagametogenesis. ....	28.
Fig. 34. Electron micrograph showing plasmodesmata in the embryo sac wall. ....	28.
Fig. 35. Electron micrograph showing polarity in the location of small vacuoles. ....	28.
Fig. 36. Electron micrograph showing pinocytosis of the embryo sac plasmalemma. ....	28.
Fig. 37. Electron micrograph of a 2-nucleate embryo sac. ....	30.
Fig. 38. Electron micrograph showing a chalazal end of a 2-nucleate embryo sac. ....	30.
Fig. 39. Electron micrograph showing the micropylar end of a 2-nucleate embryo sac. ....	30.
Fig. 40. Electron micrograph showing a protein body fusing with the major vacuole and infolding of SER to form a vacuole. ....	33.
Fig. 41. Electron micrograph showing a myelin-like body fused with the large central vacuole. ....	33.
Fig. 42. Electron micrograph showing an alternate form of a myelin-like body fused with the central vacuole. ....	33.
Fig. 43. Electron micrograph showing a Golgi body in the cytoplasm and vesicles fusing with the vacuole. ....	33.
Fig. 44. Electron micrograph showing a sagittal section of a 4-nucleate embryo sac and the extent of the inner nucellus. ....	35.
Fig. 45. Electron micrograph showing 2 chalazal nuclei in a 4-nucleate embryo sac. ....	35.
Fig. 46. Electron micrograph showing the 2 micropylar nuclei after separation and chalazal movement of 1 of the nuclei. ....	35.
Fig. 47. Electron micrograph showing the 2 chalazal nuclei after rearrangement. ....	35.
Fig. 48. Electron micrograph showing plasmodesmata in the chalazal end of the embryo	

sac wall. ....	37.
Fig. 49. Electron micrograph showing the chalazal end of embryo sac containing a myelin-like body and amyloplast. ....	37.
Fig. 50. Electron micrograph showing mitochondria and vacuoles in the embryo sac cytoplasm. ....	37.
Fig. 51. Electron micrograph showing Golgi bodies in the embryo sac cytoplasm. ....	37.
Fig. 52. Electron micrograph showing pinocytosis of the plasmalemma. ....	39.
Fig. 53. Electron micrograph showing osmiophilic and myelin-like bodies located adjacent to the central vacuole. ....	39.
Fig. 54. Electron micrograph showing a Golgi body forming vesicles and vesicles fusing with the central vacuole. ....	39.
Fig. 55. Electron micrograph showing a Golgi body producing vesicles near central vacuole. ....	39.
Fig. 56. Electron micrograph showing vesicles fused with the vacuole. ....	39.
Fig. 57. Electron micrograph showing membrane profiles of an expanded myelin-like body in the vacuole. ....	41.
Fig. 58. Electron micrograph showing membrane profiles of an expanded myelin-like body in the vacuole. ....	41.
Fig. 59. Electron micrograph showing attachment of membrane profiles to the vacuolar tonoplast. ....	41.
Fig. 60. Electron micrograph showing a myelin-like body enclosed in the vacuole. ....	41.
Fig. 61. Electron micrograph showing the youngest egg apparatus observed. ....	44.
Fig. 62. Electron micrograph of a young egg apparatus showing an egg nucleus. ....	44.
Fig. 63. Electron micrograph of a young egg apparatus showing an egg nucleus. ....	44.

Fig. 64. Electron micrograph of a young egg apparatus showing a synergid nucleus. ....	44.
Fig. 65. Electron micrograph of a young egg apparatus showing synergid nuclei. ....	44.
Fig. 66. Electron micrograph of a young egg apparatus showing synergid nuclei. ....	44.
Fig. 67. Electron micrograph of a young egg apparatus showing synergid and micropylar polar nuclei. ....	46.
Fig. 68. Electron micrograph of a young egg apparatus showing a synergid and micropylar polar nuclei. ....	46.
Fig. 69. Electron micrograph of an antipodal apparatus showing 2 cells and the chalazal polar nuclei. ....	46.
Fig. 70. Electron micrograph of the wall that separates the two most micropylar antipodal cells. ....	46.
Fig. 71. Electron micrograph of the third antipodal cell in the same embryo sac as Figs. 69 & 70. ....	46.
Fig. 72. Light micrograph of 3 egg apparatus cells at the pyramidal stage. ....	49.
Fig. 73. Fluorescent micrograph showing cellulose in egg apparatus cell walls. ....	49.
Fig. 74. Light micrograph of the same embryo sac as in Fig. 72 showing presence of small vacuoles. ....	49.
Fig. 75. Light micrograph of the same embryo sac as in Fig. 72 showing presence of small vacuoles. ....	49.
Fig. 76. Light micrograph showing egg and synergid cells. ....	51.
Fig. 77. Electron micrograph of an egg with characteristic micropylar vacuole. ....	51.
Fig. 78. Electron micrograph of egg apparatus cells with portions of 2 synergid nuclei. ....	51.
Fig. 79. Electron micrograph of a synergid with the characteristic chalazal vacuole. ....	51.
Fig. 80. Electron micrograph of the top wall of the youngest egg apparatus observed. ....	54.

Fig. 81. Electron micrograph of the egg apparatus in which the top wall shows segmentation. ....	54.
Fig. 82. Electron micrograph of a top wall of an egg apparatus that is columnar in shape. ....	54.
Fig. 83. Electron micrograph of an expanded egg cell top wall. ....	54.
Fig. 84. Electron micrograph of an expanded synergid cell top wall. ....	54.
Fig. 85. Electron micrograph of the mature egg cell top wall showing a wall packet. ....	54.
Fig. 86. Electron micrograph of an egg apparatus common wall in a young embryo sac. ...	57.
Fig. 87. Electron micrograph of a common wall in a slightly older embryo sac than in Fig. 86. ....	57.
Fig. 88. Electron micrograph showing common wall segmentation with expansion of egg apparatus. ....	57.
Fig. 89. Electron micrograph of the common wall between two synergids. ....	57.
Fig. 90. Electron micrograph of the common wall in the youngest egg apparatus observed. ....	59.
Fig. 91. Electron micrograph of the common wall in an egg apparatus slightly older than in Fig. 90. ....	59.
Fig. 92. Electron micrograph of a synergid common wall. ....	59.
Fig. 93. Electron micrograph of a synergid common wall showing swelling in the basal region near the filiform apparatus. ....	59.
Fig. 94. Electron micrograph of a young filiform apparatus in soybean. ....	61.
Fig. 95. Electron micrograph of a filiform apparatus in a mature embryo sac. ....	61.
Fig. 96. Electron micrograph showing attachment of the filiform apparatus to the synergid common wall in soybean. ....	61.
Fig. 97. Light micrograph showing that cellulose is present in the filiform apparatus and	



in egg apparatus walls. ....	61.
Fig. 98. Light micrograph of an egg apparatus showing location of the filiform apparatus in the embryo sac base. ....	63.
Fig. 99. Fluorescent micrograph showing the relationship of egg apparatus cells with the embryo sac wall. ....	63.
Fig. 100. Light micrograph of an egg apparatus showing location of the filiform apparatus in the embryo sac base. ....	63.
Fig. 101. Fluorescent micrograph showing the relationship of egg apparatus cells with the embryo sac wall. ....	63.
Fig. 102. Electron micrograph of the synergid-central cell wall after expansion. ....	65.
Fig. 103. Electron micrograph of a mature egg and synergid. ....	65.
Fig. 104. Electron micrograph of amyloplasts in the egg. ....	65.
Fig. 105. Electron micrograph of a network of RER in the synergid. ....	65.
Fig. 106. Electron micrograph showing the relationship of egg apparatus cell walls with the embryo sac wall. ....	68.
Fig. 107. Electron micrograph showing the egg attached to the embryo sac wall. ....	68.
Fig. 108. Electron micrograph showing all 3 egg apparatus cells free from the embryo sac wall. ....	68.
Fig. 109. Electron micrograph showing a profile of the egg cell. ....	68.
Fig. 110. Electron micrograph showing plasmodesmata in the wall between the egg and synergid cells. ....	70.
Fig. 111. Electron micrograph showing plasmodesmata in the walls between the egg and synergid and the synergid and central cell. ....	70.
Fig. 112. Electron micrograph showing the micropylar polar nucleus. ....	70.

Fig. 113. Electron micrograph showing an area of small wall ingrowths near the micropylar polar nucleus. ....	70.
Fig. 114. Electron micrograph showing the central cell's micropylar base. ....	73.
Fig. 115. Electron micrograph showing a plastid containing small starch grains. ....	73.
Fig. 116. Electron micrograph showing vacuoles at chalazal end of the central cell. ....	73.
Fig. 117. Electron micrograph showing central cell vacuoles with membraneous inclusions just after cellularization. ....	73.
Fig. 118. Electron micrograph showing myelin-like bodies associated with the central cell vacuole. ....	73.
Fig. 119. Electron micrograph showing a young central cell. ....	75.
Fig. 120. Electron micrograph showing the division of the central cell vacuole. ....	75.
Fig. 121. Electron micrograph showing filling in of the central cell. ....	75.
Fig. 122. Electron micrograph showing the central cell after the polar nuclei become associated. ....	75.
Fig. 123. Electron micrograph showing the polar nuclei located near the chalazal end of the egg apparatus. ....	78.
Fig. 124. Electron micrograph showing the fused membranes of the polar nuclei in Fig. 123. ....	78.
Fig. 125. Electron micrograph showing a central cell nearly filled in with cytoplasm. ....	78.
Fig. 126. Electron micrograph showing a central cell a completely filled in with cytoplasm. ....	78.
Fig. 127. Electron micrograph showing a young multigrained amyloplast with a plastid membrane. ....	80.
Fig. 128. Electron micrograph showing a section stained by the Thiéry procedure. ....	80.

Fig. 129. Light micrograph showing a PAS stained section of the central cell. ....	80.
Fig. 130. Electron micrograph showing an expanded multigrain amyloplast. ....	80.
Fig. 131. Electron micrograph showing smooth vesicular ER and dilated rough endoplasmic reticulum. ....	82.
Fig. 132. Electron micrograph showing a Golgi body in soybean central cell. ....	82.
Fig. 133. Electron micrograph showing vacuoles fused with both multigrain amyloplasts and protein bodies. ....	82.
Fig. 134. Electron micrograph showing vacuoles fused to form a network through the central cell. ....	82.
Fig. 135. Light micrograph showing Coomassie Brilliant Blue staining around multigrain amyloplasts in the central cell. ....	84.
Fig. 136. Electron micrograph showing a young antipodal apparatus. ....	84.
Fig. 137. Light micrograph showing an oblique section of an antipodal cell wall. ....	84.
Fig. 138. Fluorescent micrograph showing cellulose in an antipodal cell wall. ....	84.
Fig. 139. Electron micrograph showing an antipodal apparatus with the third cell chalazal to the other two. ....	84.
Fig. 140. Electron micrograph showing an egg at the approximate time of fertilization. ....	87.
Fig. 141. Electron micrograph showing the egg apparatus with persistent and degenerate synergids and an egg cell containing a sperm nucleus. ....	87.
Fig. 142. Electron micrograph showing scattered small vacuoles in the egg and persistent synergid cytoplasm. ....	87.
Fig. 143. Electron micrograph showing a wall separating the egg from persistent and degenerate synergids. ....	87.
Fig. 144. Electron micrograph showing the route of a pollen tube into the embryo sac. ....	89.

Fig. 145. Electron micrograph showing the terminal pore of a pollen tube. ....	89.
Fig. 146. Light micrograph of the egg and polar nucleus both containing sperm nuclei. ....	89.
Fig. 147. Electron micrograph showing the sperm nucleus in central cell cytoplasm. ....	89.
Fig. 148. Electron micrograph showing a lobe of the polar nucleus containing a small nucleolus. ....	89.
Fig. 149. Electron micrograph showing both egg and central cell plasmalemma. ....	92.
Fig. 150. Electron micrograph showing the plasmalemma of the egg and central cells separated by osmiophilic material. ....	92.
Fig. 151. Electron micrograph showing part of the wall enclosing the egg toward the persistent synergid. ....	92.
Fig. 152. Electron micrograph showing the zygote after shrinkage. ....	95.
Fig. 153. Electron micrograph showing amyloplasts in the zygote. ....	95.
Fig. 154. Light micrograph of a 2-celled proembryo showing terminal, basal and degenerate synergid cell. ....	95.
Fig. 155. Electron micrograph showing a 2-celled embryo. ....	97.
Fig. 156. Electron micrograph showing the wall separating the terminal and basal embryo cells. ....	97.
Fig. 157. Electron micrograph showing plasmodesmata in the wall between the basal and central cell near remains of the persistent synergid. ....	97.
Fig. 158. Electron micrograph showing the osmiophilic remains of the degenerate synergid in the wall between the basal and central cell. ....	97.
Fig. 159. Electron micrograph showing plasmodesmata in the wall between basal and terminal cell. ....	99.
Fig. 160. Electron micrograph showing translucent remains of the persistent synergid. ....	99.

Fig. 161. Light micrograph of the central cell after fertilization. ....	99.
Fig. 162. Electron micrograph showing the break-up of multigrain amyloplast in the central cell after fertilization. ....	99.
Fig. 163. Nomarski micrograph showing the different nucellar regions. ....	102.
Fig. 164. Electron micrograph showing wall ingrowths in cytoplasmic nucellar cells. ....	102.
Fig. 165. Electron micrograph showing cytoplasmic nucellar cells. ....	102.
Fig. 166. Light micrograph of a 2-celled proembryo after expansion of the embryo sac base. ....	102.
Fig. 167. Electron micrograph showing wall ingrowths in the embryonic basal cell. ....	105.
Fig. 168. Electron micrograph showing wall ingrowths in the embryonic basal cell. ....	105.
Fig. 169. Electron micrograph showing wall ingrowths in the chalazal end of the central cell. ....	105.
Fig. 170. Electron micrograph showing wall ingrowths scattered along the embryo sac wall in the chalazal region of the central cell. ....	105.
Fig. 171. Light micrograph of a multicellular proembryo showing suspensor, degenerate synergid and associated free nuclear endosperm. ....	107.
Fig. 172. Electron micrograph of wall ingrowths on the embryonic basal cell wall. ....	107.
Fig. 173. Electron micrograph showing wall ingrowths in the basal cell. ....	107.
Fig. 174. Electron micrograph showing wall ingrowths in the basal cell and along adjacent walls of suspensor cells. ....	107.
Fig. 175. Electron micrograph showing a wall ingrowth on a common-wall of a micropylar suspensor cell. ....	107.

## I. Introduction

Since the last century soybean has become one of the world's major food crops (Probst & Judd, 1973). Perhaps this is because soybean has a higher protein content than any other cultivated bean (Simpson & Conner-Ogorzaly, 1986). Being a member of an economically important family soybean is in a plant group which has been the subject of numerous embryological studies (see Davis, 1966; Johansen, 1945, 1950; Maheshwari, 1950; Prakash, 1979; Wardlaw, 1955). However, there remains a lack of ultrastructural information about megasporogenesis, megagametogenesis and fertilization in members of the bean family. The only ultrastructural reports to date concerning embryo sac structure in the Fabaceae include work on the mature soybean megagametophyte both before (Folsom, 1981; Folsom & Peterson, 1984; Tilton et al., 1983) and after fertilization (Dute & Peterson, 1984; Tilton et al., 1984) and on the embryology of *Phaseolus* (Clutter & Sussex, 1968; Yeung, 1980; Yeung & Clutter, 1978, 1979).

As most of the work that has been done on soybean and its taxonomic relatives used either cleared ovules or paraffin embedded tissue, an ultrastructural study of megasporogenesis, megagametogenesis, fertilization and early embryogenesis was performed to determine the fine structure of these processes. Soybean has been shown to be monosporic and undergo *Polygonum*-type embryo sac development which results in a 7-celled, 8-nucleate embryo sac (George et al., 1979; Kennell & Horner, 1985; Pamplin, 1963; Prakash & Chan, 1976). As this type of development has been referred to as "normal" and since it is found in approximately 70% of angiosperms studied (Maheshwari, 1950) a thorough understanding of embryo sac development in soybean could be important for our knowledge of megasporogenesis, megagametogenesis and fertilization in general.

Although much information has been accumulated concerning the reproductive biology of angiosperms many questions still remain. Little is known about the origin of the embryo sac's large central vacuole during megagametogenesis or how the processes of cellularization and cellular differentiation occur. Also what is the role of central cell wall ingrowths and how does timing of their development correspond to formation of the large multigrained

amyloplasts in soybean? And, finally, is fertilization in soybean similar to that observed in other plants and what are the roles of the central cell and synergids during this process?

The purpose of this research is to describe the processes of megasporogenesis, megagametogenesis, fertilization and early embryogenesis at the ultrastructural level in order to provide answers to some of these questions.

## II. Material and methods

Seeds of soybean, *Glycine max* (L.) Merr. cv. Gnome, were inoculated with *Rhizobium* and planted in a soil mix consisting of 3 pts. loam, 2 pts. sand, and 2 pts. peat. Plants were grown in the University of Alberta, Department of Botany Phytotron under a 2:3 ratio of sodium to mercury vapor high intensity lamps releasing approximately 300 - 350  $\mu\text{E}/\text{m}^2/\text{sec}$ , PAR 400 - 750 nm, at bench level and fertilized weekly with 1/2 strength modified Hoagland's solution (Hoagland & Arnon, 1950). Initially several varieties of soybean were grown in an attempt to select the one most suited for this research. This decision was based on plant vigor in the growth chamber, length of time from planting to bud formation and the number of flowers per raceme. A dwarf variety, Gnome, was finally selected. Although the number of flowers per raceme of Gnome was less than optimal, (other varieties typically had more flowers per raceme, in some cases up to 20), the plant responded well to conditions in the growth chamber and would normally produce usable material 4 - 6 wk after planting.

Flowers were dissected under a stereo microscope. During this process photographs were taken of either the flower or ovary using a Wild Photoautomat MPS 45 attached to a Wild M5 stereomicroscope. The Wild stereomicroscope was also used to measure the length of ovaries.

Because the size and shape of the tissue make orientation very difficult the ovules were left attached to carpel walls. The ovary was cut into segments each of which contained a single ovule. Sections of tissue were placed in vials containing the primary fixative and processed by a variety of methods. Many different combinations of fixatives were tried in the process of selecting the one most suited for the tissue. Procedures suggested by Hepler (1981), Park et al. (1982) and Gordon-Weeks et al. (1982) were tried but did not prove successful. All chemically fixed tissue destined for observation with the transmission electron microscope was processed by one of the following protocols:



3.25% glutaraldehyde in 0.075M sodium cacodylate, pH 7.0 overnight at room temperature in 15 psi vacuum washed 3 times in the same buffer and post-fixed with 2% OsO<sub>4</sub> in 0.05 M sodium cacodylate buffer, pH 7.0;

3% glutaraldehyde and 1% Alcian Blue 8GX in 0.05 M sodium cacodylate, pH 7.0 (Behnke & Zelander, 1970; Pettitt, 1977; Scott & Dorling, 1965) overnight at room temperature in 15 psi vacuum, washed 3 times in the same buffer and post-fixed with 2% OsO<sub>4</sub> in 0.05 M sodium cacodylate buffer, pH 7.0;

2% formaldehyde and 3% glutaraldehyde in 0.05 M phosphate buffer, pH 7.0 overnight at room temperature in 15 psi vacuum, washed 3 times in the same buffer and post-fixed with 2% OsO<sub>4</sub> in 0.05 M sodium cacodylate buffer, pH 7.0;

3.25% glutaraldehyde and 0.05% ruthenium red in 0.075M sodium cacodylate, pH 7.0 overnight at room temperature in 15 psi vacuum washed 3 times in the same buffer and then post-fixed with 2% OsO<sub>4</sub> and 0.05% ruthenium red in 0.05 M sodium cacodylate buffer, pH 7.0 (Luft, 1971).

After many different tissue runs it was found, that for general use, the combination of 3.25% glutaraldehyde and 2% OsO<sub>4</sub> gave the best results.

Tissue was taken out of osmium and washed briefly in the 0.05 M sodium cacodylate buffer, pH 7.0, then transferred to distilled water to remove unbound osmium. All material was dehydrated in either a graded alcohol or ACS spectro grade acetone series (30, 50, 60, 70, 95 and 100%). Each step lasted from 10 to 15 min and all were carried out at room temperature. Tissue embedded in Epon 812 (Mollenhauer, 1964) was dehydrated in an alcohol series and then transferred through two, 10 min, changes of propylene oxide. Material to be embedded in Spurr's resin (Spurr, 1969) was transferred directly from 100% acetone to the first step in the infiltration process. For the Spurr embedded material the process was actually a variant of one used by Carrol and Mayhew (1976). Their original technique used alcohol as

a transition solvent with the tissue under vacuum, 15 psi, during the entire infiltration process. In my protocol however acetone was ultimately substituted for alcohol because it eliminated infiltration problems. The 3 intermediate steps between acetone and 100% resin were 2:1, 1:1, and 1:2 (100% acetone : Spurr's resin) each lasting a period of 24 hr. The change in transition solvent required a modification of the Carroll and Mayhew (1976) technique. Because of the increased volatility of acetone in vacuum when compared to alcohol the number of hr that the tissue could be exposed to vacuum had to be decreased. Only in the last 2 - 3 hr of each step was the tissue treated with acetone/resin mixture exposed to 15 psi vacuum. Even though the tissue was under vacuum for a shorter period of time there still was an improvement in infiltration. Once the tissue was in 100% Spurr's it was put back into the vacuum for a further 24 hours then into fresh resin in the embedding flats before being returned to the vacuum for a further 3 - 4 hours. The plastic was cured overnight in a 70° C oven.

Blocks were sectioned using either a Reichert OM U2 or Ultracut E ultramicrotome with a diamond knife. Silver sections were collected on formvar coated copper or nickel grids. 0.25% formvar in dichloroethane (Roland, 1978). Grids were normally stained with uranyl acetate (1:1 aqueous saturated uranyl acetate to 95% ethanol) and lead citrate (Venable & Coggeshall, 1965). Grids were processed together using a Hiraoka supporting platform (Polyscience, Inc., Warrington, Pa.). Staining solutions were held in a small plastic weighing boat, capacity 7 ml, and the platform holding the grids was inverted and placed on the dish. The staining protocol was either 4 min in uranyl acetate and 3 min in lead citrate or, following the recommendations of Daddow (1983), 4 min in lead citrate, 40 min in uranyl acetate, and a further 20 min in lead citrate. After lead citrate the grids were washed in 4 separate 100 ml beakers of degassed distilled water, the first containing 0.2 ml 10 N NaOH. After the uranyl acetate treatment grids were washed in two beakers of 50% ethanol and then 4 of degassed distilled water.

At the EM level polysaccharides were detected with the periodic acid -

~~thiocarbohydrazide~~ - silver proteinate method (Thiery, 1967), using thiocarbohydrazide

treatments for 6 hr on gold formvar coated grids. Sections used for this were first treated with 3%  $H_2O_2$  (diluted from 30%  $H_2O_2$  immediately before use) and then oxidized with 1% periodic acid for 20 min. at room temperature (Bechtel & Pomeranz, 1981). Control sections were made by following the same protocol except distilled  $H_2O$  was substituted for periodic acid. After treatment with silver proteinate sections were viewed and photographed without any further grid staining.

Sections were viewed with either a Philips EM 200 or 410 transmission electron microscope. The acceleration voltage used on the EM 200 was 60 kv while on the 410 80 kv. Electron micrographs were taken with Kodak fine grain release positive film 5302 and developed for 5 min in full strength Kodak D-19.

Material for light microscopy came from that fixed and embedded for electron microscopy or was fixed in either 3.25% glutaraldehyde in 0.05 M sodium cacodylate buffer, pH 7.0, Carnoy II (Lillie & Fullmer, 1976), or Newcomer's Carnoy substitute (Newcomer, 1953) and embedded in glycol methacrylate (Cole & Sykes, 1974; O'Brien and McCully, 1981) or in LKB Histo-resin. Sections 1 to 2  $\mu m$  were cut with glass knives and fixed to either plain or coated slides (Jensen, 1962) with a conventional horplate or at 80° C using a LKB Multiplate.

Toluidine blue O (TBO) was used as a general stain for all plastic embedded sections (Yeung, 1984). Insoluble carbohydrates were localized using the periodic acid - Schiff stain (PAS) technique (Feder & O'Brien, 1968). Free aldehydes were blocked using 2,4 dinitrophenylhydrazine (DNPH) (Feder & O'Brien, 1968). Proteins were localized using 0.25% Coomassie Brilliant Blue G - 250 in 87 pts. water, 10 pts. methanol, and 3 pts. glacial acetic acid (Heslop-Harrison, 1979). Callose was localized with 0.05% water soluble aniline blue in 0.067 M, pH 8.5 potassium phosphate buffer (Smith & McCully, 1978) while cellulose was stained with 0.1% aqueous Calcoflour M2R NEW (Hughes & McCully, 1975; Wood, 1980; Yeung, 1984). In both cases it was found that the fluoresceins worked best when the plastic was removed from the sections using sodium methoxide, a solution made by saturating sodium hydroxide in absolute methanol (Sutherland & McCully, 1976). After a treatment of 1

- 2 min the sections were washed briefly with methanol and then water before staining. All bright-field, phase and Nomarski differential interference photomicrographs were taken with a Zeiss Photomicroscope I equipped with a Zeiss III RS epi-fluorescence condenser and a 50 watt light source, excitation filter BP365/11 and barrier filter LP 397, using both the internal camera system and a Zeiss MC 63 35mm camera attachment.

### III. Results

In soybean, *Glycine max* cv. Gnome, the ovary usually contains 2 or 3 ovules. During the early stages of megasporogenesis and megagametogenesis no synchrony was found in ovule development within a single ovary. Nor did individual ovules show any correlation between their relative position and developmental stage. Length of ovary was finally chosen as the main morphological reference character because it served as an indicator of mean developmental stage of ovules in the ovary.

#### Megasporogenesis through cellularization:

The developing megaspore mother cell is enclosed by several layers of nucellar cells (Figs. 1 & 2). Because of its size and prominent nucleus the megasporocyte is more conspicuous than the rest of the nucellus (Fig. 2). Its cytoplasmic density and organelle content are very similar to surrounding nucellar cells. Plasmodesmata are found in the walls of the megaspore mother cell connecting it to adjacent nucellar cells (Figs. 3 & 4). The megaspore mother cell's cytoplasm contains a number of mitochondria (Fig. 5) and vacuoles (Figs. 5 & 6). At certain developmental stages areas of the megasporocyte wall are relatively thick (Fig. 6). Staining with the fluorescein aniline blue, which is specific for callose, shows an unique fluorescence in the micropylar region of the megasporocyte wall (Figs. 7 & 8). Expansion of the megasporocyte results in a more rectangular cell (Fig. 9) which has a centrally placed nucleus, randomly distributed organelles, plasmodesmata in its walls (Fig. 10) and an elevated number of vacuoles located in both the micropylar (Fig. 11) and chalazal ends (Fig. 12). Concurrent with this the plasma membrane shows invagination of the plasma membrane (Figs. 10 & 12).

During the expansion of the megaspore mother cell changes occur in the walls and cytoplasm of adjacent nucellar cells resulting in both an increase in wall thickness and cytoplasmic density (Fig. 9). These changes differentiate the nucellar cells adjacent to the megaspore mother cell from the more peripheral nucellar cells that are characterized by

**Megasporocytes of soybean.**

**Fig. 1.** Young soybean ovule showing nucellus, megasporocyte and integuments. Toluidine blue oxide stain (TBO). L.M. x625.

**Fig. 2.** Portion of an ovule showing nucellus, megaspore and one of the two integuments. E.M. x1,360.

**Fig. 3.** Enlargement of Fig. 2 showing nucleus with diffuse chromatin. E.M. x5,200.

**Fig. 4.** Plasmodesmata connecting the megasporocyte to surrounding nucellar cells. Note plasmodesmata in the walls between nucellar cells. E.M. x6,020.

**Key to Abbreviations:** I, integuments; M, megaspore; Mb, myelin-like bodies; N, nucleus; Nu, nucellus; P, plasmodesmata.



Electron and fluorescent micrographs of soybean megasporocytes.

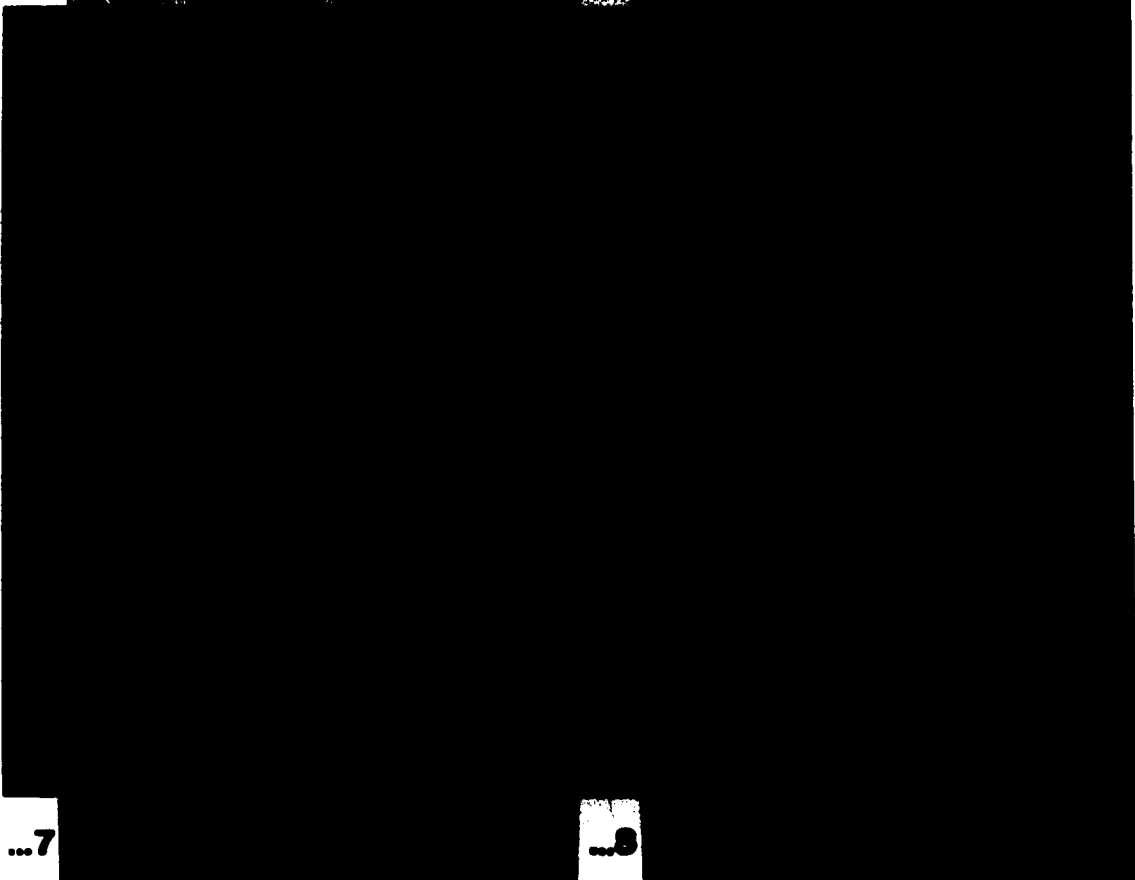
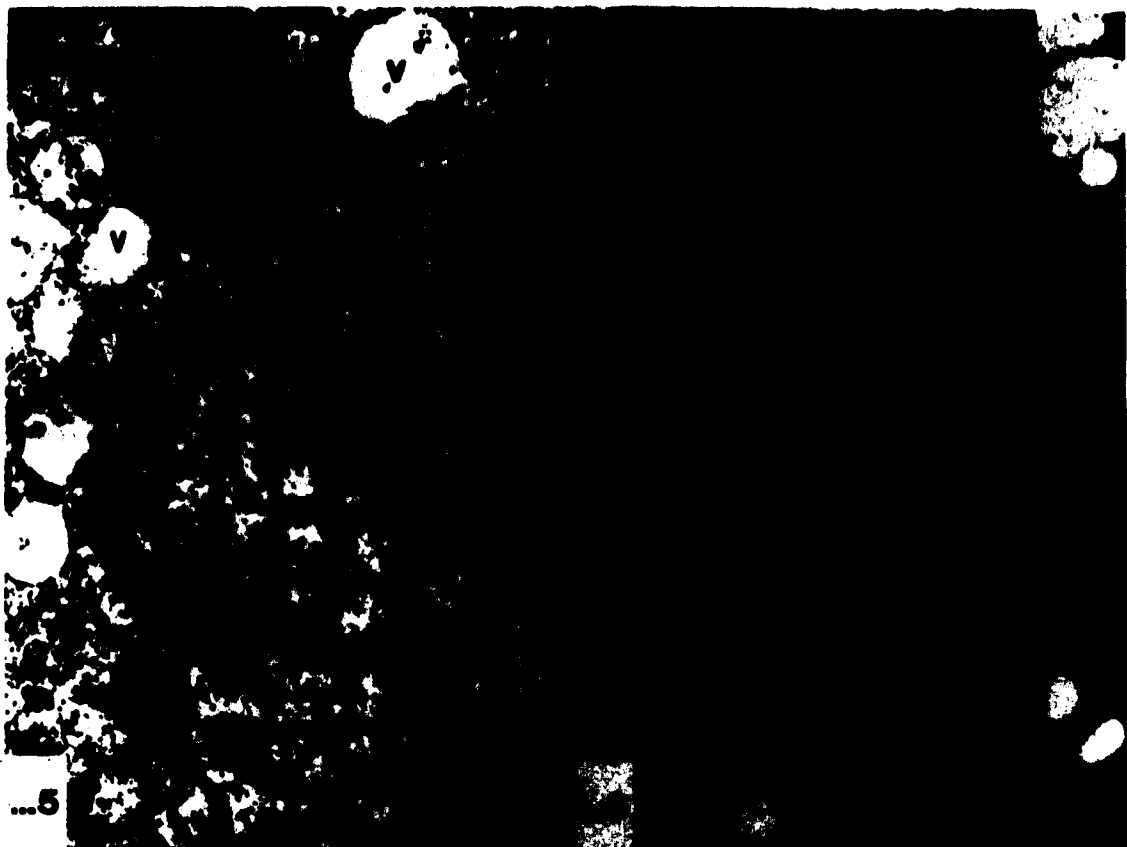
Fig. 5. Mitochondria, vacuoles and a protein body in the megasporocyte. E.M. x29,200.

Fig. 6. Megasporocyte of soybean after callose deposition. Note thickened wall (W). E.M. x15,200.

Figs. 7 & 8. Fluorescent micrographs showing callose deposition only along the micropylar walls of the megasporocyte. x980.

Key to Abbreviations: M, mitochondria; N, nucleus; Pb, protein body; V, vacuole.





**Expanded megasporocyte and inner nucellus of soybean.**

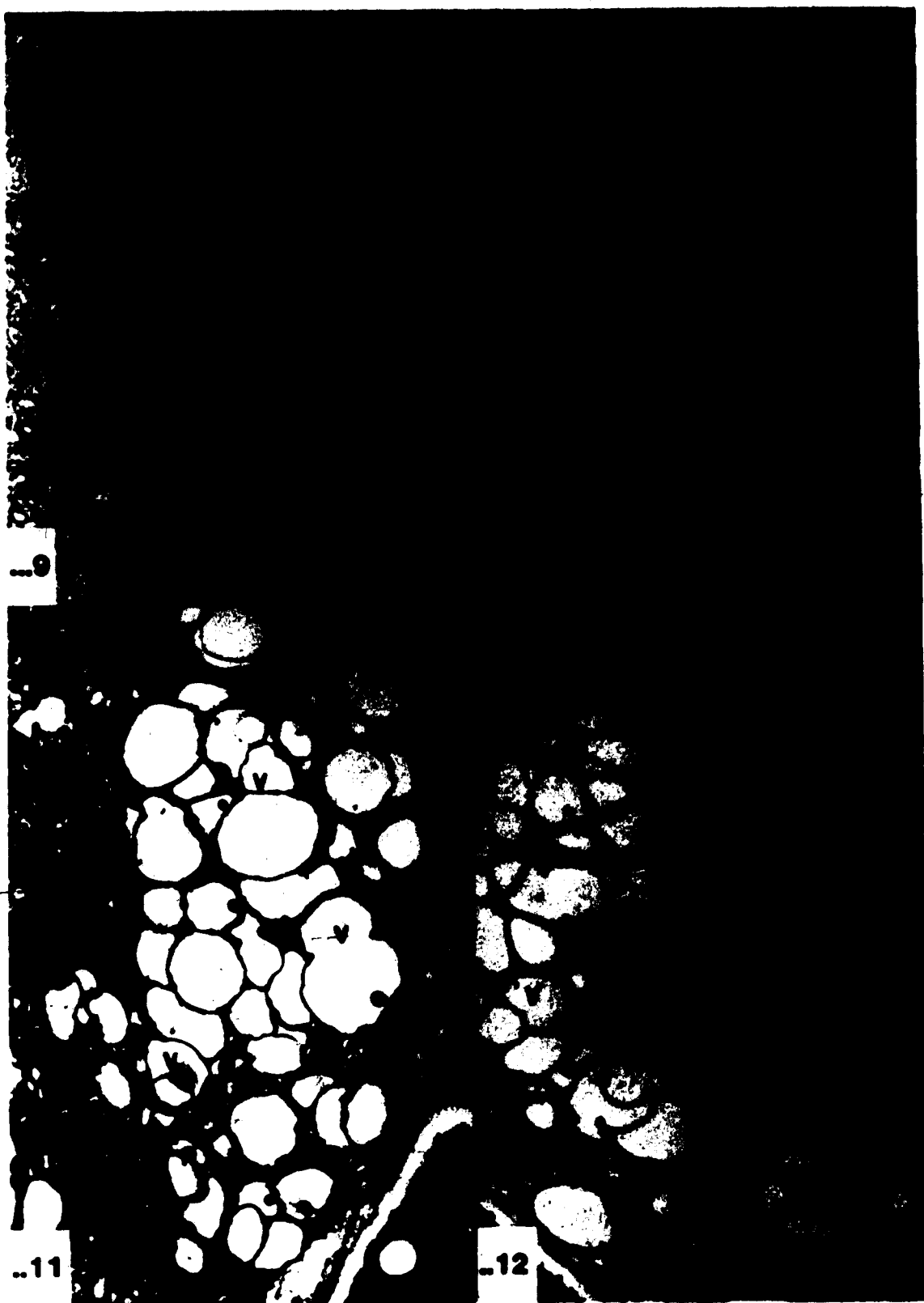
**Fig. 9.** Expanded megasporocyte and associated inner nucellar cells. E.M. x3,560.

**Fig. 10.** Expanded megasporocyte showing invaginations of the plasmalemma (arrow) and plasmodesmata in the megasporocyte wall. E.M. x19,600.

**Fig. 11.** Collection of vacuoles in the micropylar end of the expanded megasporocyte. E.M. x20,000.

**Fig. 12.** Collection of vacuoles in the chalazal end of the expanded megasporocyte. Note the pinocytotic activity of the plasmalemma (arrow). E.M. x21,000.

**Key to Abbreviations:** G, golgi body; In, inner nucellar cell; M, megaspore; Nu, nucellus; P, plasmodesmata; V, vacuole.



thinner walls and more translucent cytoplasm. I propose that this cellular region be referred to as the "inner nucellus" to differentiate it from the remainder of the nucellus, the "outer nucellus". Once the inner nucellar cells are formed their characteristics do not appear to vary until they are destroyed by embryo sac expansion. Figures 9, 13 - 16 show parts of the inner nucellar cells from ovules at different developmental stages. The fluorescein aniline blue shows that the walls of the inner and outer nucellus are similar in containing only low levels of callose (Fig. 17). Calcofluor White M2R indicates the presence of cellulose in the walls of both cell types (Fig. 18). The walls of the inner and outer nucellus are also similar in that both contain numerous plasmodesmata (Figs. 9, 13, 14 & 16). Staining sections with the metachromatic stain TBO suggests that inner nucellar cells contain an elevated level of RNA (Fig. 19). Ultrastructural observations show that differences in cytoplasmic density between the two nucellar cell types results from an increase in ribosome concentration of the inner nucellar cells. Transitional cells occur adjacent to the inner nucellus which are intermediate in cytoplasmic density and/or wall thickness. When an inner nucellar cell is adjacent to either an outer or a transitional nucellar cell the wall is of an uneven thickness. The thicker side is toward the inner nucellar cell (Figs. 14 & 15).

It is assumed that meiosis occurs in the megasporocyte resulting in formation of a linear tetrad of megaspores (Figs. 20 & 21) with the chalazal megaspore being the largest of the four (Fig. 22). Each of the megaspores is highly vacuolated and contains a large nucleus. Staining with aniline blue shows that the walls separating each of the megaspores from one another contains callose (Fig. 17). These walls are perpendicular to the long axis of the nucellus (Fig. 19). No fluorescence was seen on any of the lateral walls of the megaspores. Staining of the same tissue with Calcofluor White M2R did not result in the fluorescence of the wall separating the megaspores (Fig. 18). Figure 24 shows one of the walls that separate the megaspores at a higher magnification. This wall differs from other walls of the inner or outer nucellus in that the fine striations contained in the walls of the nucellus are not evident in the walls that separate the megaspores. Megaspore walls have an amorphous structure, the only electron density associated with the wall occurs in a band of irregular thickness along one

Inner nucellar cells in the soybean ovule.

Fig. 13. Inner, outer and transitional nucellar cells. Plasmodesmata connect all 3 cell types. E.M. x9,040.

Fig. 14. Inner and outer nucellar cells. Arrows indicate the middle lamella. E.M. x16,000.

Fig. 15. Enlargment of Fig. 13 showing the middle lamella between 2 inner nucellar cells and between an inner and transitional nucellar cell. E.M. x44,000.

Fig. 16. Inner, outer and transitional nucellar cells. E. M. x8,400.

Key to Abbreviations: In, inner nucellar cell; On, outer nucellar cell; P, plasmodesmata; Tn, transitional nucellar cell.



On

-18

-18

-18

**Callose wall separating megaspores in soybean.**

**Fig. 17.** Aniline blue staining of thin section showing one of the callose walls separating 2 megaspores. Note lack of callose staining along lateral walls. x625.

**Fig. 18.** Calcofluor White staining of thin sections in Fig. 17 shows presence of cellulose in walls. No cellulose was shown in the callosic megaspore wall. x625.

**Fig. 19.** TBO staining of the same section as in Fig. 18. The light micrograph shows the callosic wall (arrow) along with darkly staining inner nucellar cells. x625.

**Key to Abbreviations:** Cw, callose wall; In, inner nucellar cell; M, megaspore; On, outer nucellar cell.

3



**Megaspores in soybean.**

**Fig. 20.** One of the megaspores showing micropylar callosic wall (arrow) and nucleus. E.M. x1,470.

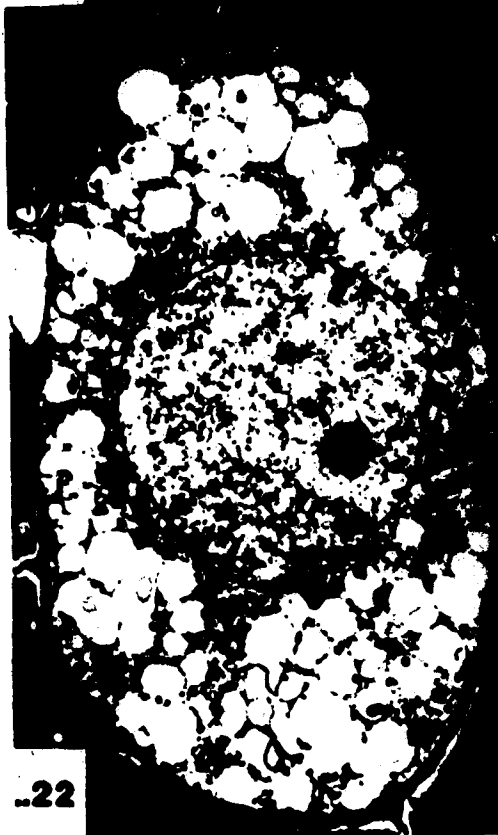
**Fig. 21.** Two megaspores showing highly vacuolate nature of these cells. E.M. x4,400.

**Fig. 22.** The chalazal, functional megaspore. E.M. x5,200.

**Fig. 23.** High magnification of megaspore's cytoplasm showing myelin-like body, strands of rough endoplasmic reticulum and vacuoles. E.M. x8,400.

**Key to Abbreviations:** Cw, callose wall; In, inner nucellar cell; M, megaspore; Mb, myelin-like body; On, outer nucellar cell. Pb, protein body; Rer, rough endoplasmic reticulum; V, vacuole.

120



22



23



Callosic wall and expansion of the functional megaspore.

**Fig. 24.** Callosic wall with dark pore-like areas (arrows) and a band of electron opaque material along one side of the wall. x29,200.

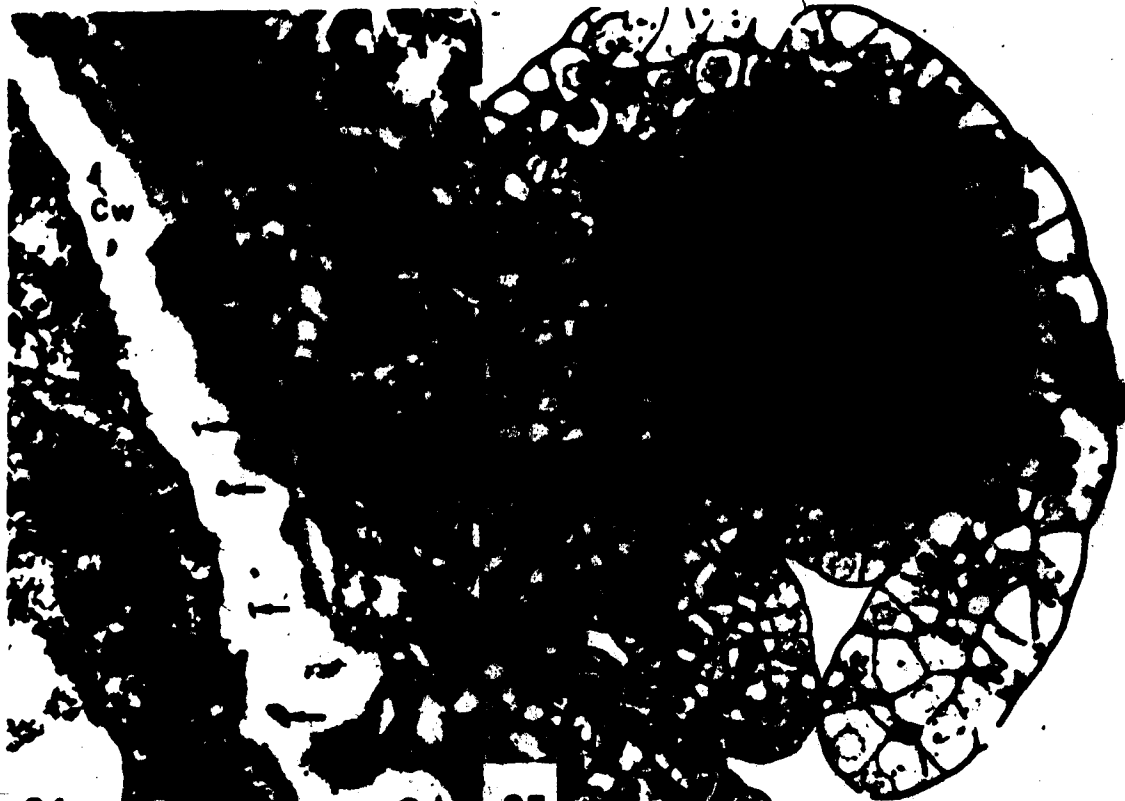
**Fig. 25.** Expanded functional megaspore and the remains of the degenerated megaspores (arrow). L.M. x625.

**Fig. 26.** The dark osmiophilic remains of the 3 micropylar megaspores. E.M. x11,200.

**Fig. 27.** Aniline blue stained section showing the callosic wall lining the micropylar extent of the megaspore. x980.

**Fig. 28.** Calcofluor White staining shows cellulose is present in the micropylar wall (arrow) of the functional megaspore in Fig. 27. L.M. x980.

**Key to Abbreviations:** Cw, callose wall; Dm, degenerated megaspore; Fm, functional megaspore; Pb, protein body; V, vacuole.



..24

..25



..26

..27

..28

side of the wall and small round areas in the electron translucent region of the wall that may be vestiges of plasmodesmata (Fig. 24). Plasmodesmata were only seen in the chalazal megaspore in walls common with the nucellus (Fig. 22). Besides the diffuse vacuome that characterizes the megaspores (Fig. 21) protein bodies, mitochondria, myelin-like bodies and segments of rough endoplasmic reticulum (RER) (Fig. 23) are seen.

The three micropylar megaspores degenerate leaving a single large chalazal megaspore (Figs. 25 & 26). Staining of sections from the ovule used for Fig. 25 with aniline blue (Fig. 27) and Calcofluor White (Fig. 28) show that the aniline blue positive wall is now displaced toward the micropylar region of the embryo sac and that the micropylar wall of the megaspore is now Calcofluor positive.

Continued expansion of the functional megaspore is accompanied by formation of various sized vacuoles (Fig. 29). Large osmiophilic bodies are present in the cytoplasm, some of which are closely associated with areas of membrane resembling myelin-like bodies (Fig. 30). The activity of the Golgi apparatus in this cell is particularly conspicuous (Fig. 31). Most Golgi seem to be located near vacuoles and the vesicles formed appear to be fusing with vacuoles. Protein bodies and myelin-like bodies are also found fusing with vacuoles at this time (Fig. 32).

The metaphase plate of the first mitotic division in megagametogenesis is roughly perpendicular to the long axis of the embryo sac (Fig. 33). The embryo sac at this time is connected to the nucellus by plasmodesmata (Fig. 34) and the cytoplasm has lost all of its large vacuoles with its vacuome now consisting of a diffuse assemblage of smaller vacuoles (Figs. 34 & 35). Mitochondria, strands of RER and plastids are also present at this developmental stage (Figs. 35 & 36). Micrographs such as Fig. 35 suggest that there is a polarity in the embryo sac at this stage with most of the vacuoles located in its micropylar region. Also, during this phase of development invaginations of the plasma membrane seems to be occurring in the micropylar region of the embryo sac (Figs. 35 & 36).

After the mitotic chromosomes separate and the two nuclei are re-established the large central vacuole is formed (Figs. 37 - 39). During this developmental stage the plasmalemma

**One-nucleate embryo sac.**

**Fig. 29.** One-nucleate embryo sac shows centrally placed nucleus and an assemblage of vacuoles. E.M. x3,560.

**Fig. 30.** A condensed myelin-like body associated with a vacuole. E.M. x20,340.

**Fig. 31.** Golgi bodies producing vesicles. Some vesicles are seen fusing with a vacuole. E.M. x58,800.

**Fig. 32.** Protein body and myelin-like body fused with a vacuole. E.M. x35,600.

**Key to Abbreviations:** G, golgi body; Mb, myelin-like body; N, nucleus; P, plasmodesmata; Pb, protein body; V, vacuole; Ve, vesicle.



Transition from 1- to 2-nucleate embryo sac in soybean.

Fig. 33. Metaphase plate (arrow) perpendicular to the long axis of the embryo sac during the first mitotic division of megagametogenesis. L.M. x625.

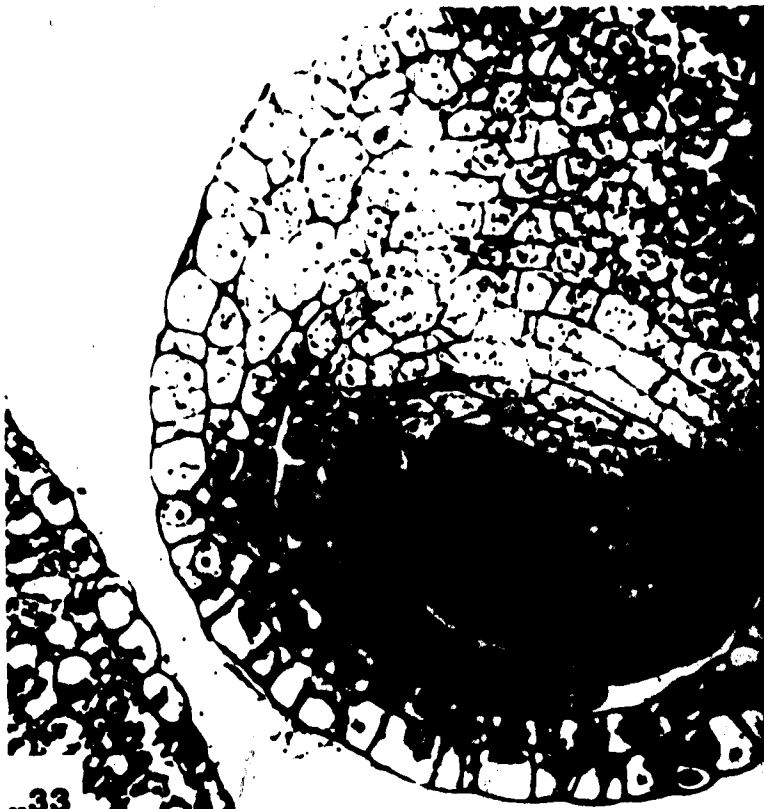
Fig. 34. Plasmodesmata in the embryo sac wall. E.M. x6,600.

Fig. 35. Cytoplasm in the embryo sac showing polarity in the location of the small vacuoles. Note the invaginations of the plasmalemma (arrow). E.M. x9,040.

Fig. 36. Invagination of the plasmalemma in the embryo sac (arrows). E.M. x20,000.

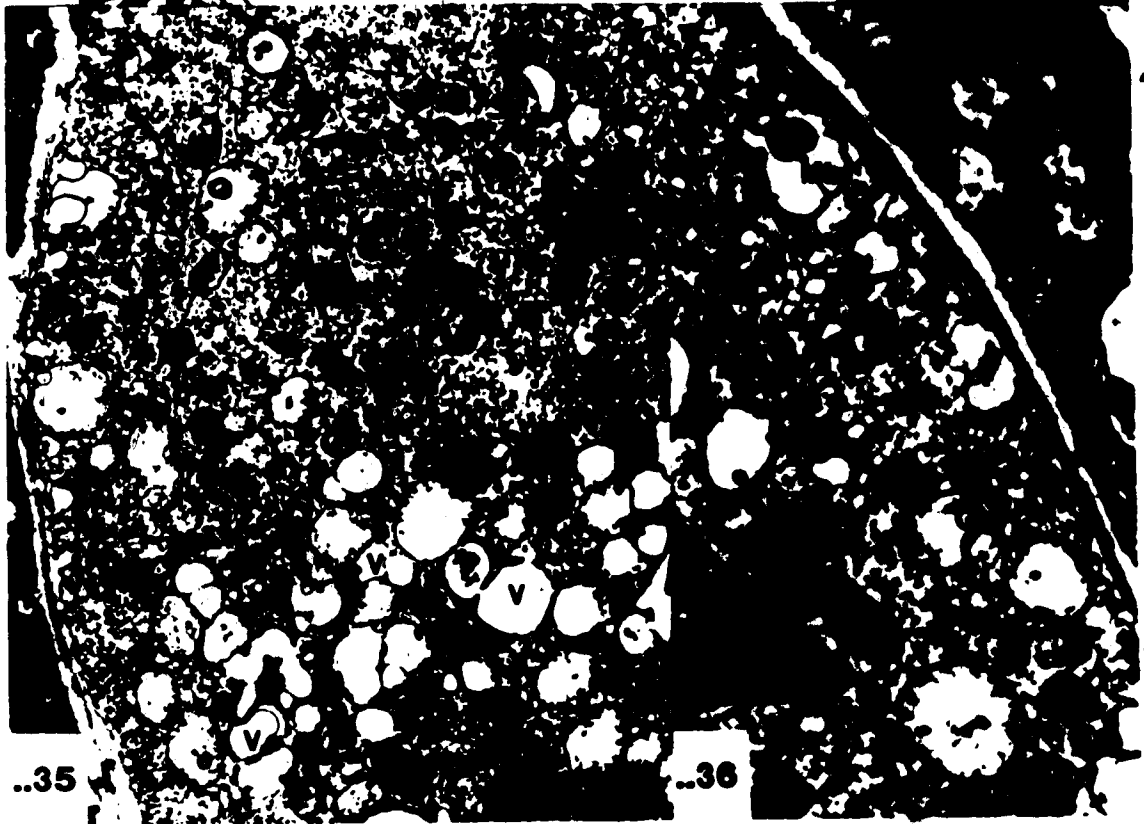
Key to Abbreviations: G, golgi body; Mb, myelin-like body; P, plasmodesmata; V, vacuole.





..33

..34



..35

..36

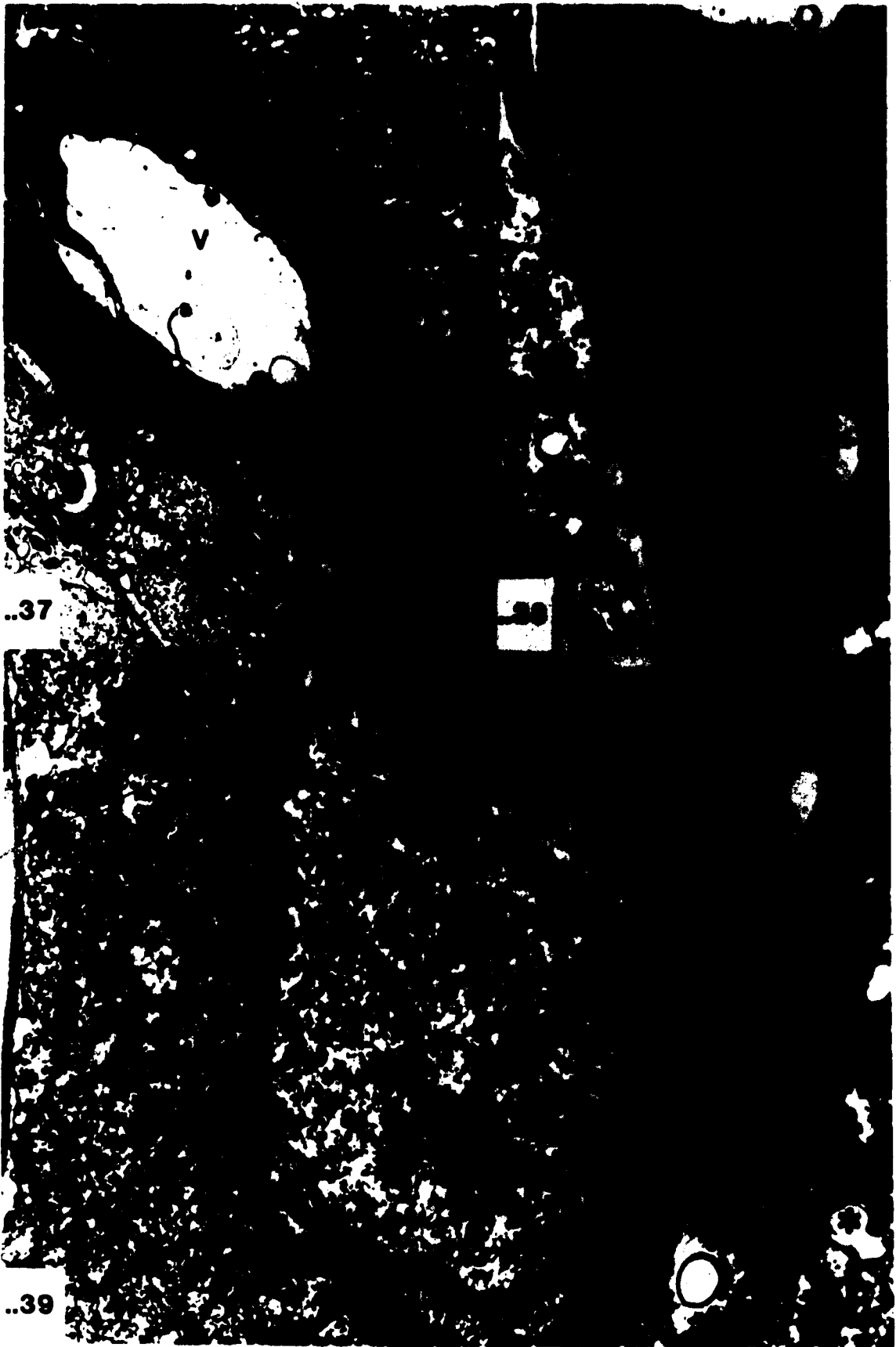
Two-nucleate embryo sac in soybean.

Fig. 37. A sagittal section of the 2-nucleate embryo sac with a large central vacuole. E.M. x3,440.

Fig. 38. Chalazal end of the 2-nucleate embryo sac showing nucleus and invaginations of the plasmalemma (arrows). E.M. x9,100.

Fig. 39. Micropylar end of the 2-nucleate embryo sac showing the nucleus and invaginations of the plasmalemma (arrows). Note infolding of smooth endoplasmic reticulum (SER) to form a vacuole (asterisk). E.M. x31,200.

Key to Abbreviations: G, golgi body; M, mitochondria; N, nucleus; Ob, osmiophilic body; V, vacuole.



..37

..39

continues to produce invaginate (Figs. 38 & 39). Also, infolding of smooth endoplasmic reticulum (SER) also results in vacuole formation (Figs. 39 & 40). Myelin-like bodies (Figs. 41 & 42), protein bodies (Fig. 40) and Golgi vesicles (Fig. 43) are often seen fusing with the central vacuole. The cytoplasm of the 2-nucleate embryo sac is seen to be filled with mitochondria (Fig. 39), Golgi bodies (Fig. 43) and many osmophilic bodies (Figs. 37, 38 & 40).

The second mitotic division results in a 4-nucleate embryo sac. By this developmental stage the inner nucellus is almost completely destroyed in areas associated with the micropylar region of the embryo sac (Fig. 44). The plane of division as reflected by the position of the resultant nuclei in the micropylar region is perpendicular to that of the previous division (Fig. 44). However, the plane of division appears to be somewhat more variable in the chalazal region where it is oblique ranging somewhere between perpendicular to parallel to the long axis of the embryo sac (Fig. 45). During the development of the 4-nucleate embryo sac there are changes in the position of the nuclei. In the micropylar region of the embryo sac the 2 nuclei separate and one then assumes a position slightly more chalazal than the other (Fig. 46). In the chalazal portion of the embryo sac the 2 nuclei move from their oblique position to one that is parallel to the long axis of the embryo sac (Fig. 47). Plasmodesmata connect the embryo sac to the cells of the inner nucellus in the chalazal region of the embryo sac (Figs. 45, 47 & 48). A few of the previously undifferentiated plastids form starch grains (Fig. 49) and the cytoplasm is filled with myelin-like bodies (Figs. 47 & 49), vacuoles (Figs. 45 - 47, 49 & 50) and mitochondria (Fig. 50). Golgi bodies occur throughout the cytoplasm (Fig. 49) but their activity is especially intense in later stages of development (Fig. 51). The plasma membrane continues to exhibit membrane configurations that indicate with pinocytotic activity (Fig. 52) and much of the Golgi apparatus seems to be located near the large central vacuole where many of its vesicles are seen fusing with this vacuole (Figs. 53 - 56).

In later stages of development in the 4-nucleate embryo sac there appears to be an increase in membrane systems found within the central vacuole (Figs. 57 - 60). Many osmophilic bodies are produced throughout the cytoplasm (Figs. 46 & 47). These bodies are

**Cytoplasm of the 2-nucleate embryo sac.**

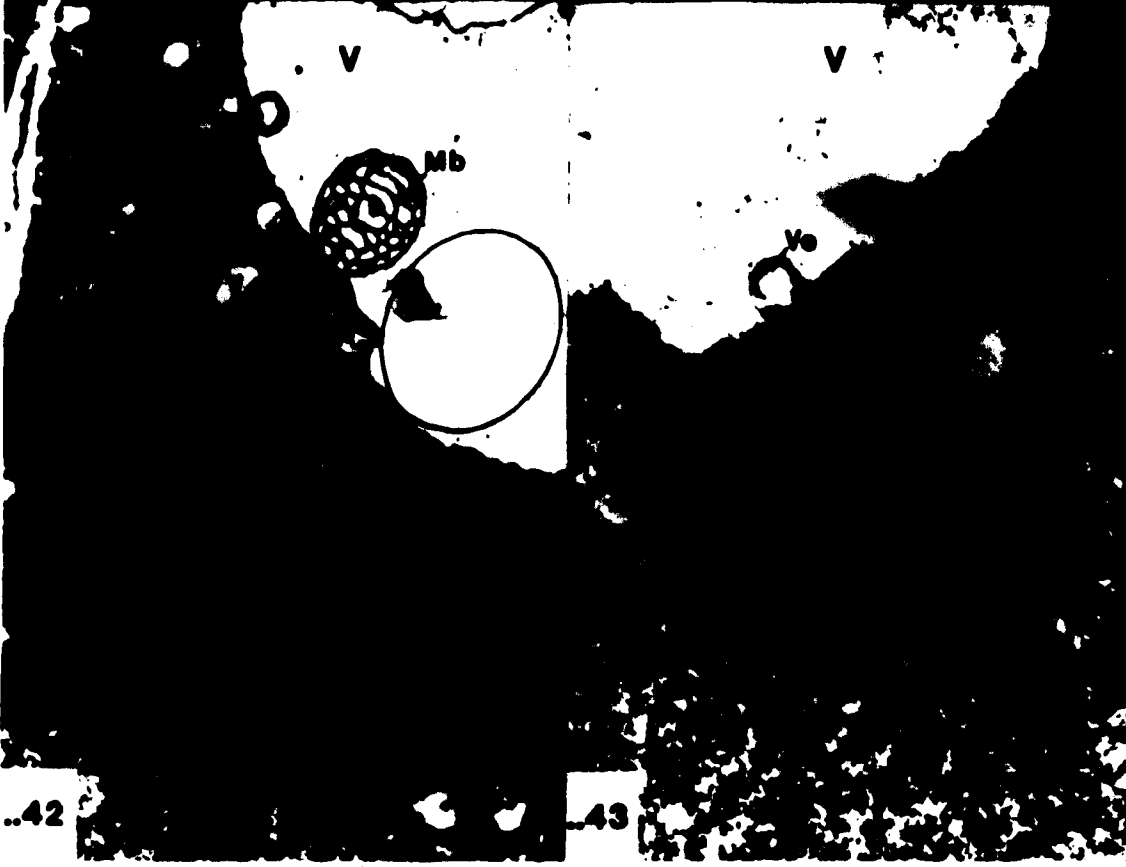
**Fig. 40.** Protein body fusing with the major vacuole and infolding of SER to form a vacuole (asterisk). E.M. x48,800.

**Fig. 41.** Myelin-like body fused with the large central vacuole. E.M. x14,400.

**Fig. 42.** Another form of a myelin-like body fused with the central vacuole. E.M. x17,600.

**Fig. 43.** Golgi body in the cytoplasm and vesicles fusing with the vacuole. E.M. x35,600.

**Key to Abbreviations:** G, golgi body; Mb, myelin-like body; N, nucleus; Ob, osmiophilic body; Pb, protein body; V, vacuole; Ve, vesicle.



Four-nucleate embryo sac in soybean.

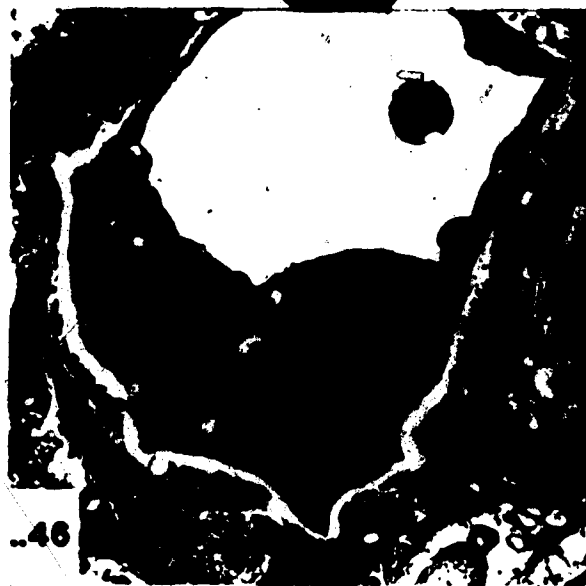
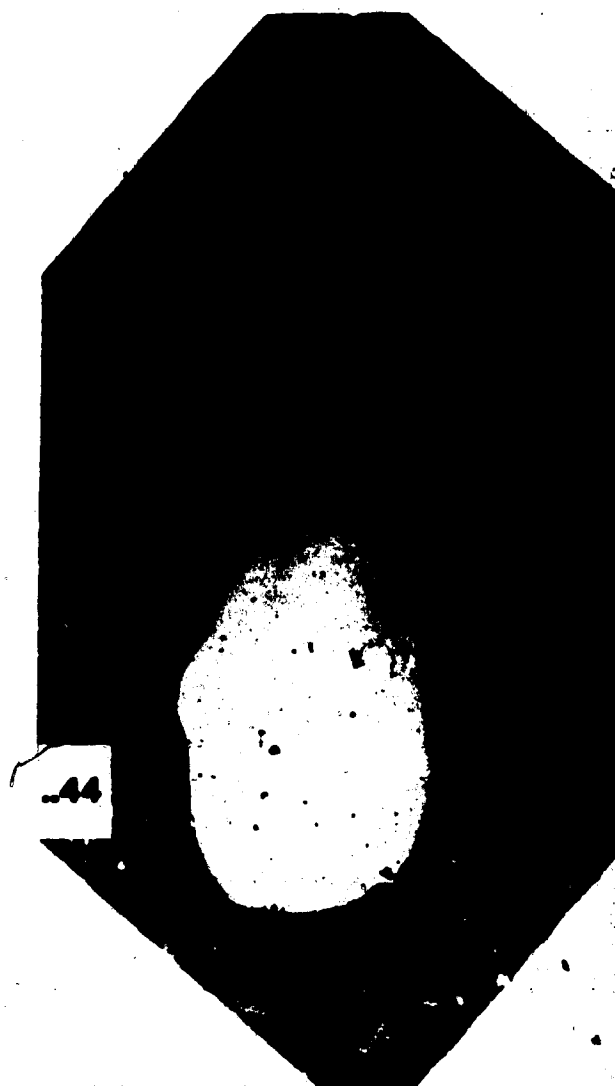
Fig. 44. Sagittal section showing micropylar nuclei in the embryo sac and extent of the inner nucellus. E.M. x1,840.

Fig. 45. The 2 chalazal nuclei in the same sac as Fig. 44. E.M. x3,440.

Fig. 46. Two micropylar nuclei after separation and chalazal movement of one of the nuclei. E.M. x3,560.

Fig. 47. The 2 chalazal nuclei after rearrangement. Both nuclei are parallel to the long axis of the embryo sac. E.M. x5,340.

Key to Abbreviations: inner nucellar cell; Mb, myelin-like body; N, nucleus; Ob, osmiophilic body; P, plasmodesmata; Pb, protein body; V, vacuole.





Cytoplasm of the 4-nucleate embryo sac.

Fig. 48. Plasmodesmata in the chalazal end of the embryo sac wall. E.M. x33,200.

Fig. 49. Chalazal end of the embryo sac showing myelin-like body and amyloplast. E.M. x20,800.

Fig. 50. Mitochondria and vacuoles in the embryo sac cytoplasm. E.M. x26,400.

Fig. 51. Golgi bodies in the embryo sac cytoplasm. E.M. x33,200.

Key to Abbreviations: A, amyloplast; G, golgi body; In, inner nucellar cell; Mb, myelin-like body; Ob, osmiophilic body; V, vacuole; Ve, vesicle.



Cytoplasm of the 4-nucleate embryo sac.

Fig. 52. Invagination of the plasmalemma (arrows). E.M. x29,200.

Fig. 53. Osmiophilic and myelin-like body located adjacent to the central vacuole. E.M. x20,000.

Fig. 54. Golgi body forming vesicles and vesicles fusing with the central vacuole. E.M. x44,000.

Fig. 55. Golgi body producing vesicles some of which appear to be fusing with the central vacuole. E.M. x41,600.

Fig. 56. Vesicle fused with the vacuole (Ve). E.M. x86,000.

Key to Abbreviations: G, golgi body; Mb, myelin-like body; Ob, osmiophilic body; V, vacuole; Ve, vesicle.



Membrane proliferations associated with the major vacuole of the 4-nucleate embryo sac.

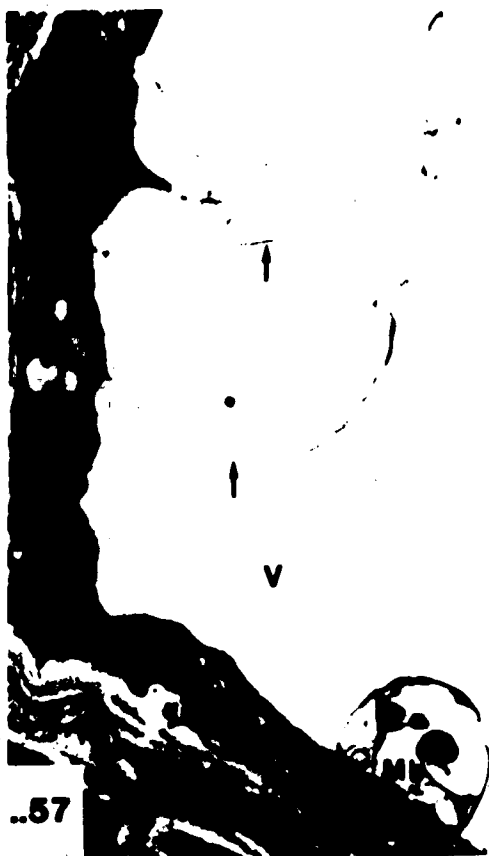
Fig. 57. Membrane profiles (arrows) of an expanded myelin-like body in the vacuole. E.M. x20,000.

Fig. 58. Membrane profile (arrows) of an expanded myelin-like body in the vacuole. E.M. x20,000.

Fig. 59. Attachment of membrane profiles to the vacuolar tonoplast (arrows). E.M. x35,600.

Fig. 60. Myelin-like body enclosed in the vacuole. E.M. x44,000.

**Key to Abbreviations:** G, golgi body; Mb, myelin-like body; Ob, osmiophilic body; V, vacuole.



often found associated with or are located on the periphery of a vacuole (Figs. 52, 53 & 57).

The third mitotic division results in an 8-nucleate 7-celled embryo sac. The process of karyokinesis and cytokinesis appear to be closely tied since no 8-nucleate, acellular embryo sac was found in the course of the study. Figure 61 shows 2 of the cells of the egg apparatus at the youngest developmental stage observed. The cells have dense cytoplasm without the scattered vacuoles common in the cytoplasm of 4-nucleate embryo sac. Figures 62 - 68 show sections of a young egg apparatus from an embryo sac which is slightly older, ~~less~~ dense, and more vacuolate than the one shown in Fig. 61. It appears that the density of the cytoplasm and the lack of vacuoles are correlated with the developmental stage of the egg apparatus. At this stage of development it is difficult to determine if a particular egg apparatus cell is an egg or a synergid because none of the most obvious cellular characteristics are present. In the mature egg apparatus some of the differences are the points of attachment to the embryo sac wall, the relative positions of the largest vacuole and the nucleus in the cell, the presence or absence of a filiform apparatus and the size and distribution of wall packets around the chalazal end of the cells (Folsom & Peterson, 1984).

Inspection of an egg apparatus slightly older than that in Fig. 61 reveals the relative positions of nuclei and walls after cellularization has occurred. When viewed in this manner it is possible, even before development of the characteristic large vacuole, to classify an egg apparatus cell as either an egg or synergid. Because of relative position, the cells with the lowermost nuclei (Fig. 66) are assumed to be synergids while that with the uppermost nucleus an egg (Figs. 62 & 63). From this series (Figs. 62 - 68) of micrographs it is apparent that the cells of the egg apparatus are separated from one another and the central cell by three walls forming two distinct sets. The first set is comprised of a wall, the top wall, which is roughly perpendicular to the long axis of the embryo sac and separates the cells of the egg apparatus from the central cell (Figs. 62 - 68). The second set is composed of two walls, the egg apparatus common walls, that divides the micropylar base of the embryo sac into the cells of the egg apparatus (Figs. 63 & 64). One wall in the second set of two walls is parallel to the embryo sac's long axis and continuous across the entire megagametophyte base dividing it into

Young egg apparatus in soybean.

Fig. 61. Youngest egg apparatus observed. Note dark cytoplasm and thick walls. E.M. x6,600.

Figs. 62-66. Series of micrographs through an egg apparatus slightly older than that in Fig. 61 showing the 3 walls which separate egg and synergid cells from each other and the central cell. Figs. 62 & 63 show an egg nucleus while Figs. 64 - 66 show synergid nuclei. Figs. 63 & 64 show the third egg apparatus wall (arrows) which separates the egg from the synergid in one-half of the embryo sac base. Figs. 62 - 66 all show the top and common wall of the egg apparatus. E.M. x4,300.

Key to Abbreviations: Cc, central cell; Cw, common wall; Ea, egg apparatus cell; En, egg nucleus; Esw, embryo sac wall; Mpn, micropylar polar nucleus; Sn, synergid nucleus; Tw, top wall.



Cc

..61

..63

..65

..68

Young egg and antipodal apparatus in soybean.

Figs. 67 & 68. Continues series begun with Fig. 62. Micrographs show both synergids and micropylar polar nucleus. E.M. x4,300.

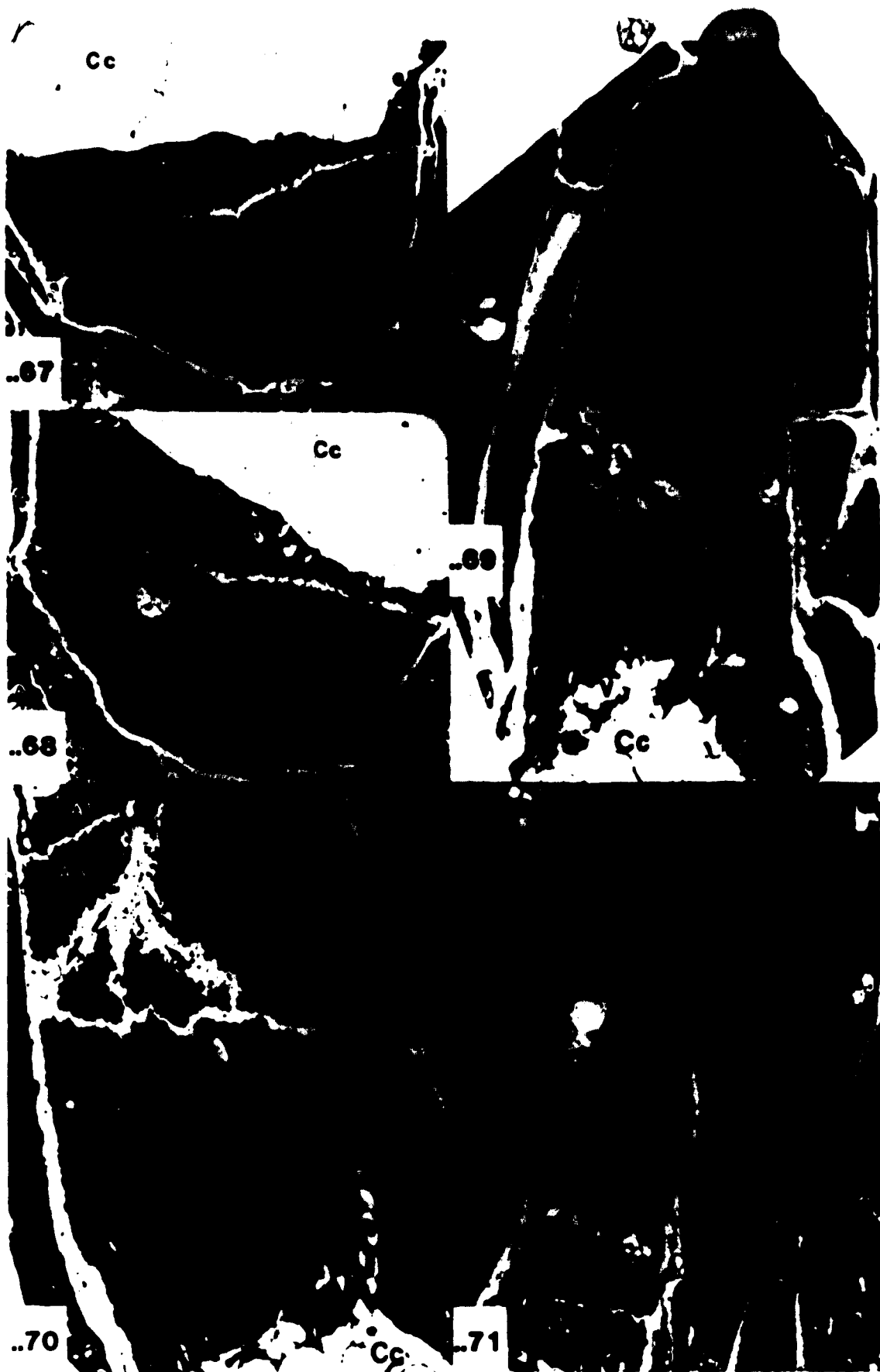
Sections through an antipodal apparatus showing all antipodal cells (A1, A2, A3).

Fig. 69. Antipodal apparatus showing 2 cells and the chalazal polar nucleus. E.M. x4,400.

Fig. 70. Median section of the wall which separates the two most micropylar antipodal cells containing cross sections of plasmodesmata (arrows). E.M. x6,600.

Fig. 71. Third antipodal cell in the same embryo sac as Figs. 69 & 70. E.M. x3,440.

Key to Abbreviations: Cc, central cell; Cpn, chalazal polar nucleus; Cw, common wall; Mpn, micropylar polar nucleus; P, plasmodesmata; Pb, protein body; Tw, top wall; V, vacuole.



two roughly equal halves (Figs. 62 - 68). In one of these halves an egg and synergid are formed (Figs. 63 - 66) while the other contains a single synergid (Figs. 62 - 68). The second wall, in the second set of egg apparatus walls is oblique to the other two walls and separates the egg and synergid from one another.

The central cell and antipodal apparatus are also formed at this time. The major features of the central cell are the vacuole that develops during the 2- and 4-nucleate stages (Fig. 62) and the polar nuclei that are found at the micropylar (Figs. 67 & 68) and chalazal (Fig. 69) ends of the cell. Wall ingrowths and multigrain amyloplasts (starch packets), prominent features of the mature soybean central cell (Folsom & Peterson, 1984) are not present at this time.

The arrangement and shape of antipodal cells reflect the nuclear position during the late 4-nucleate stage and embryo sac structure at that time. Structurally the chalazal-most portion of the embryo sac is cone shaped at the late 4-nucleate stage (Fig. 69). During cellularization 3 walls form separating the antipodal cells from each other and the central cell (Figs. 69 - 71). Two of these walls are parallel to each other and perpendicular to the long axis of the embryo sac (Figs. 69 & 71). The third wall forms between these two new walls and is parallel to the long axis of embryo sac (Fig. 70).

#### The development of the cells of the egg apparatus:

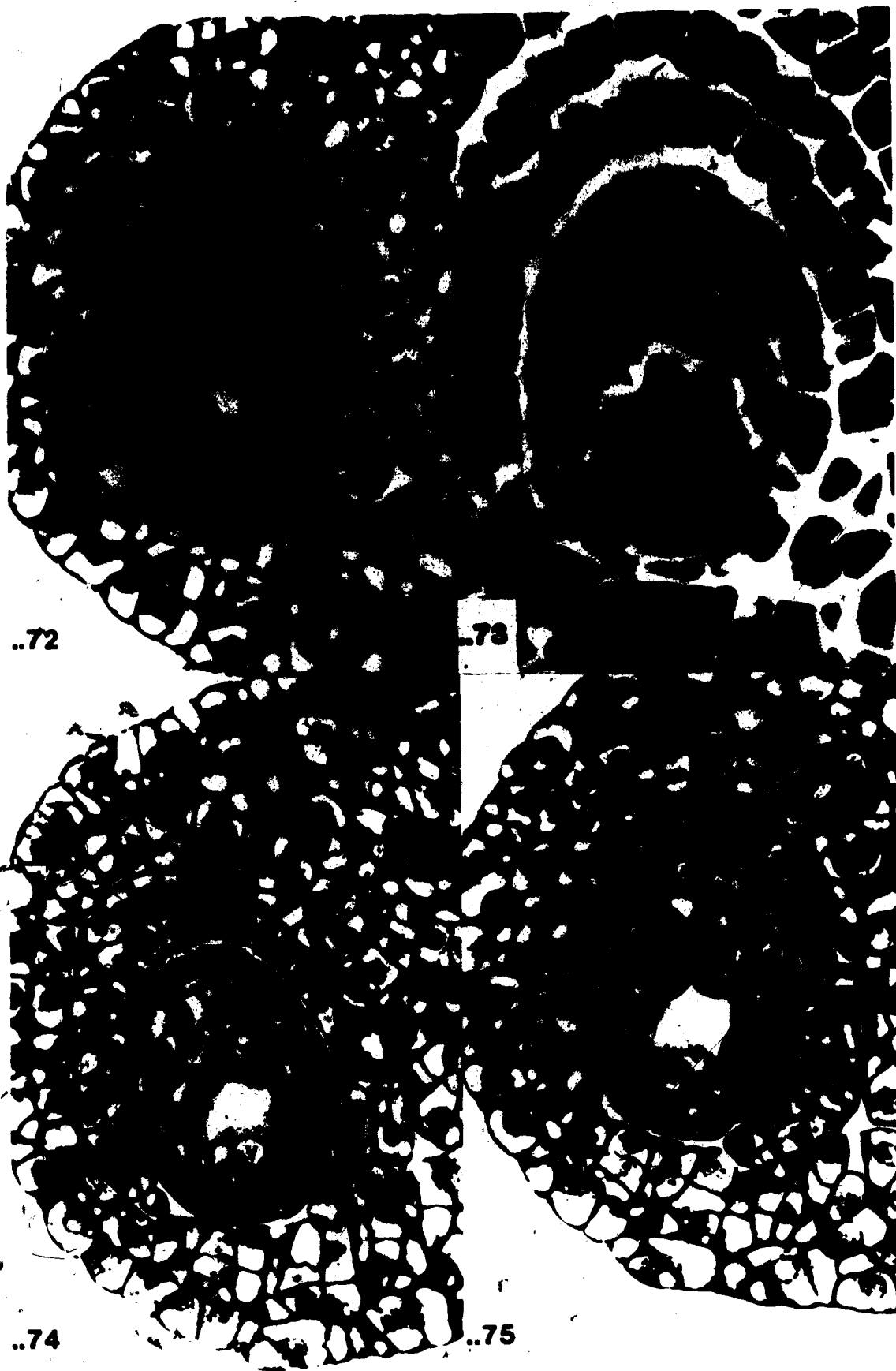
In soybean the cytoplasm of each egg apparatus cell immediately after cellularization is extremely dense with a large nucleus and a few small vacuoles and is enclosed in thick, highly dissected walls. The walls that separate cells of the egg apparatus from one another are roughly perpendicular to the one that isolates the egg apparatus from the central cell (Fig. 61). The formation of vacuoles micropylar to the egg nucleus and chalazal to the synergids nuclei are the first events that allow the egg apparatus cells to be easily distinguished from one another. When the egg apparatus cells are pyramidal in shape these vacuoles are small (Fig. 72) but later enlarge as the egg and synergids develop a columnar shape (Fig. 76).

Egg apparatus cells showing a pyramidal shape.

Fig. 72. Three egg apparatus cells (asterisks) at the pyramidal stage. L.M. x625.

Fig. 73. Same section as Fig. 72 stained with Calcofluor White showing cellulose in egg apparatus cell walls (W). x980.

Figs. 74 & 75. Sections through the same embryo sac as in Fig. 72 showing presence of small vacuoles (V). L.M. x625.



Columnar shaped egg apparatus cells.

Fig. 76. Light micrograph showing egg and synergid cells. TBO. x750.

Series of micrographs through a columnar shaped egg apparatus showing attachment of cells to the embryo sac wall.

Fig. 77. Egg with characteristic micropylar vacuole. E.M. x9,900.

Fig. 78. Three egg apparatus cells with portions of 2 synergid nuclei. E.M. x3,560.

Fig. 79. Synergid with characteristic chalazal vacuole. E.M. x5,200.

Key to Abbreviations: Cc, central cell; E, egg; Esw, embryo sac wall; Ma, multigrain amyloplast; N, nucleus; S, synergid; V, vacuole; Wi, wall ingrowth.





Figures 77 - 79 are all from an embryo sac in which the egg apparatus cells have expanded, each containing a large vacuole. Other than nuclear and vacuolar positions there is no difference among egg apparatus cells in their cytoplasm, nature of the surrounding walls, or point of attachment to the embryo sac wall.

Throughout expansion and differentiation of the egg apparatus there are progressive increases in length and corresponding decreases in cell wall thickness and cytoplasmic density. When measurements are made of the youngest embryo sac observed in this study the egg apparatus cells had a maximum length of  $24\text{ }\mu\text{m}$ . During the course of development there is a greater than 11-fold increase in cell length to approximately  $27\text{ }\mu\text{m}$ . The effect of the elongation process can be seen in all of the egg apparatus walls but is most obvious in the top wall and the chalazal region of the walls separating the egg and synergid cells.

As already stated the egg apparatus consists of 2 sets of walls. Initially these walls are all structurally similar in that they are heavily dissected by electron dense bands suggestive of plasmodesmata and lack a middle lamella (Figs. 61 & 80). The first set is composed entirely of the top wall that separates the chalazal region of the egg apparatus cells from the central cell while the second set is a system of two walls that separate the synergids from one another and the egg cell. Although there are some regional variations in thickness, the egg apparatus top wall is initially  $400\text{ nm}$  thick (Fig. 80). During its initial expansion this wall separates into discrete units that appear to have been previously defined by these electron dense bands (Fig. 81). Next a thinning of the wall occurs as its thickness decreases by at least 50% in some areas (Fig. 82). The result is a wall consisting of discrete wall packets approximately  $205\text{ nm}$  in thickness separated by areas of plasma membrane contact in the egg (Fig. 83). There appear to be more and larger wall packets per unit length in the egg than the synergids (compare Figs. 83 & 84). The dimensions of these packets can later increase, presumably due to Golgi activity (Fig. 85).

The second system of walls are often referred to as the common walls of the egg apparatus. In the chalazal-most area of the common walls where they fuse with the top wall of the egg apparatus, the wall also undergoes thinning and segmentation resulting in a

Egg apparatus, top wall showing thinning and segmentation with cellular expansion.  
All electron micrographs x40,000.

Fig. 80. Youngest egg apparatus observed.

Fig. 81. Egg apparatus in which the top wall shows segmentation (arrow).

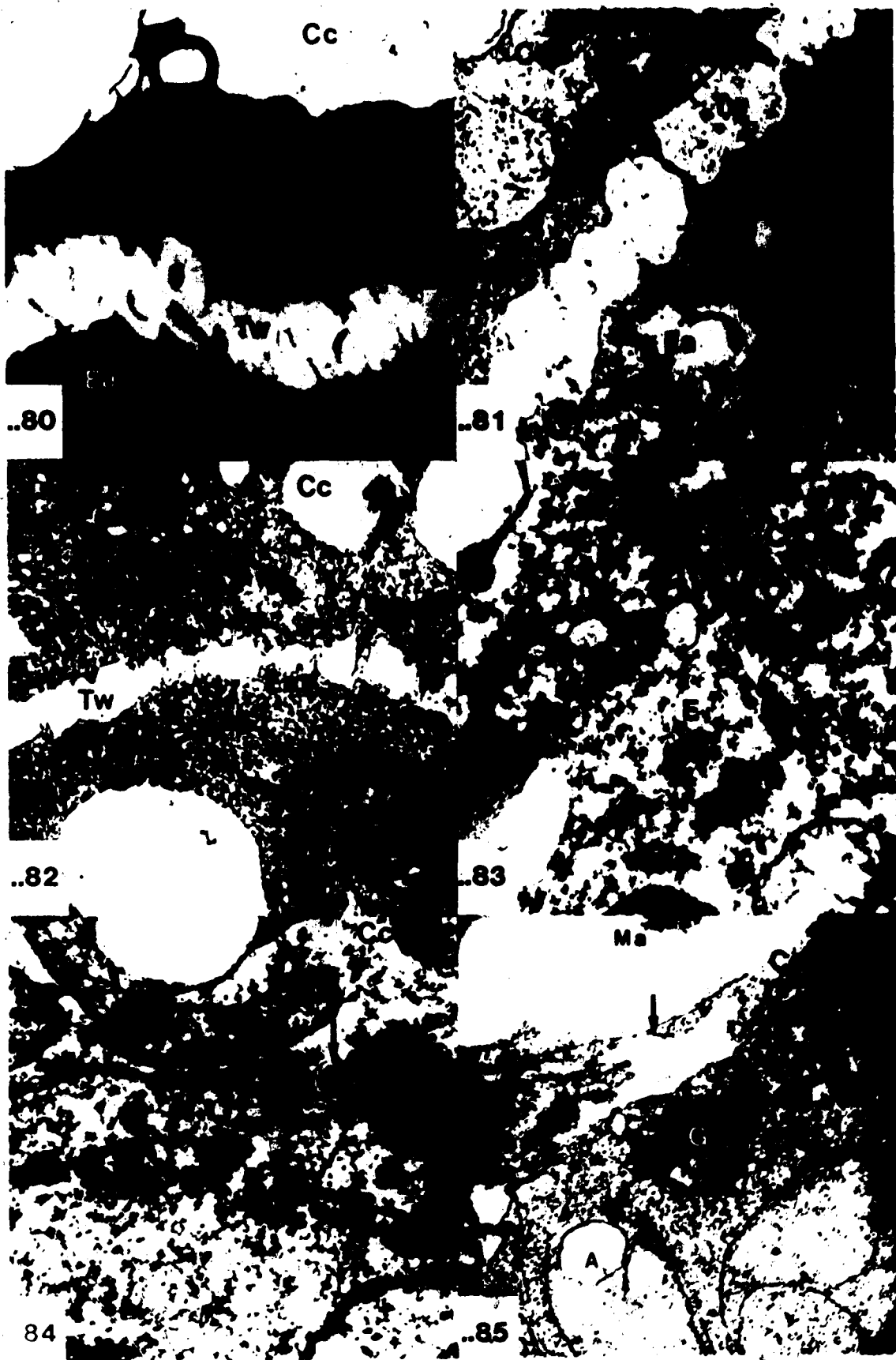
Fig. 82. Top wall of a columnar shaped egg apparatus.

Fig. 83. Top wall of an expanded egg cell. Note wall packets (arrows) separated by thin areas.

Fig. 84. Top wall of an expanded synergid cell. Note fewer wall packets (arrows) per unit length than in the egg (Fig. 83).

Fig. 85. Top wall of mature egg cell showing a wall packet (arrow). Expansion of wall packets appears to occur through golgi activity.

Key to Abbreviations: A, amyloplast; Cc, central cell; E, egg; Ea, egg apparatus cell; G, golgi body; Ma, multigrain amyloplast; Pb, protein body; S, synergid; Tw, top wall.



decrease in thickness from 270 nm to areas of membrane contact with wall packets of 150 nm in diameter. Overall expansion of the egg apparatus results in the development of the characteristic "Y" shaped intersection which forms at the point of attachment of the common walls to the egg apparatus top wall (Figs. 86 - 89). The base of the egg apparatus common walls also undergoes a thinning from approximately 280 to 120 nm before the development of the filiform apparatus (Figs. 90 & 91).

The filiform apparatus forms after the differentiation and expansion of egg apparatus cells. Examination of sections through an egg apparatus reveals that the first sign of a filiform apparatus is a swelling in the base of the synergids' common wall (Figs. 92 & 93). The filiform apparatus first appears as a number of finger-like projections that radiate from the common wall of the synergids (Fig. 94). In later stages of development these projections continue to grow further into the synergid cytoplasm (Fig. 95). At this later stage of development, the filiform apparatus has grown extensively into synergid cytoplasm but the area of attachment to the base of the common wall does not appear to expand (Figs. 96 & 97). Cross sections of the micropylar end of an embryo sac show that the filiform apparatus forms not only at the micropylar base but also at the center of the wall between the two synergids (Figs. 98 - 101). In a cross sectional view the filiform apparatus also shows the restricted point of attachment to the synergid-synergid wall seen in longitudinal section. The filiform apparatus along with the walls that surround the cells of the egg apparatus fluoresce after being stained with Calcofluor White M2R (Figs. 73, 97, 99 & 101).

As shown earlier, the egg apparatus begins as a group of cells with a relatively flat top wall that is fused to the embryo sac wall and separates the egg apparatus from the central cell. When the angle between the top wall of the egg apparatus and the embryo sac wall contained in the central cell is determined it ranges from acute to obtuse (Figs. 61 & 62). With expansion of the egg apparatus cells this angle becomes strictly acute often approaching 15° (Fig. 102).

As the egg apparatus cells expand their cytoplasmic contents become more recognizable. The cytoplasm of these cells is uniformly dense at maturity. In both cell types

Attachment of common wall to the egg apparatus top wall.

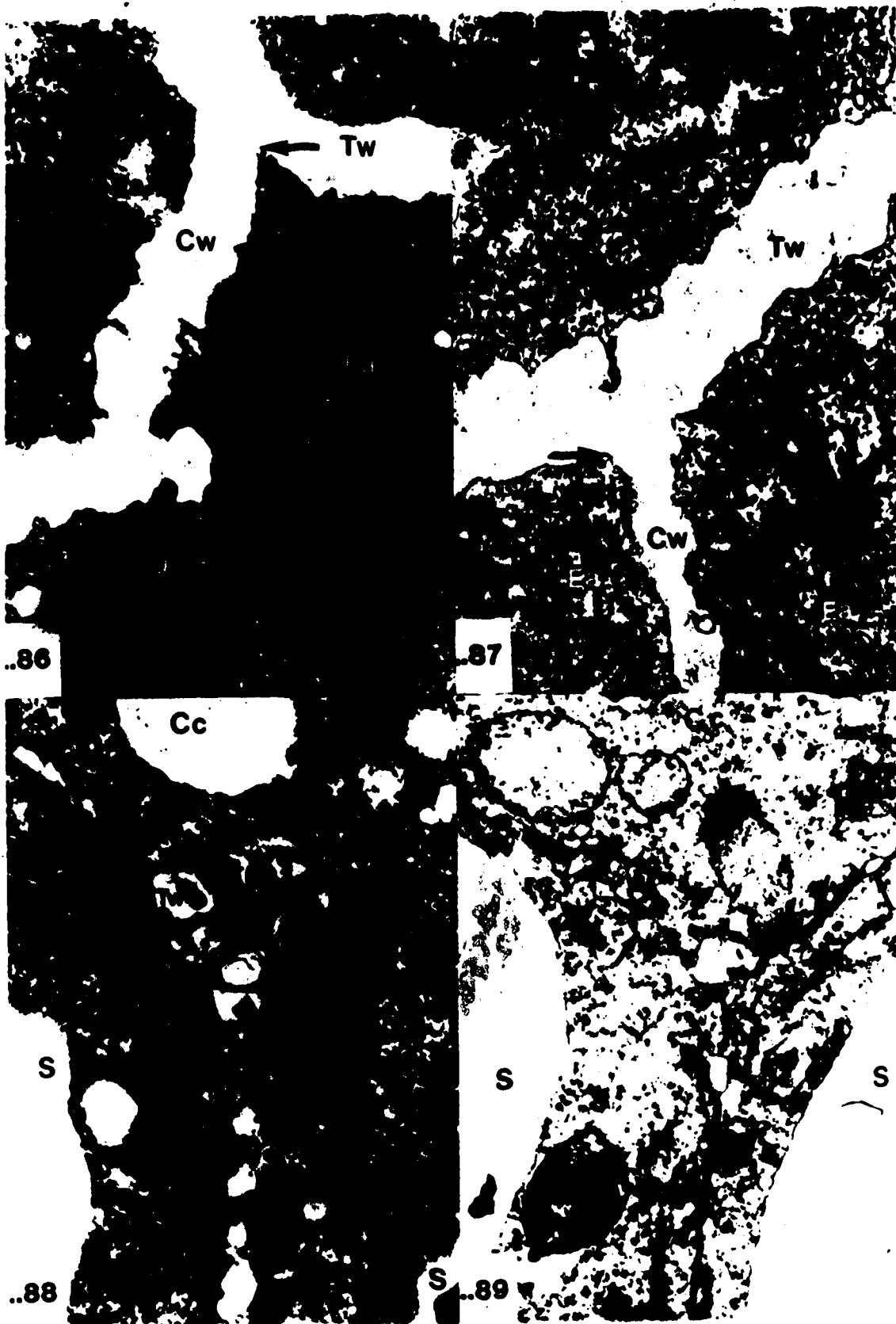
Fig. 86. Egg apparatus in a young embryo sac. The common wall is 270 nm thick (arrows) at the point of attachment to the top wall. E.M. x44,000.

Fig. 87. Slightly older embryo sac than in Fig. 86. Common wall is 240 nm thick at point of attachment (arrows). E.M. x41,600.

Fig. 88. Shows segmentation of common wall with expansion of egg apparatus. E.M. x29,200.

Fig. 89. Common wall between two synergids. Wall packets (arrows) are separated by membrane areas. E.M. x26,400.

Key to Abbreviations: Cc, central cell; Cw, common wall; Ea, egg apparatus cell; S, synergid; Tw, top wall.



Base of egg apparatus common wall.

Fig. 90. A common wall in the youngest egg apparatus observed. E.M. x44,000.

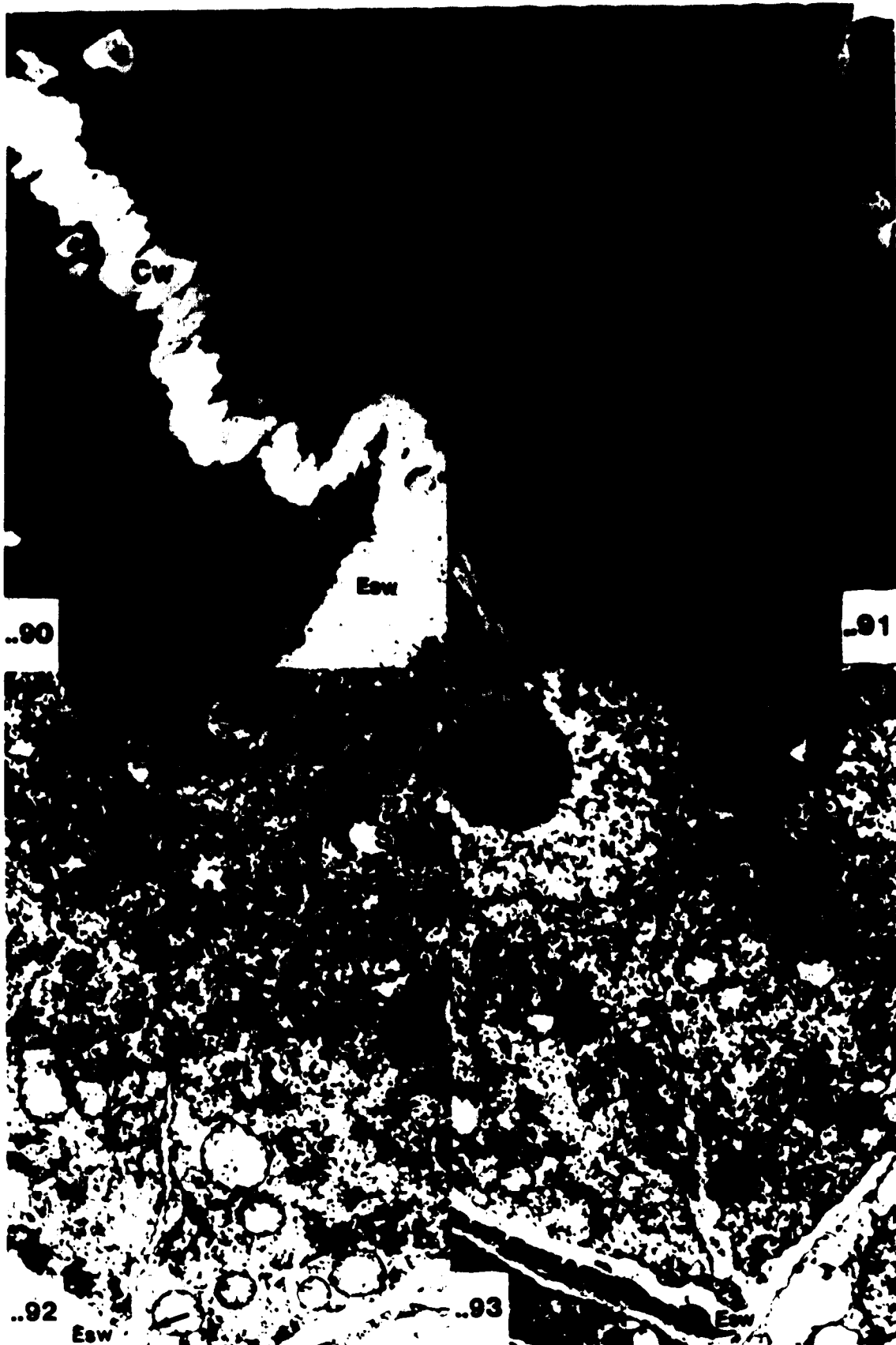
Fig. 91. Wall in egg apparatus older than in Fig. 90. Note thinning of wall. E.M. x16,000.

Figs. 92 & 93 begin a sequence showing swelling of synergid's common wall as sections approach the filiform apparatus.

Fig. 92. Synergid common wall in egg apparatus older than in Figs. 90 & 91. Note absence of swelling in the basal part of the common wall (arrows). E.M. x11,200.

Fig. 93. Synergid common wall showing swelling in the basal region near the filiform apparatus (arrows). E.M. x9,040.

Key to Abbreviations: Cw, common wall; Ea, egg apparatus cell; Esw, embryo sac wall; Mb, myelin-like body; N, nucleus; P, plasmodesmata; S, synergid.





**Filiform apparatus in soybean.**

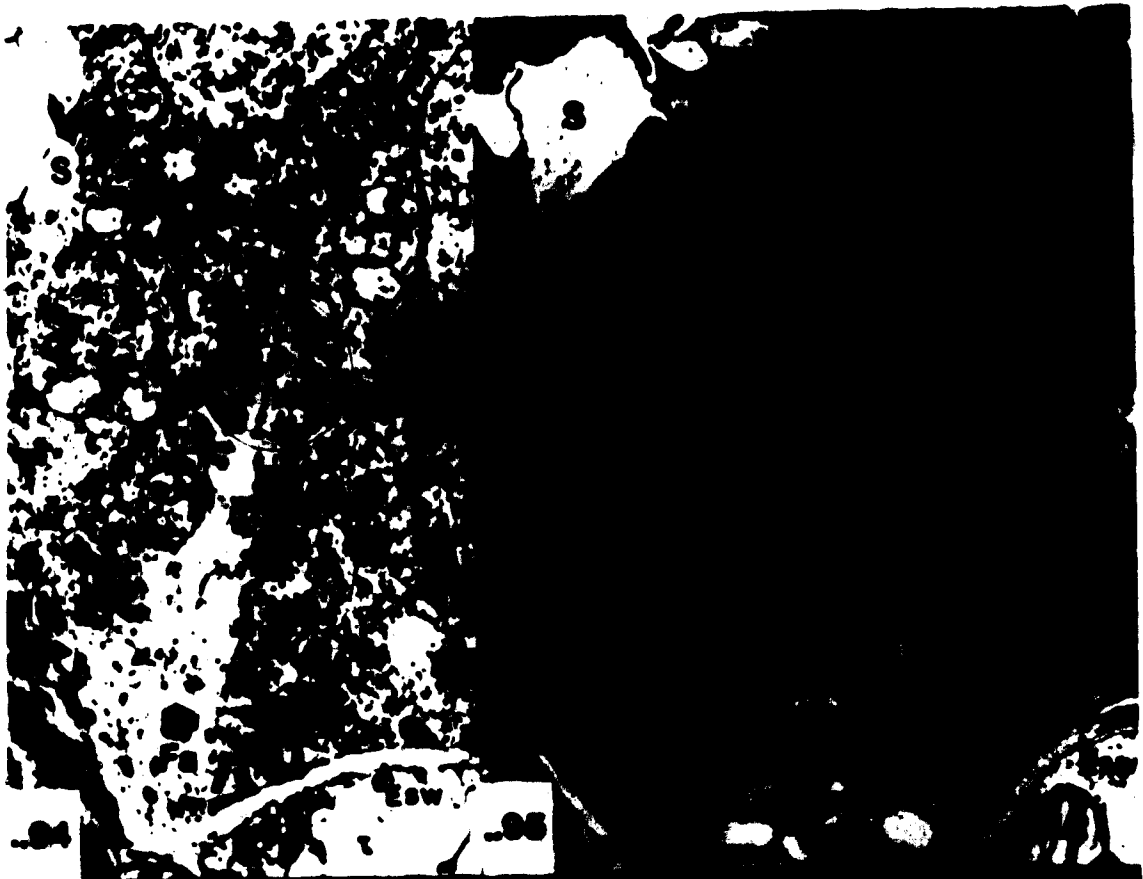
**Fig. 94.** Continues series begun in Fig. 90. Young filiform apparatus in soybean. E.M. x9,040.

**Fig. 95.** A filiform apparatus in a mature embryo sac. E.M. x6,600.

**Fig. 96.** Section showing restricted nature of filiform apparatus attachment to the synergid common wall in soybean. E.M. x17,600.

**Fig. 97.** Calcofluor staining indicates that cellulose is present in the filiform apparatus at the base of the synergid's common wall and egg apparatus walls (arrow heads). x980.

**Key to Abbreviations:** Esw, embryo sac wall; Fa, filiform apparatus; M, mitochondria; N, nucleus; P, plasmodesmata; S, synergid.



Cross sections of the soybean filiform apparatus.

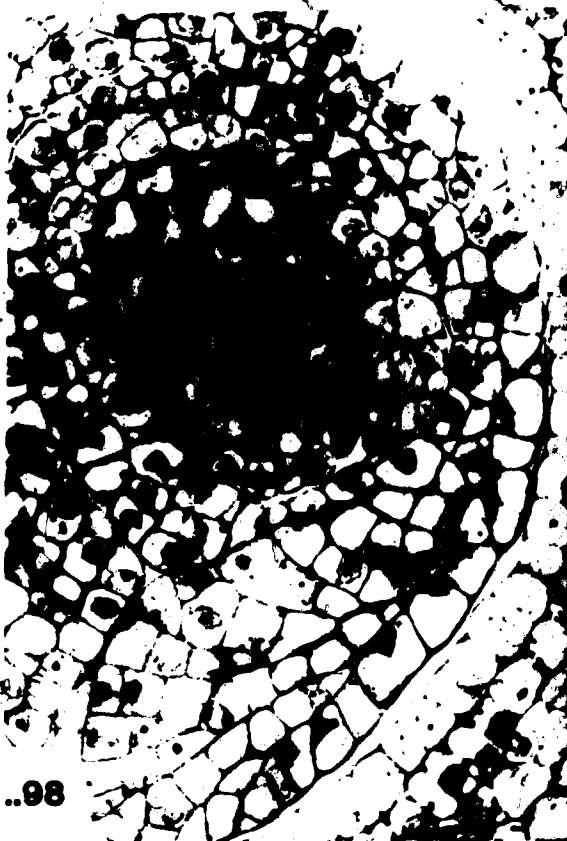
Fig. 98. Base of egg apparatus showing location of the filiform apparatus in the embryo sac. L.M. x625.

Fig. 99. Same section as Fig. 98 after staining with Calcofluor White. The section shows the relationship of the egg apparatus cells with the embryo sac wall. x980.

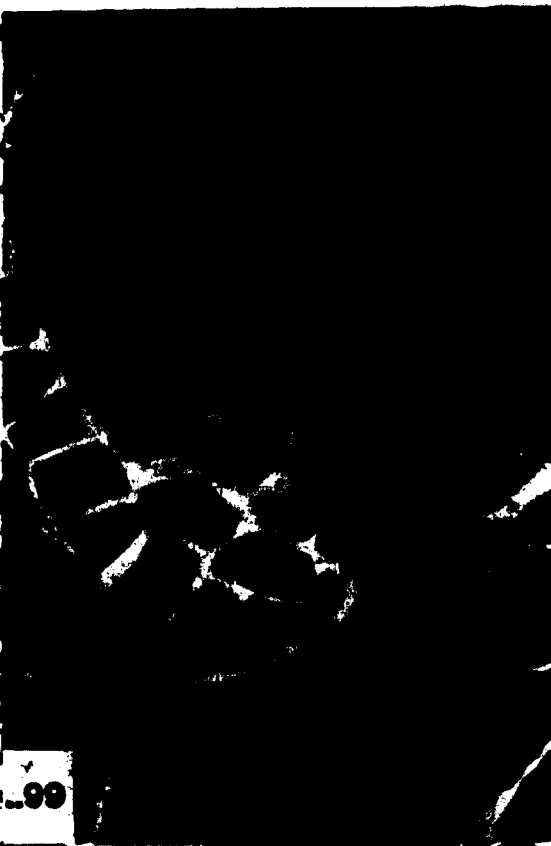
Fig. 100. Section chalazal to that in Fig. 98. L.M. x625.

Fig. 101. Same section as in Fig. 100 after staining with Calcofluor White showing the relationship of egg apparatus cells with the embryo sac wall. x980.

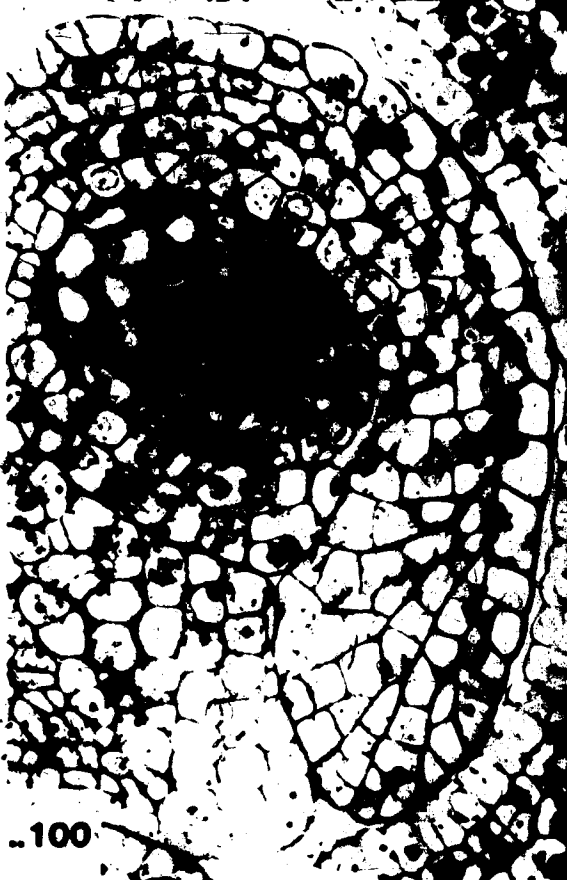
Key to Abbreviations: Cc, central cell; E, egg; Esw, embryo sac wall; S, synergid.



..98



..99



..100



..101

Egg apparatus cells after expansion.

Fig. 102. Synergids after expansion. Angle between synergid top wall (arrows) and embryo sac wall is approximately 15°. E.M. x8,400.

Fig. 103. Mature egg and synergid. E.M. x6,600.

Fig. 104. Egg cytoplasm containing amyloplasts. E.M. x20,800.

Fig. 105. Synergid cytoplasm containing a network of RER. E.M. x20,800.

Key to Abbreviations: A, amyloplast; Cc, central cell; E, egg; Esw, embryo sac wall; G, golgi body; Ma, multigrain amyloplast; N, nucleus; Rer, rough endoplasmic reticulum; V, vacuole; Wi, wall ingrowth.



lipoid bodies are distributed throughout the cytoplasm and Golgi bodies tend to occur near the walls (Figs. 103 - 105). The egg is distinguished by the chalazal position of its nucleus with respect to its major vacuole (Fig. 103) and by the possession of amyloplasts (Fig. 104). In contrast the synergids appear to lack amyloplasts and contain networks of rough endoplasmic reticulum (RER), a chalazal vacuole, and micropylar nuclei (Figs. 102, 103 & 105).

After cellularization a large part of the wall initially enclosing each of the egg apparatus cells is made up of embryo sac wall (Figs. 63 & 64). As egg and synergid cells expand into the central cell the total amount of wall that encloses these cells increases. This results in a decrease in the relative percentage of embryo sac wall that encloses each of the egg apparatus cells. In a mature embryo sac, a series of cross sections progressing from the micropylar base to the chalazal terminus shows the cellular arrangement along with the extent of attachment to the embryo sac wall. These sections show that a synergid is the first cell to begin to lose contact with the embryo sac wall (Fig. 99). Further from the embryo sac's micropylar base this synergid becomes completely separate from the embryo sac wall and a portion of the lateral wall of the egg is also free (Fig. 101). More chalazally the other synergid starts to separate from the embryo sac wall as well (Fig. 106). About midway up the synergids, in the region of their nuclei, both cells are free and only a portion of the egg is still fused to the embryo sac wall (Fig. 107). Chalazal to the synergid nuclei all of the cells are free from the embryo sac wall (Fig. 108). Ultimately both synergids disappear and only the egg cell profile remains (Fig. 109).

Inspection of egg apparatus cells after expansion reveals plasmodesmata in the wall between synergid cells chalazal to the filiform apparatus (Figs. 94 & 95) and in the walls between the egg and synergid cells (Figs. 110 & 111). Plasmodesmata also occur in the wall between synergids and central cell in the region of the synergid hook (Figs. 102 & 103) and in the area of the egg hook in the wall common to the egg and central cell (Fig. 111). However, no plasmodesmata were found in the embryo sac wall between the egg apparatus cells and nucellus.

Cross section of egg apparatus cells showing relationship of cells with the embryo sac wall.

Fig. 106. Synergid free from the embryo sac wall while the other synergid and egg cell are still fused with the embryo sac wall. Note distribution of wall ingrowths in the central cell near the egg apparatus cells. E.M. x3,440.

Fig. 107. Section more chalazal to that in Fig. 106. The egg is the only cell still attached to the embryo sac wall (arrows). E.M. x7,800.

Fig. 108. All egg apparatus cells are now free from the embryo sac wall. Note distribution of central cell wall ingrowths near the egg and one of the synergids. E.M. x3,440.

Fig. 109. Section chalazal to that in Fig. 108, showing only profile of the egg cell. E.M. x2,000.

Key to Abbreviations: Cc, central cell; E, egg; Esw, embryo sac wall; Ma, multigrain amyloplast; P, plasmodesmata; S, synergid; V, vacuole; Wi, wall ingrowth.





The egg apparatus and central cell in soybean.

Fig. 110. Plasmodesmata (arrows) in the wall between egg and synergid cells. B.M. x31,200.

Fig. 111. Plasmodesmata (arrows) in the walls between the egg and synergid and the synergid and central cell. E.M. x14,000.

Fig. 112. Micropylar polar nucleus. E.M. x11,200.

Fig. 113. Area of small wall ingrowths (arrows) near the micropylar polar nucleus. E.M. x33,200.

Key to Abbreviations: Cc, central cell; E, egg; Mpn, micropylar polar nucleus; S, synergid.



### Developmental changes of the central cell:

After embryo sac cellularization the central cell undergoes various developmental changes before fertilization. It has been shown that the major characteristic of the mature soybean central cell includes the presence of many multigrain amyloplasts (starch packets), a pair of nuclei whose membranes are partially fused and an area of wall ingrowths that occurs at the cell's micropylar base (Folsom & Peterson, 1984).

The central cell throughout its development is delimited by embryo sac wall, the top wall of the egg apparatus (Fig. 61) and for a certain length of time the antipodals' chalazal walls (Figs. 69 - 71). Initially polar nuclei are located at the micropylar (Figs. 67 & 68) and chalazal ends (Fig. 70) of the young central cell. The remainder of the cell is filled with a large vacuole, a remnant of the one present in the 4-nucleate embryo sac. Cytoplasm is mainly associated with the nuclei at both ends and to a lesser extent along the lateral walls of the cell. The first sign of wall-ingrowth formation occurs in the micropylar base of the central cell near one of the polar nuclei (Figs. 112 & 113). Wall ingrowths were not observed on the other side of the same embryo sac (Fig. 114).

The young central cell amyloplasts are initially found near wall ingrowths (Fig. 115). Mitochondria and protein bodies are also found in the cytoplasm (Figs. 114 & 116). The few small vacuoles in the cytoplasm at this time appear to be restricted to areas near the polar nuclei (Figs. 70 & 116). The vacuole in the central cell is like that of the late 4-nucleate embryo sac since it contains many membranous inclusions which appear to form a subdividing network (Fig. 117). Myelin-like and osmiophilic bodies are often seen along the periphery of the vacuole (Figs. 118 - 120). Dark osmiophilic bodies seem to expand and to have some developmental association with the myelin-like bodies (Figs. 118 & 119).

Initially there is only a thin layer of cytoplasm along lateral walls of the central cell and a large central vacuole (Fig. 117). As the central cell begins to fill in (Fig. 119) the vacuole appears to be segmented by the movement of cytoplasm along lines previously established by membranous inclusions within the vacuole (Figs. 117 & 120). As a result, the small vacuoles initially found along the lateral walls of the cell are now found throughout.

Central cell of soybean.

Fig. 114. Micropylar base of the central cell opposite the side that contains the micropylar polar nucleus. Note the absence of wall ingrowths on the embryo sac wall. E.M. x17,600.

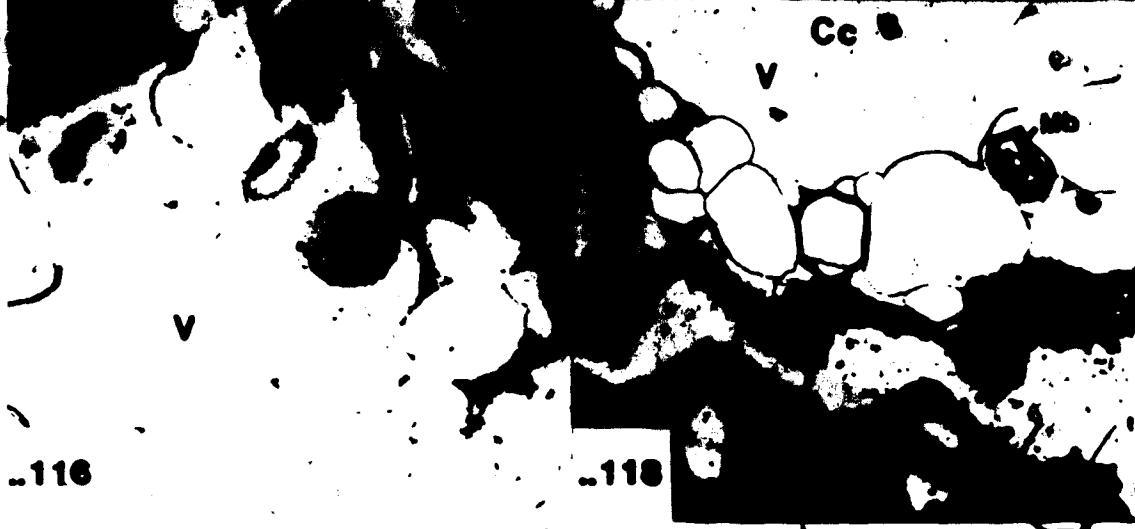
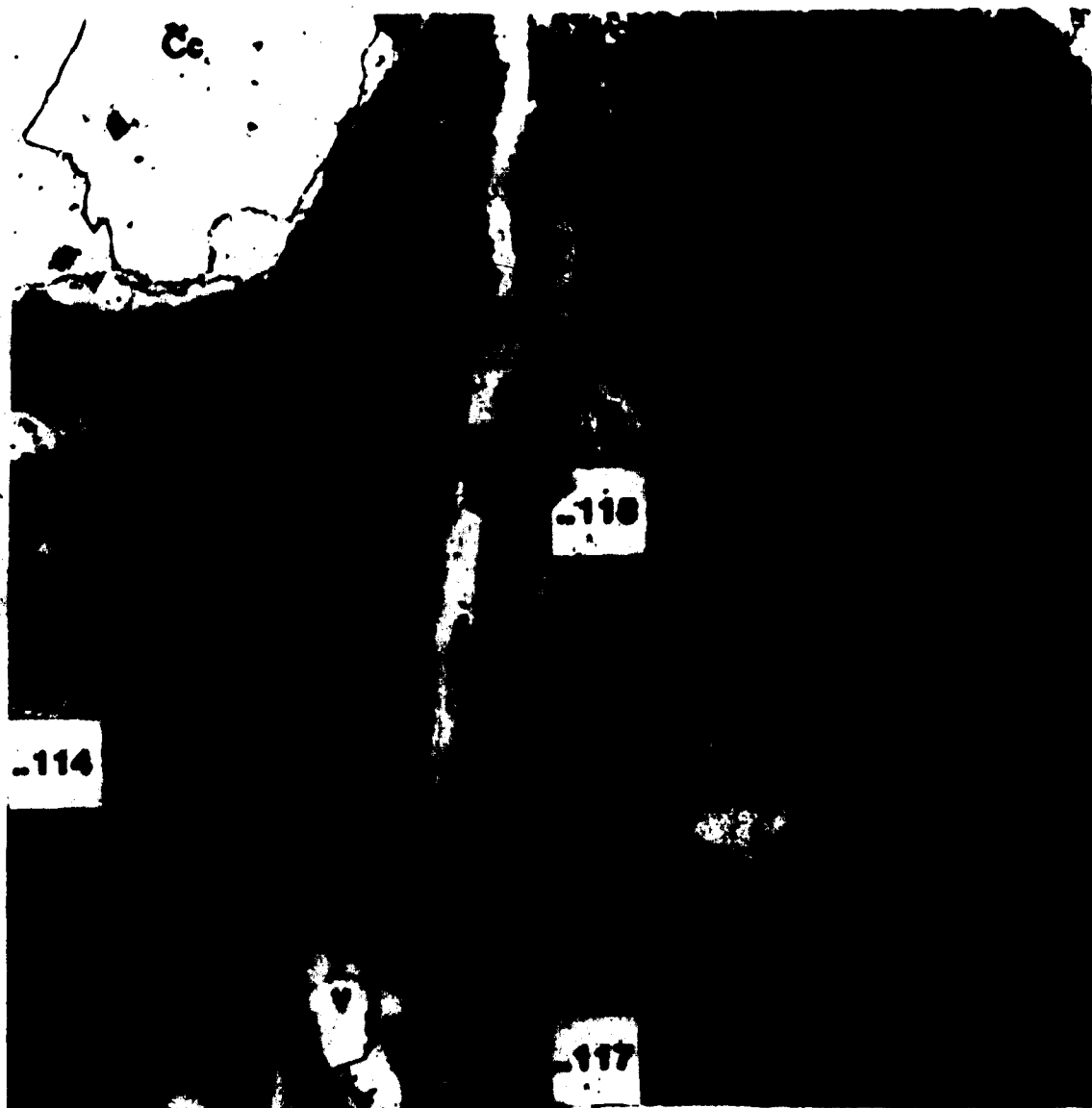
Fig. 115. A plastid containing a few small starch grains near the area of young wall ingrowths. E.M. x58,800.

Fig. 116. Vacuoles in cytoplasm at chalazal end of the central cell. E.M. x14,000.

Fig. 117. Central cell vacuole with membraneous inclusions after cellularization. E.M. x3,600.

Fig. 118. Myelin-like bodies associated with the central cell vacuole. E.M. x20,000.

Key to Abbreviations: A, amyloplast; Cc, central cell; Cpn, chalazal-polar nucleus; Ea, egg apparatus cell; Esw, embryo sac wall; Mb, myelin-like body; Pb, protein body; V, vacuole.



Central cell of soybean during the filling in phase.

Fig. 119. Development of several multigrain amyloplasts in the young central cell and occurrence of osmiophilic bodies associated with the vacuole. E.M. x8,400.

Fig. 120. Movement of cytoplasm into space previously occupied by the vacuole along lines established by membraneous inclusions (arrows). E.M. x11,200.

Fig. 121. Late stage of central cell filling in process. Note thin area of cytoplasm between the vacuoles (arrows). E.M. x20,800.

Fig. 122. The polar nuclei become associated while the central cell is still quite vacuolate. E.M. x4,400.

Key to Abbreviations: A, amyloplast; Cc, central cell; Ea, egg apparatus cell; Ma, multigrain amyloplast; Ob, osmiophilic body; Pb, protein body; V, vacuole.



-110

-120

-121

-122



During early developmental stages in the central cell protein bodies are often seen fusing with parts of the vacuome (Figs. 116 & 121).

As the central cell starts to fill in and vacuole fragment, the chalazal polar nucleus moves in a micropylar direction while the micropylar polar nucleus moves chalazally (Fig. 122). The two nuclei appear to start fusing soon after they become paired and are located near the chalazal end of the egg apparatus (Figs. 123 & 124). Once paired the polar nuclei retain this central position (Figs. 125 & 126).

Besides presence of polar nuclei, other major features of the central cell are the area of wall ingrowths in the cell's micropylar base (Figs. 79, 102, 106 & 108) and multigrain amyloplasts that occur throughout the cell (Fig. 127). Central cell wall ingrowths are not evenly distributed around the circumference of the cell's micropylar base but tend to occur on areas of the embryo sac wall closely associated with the egg apparatus cells (Figs. 106 & 108). Multigrain amyloplasts are shown to consist of grains containing insoluble carbohydrate by both the Thiéry (Fig. 128) and PAS test (Fig. 129). Central cell amyloplasts differentiate after cellularization but before fusion of the polar nuclei. They are initially found as plastids containing a few small starch grains (Figs. 115 & 127) but ultimately expand to the point where the plastid membrane is difficult to discern (Fig. 130).

At the developmental stage when vacuolar contraction ends and expansion begins the central cell cytoplasm contains a large amount of dilated RER. Some of this RER can be seen terminating in areas of smooth vesicular ER (Fig. 131). Concomitant with vacuolar expansion is the fusion of vacuoles to multigrain amyloplasts (Fig. 132). Initially these vacuoles can be seen throughout the cytoplasm fusing not only with multigrain amyloplasts but also with protein bodies (Fig. 133). Many small vacuoles attach to each starch packet ultimately fusing with one another establishing a continuous network throughout the central cell (Fig. 134). This network of vacuoles often contains flocculent material (Fig. 134). Staining with Coomassie Brilliant Blue shows that areas around the multigrain amyloplasts contain protein (Fig. 135).

Central cell of soybean.

Fig. 123. Polar nuclei located near the chalazal end of the egg apparatus. E.M. x5,720.

Fig. 124. Fused membranes of polar nuclei in Fig. 123 (arrow). E.M. x29,200.

Fig. 125. Nearly filled in central cell. Note majority of vacuoles remaining are located in the cell's chalazal end. E.M. x3,440.

Fig. 126. Completely filled in central cell. E.M. x2,700.

Key to Abbreviations: A, antipodals; Ma, multigrain amyloplast; Pb, protein body; Pn, polar nuclei; Pnm, polar nuclear membrane; S, synergid; V, vacuole.



Multigrain amyloplast in the soybean central cell.

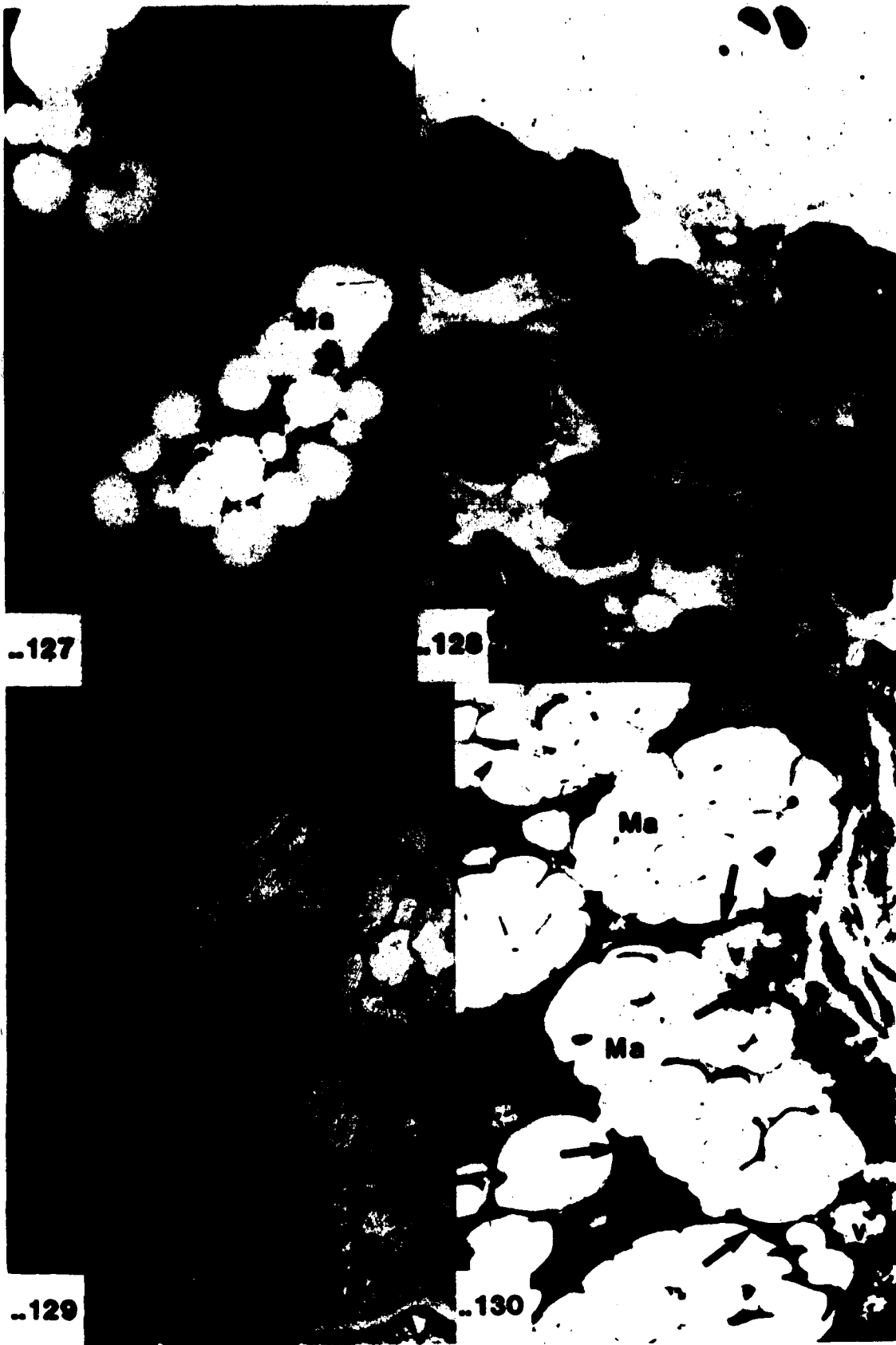
Fig. 127. A young multigrained amyloplast showing its plastid membrane (arrows).  
E.M. x29,200.

Fig. 128. Section stained by the Thiéry procedure showing insoluble polysaccharides.  
E.M. x9,040.

Fig. 129. PAS stained section shows extent of multigrain amyloplasts in the central cell. L.M. x660.

Fig. 130. Expanded multigrain amyloplast with the plastid membrane still evident in certain areas (arrows). E.M. x9,200.

Key to Abbreviations: Cc, central cell; Ma, multigrain amyloplast; Pb, protein body;  
V, vacuole.



**Soybean central cell cytoplasm and multigrain amyloplast.**

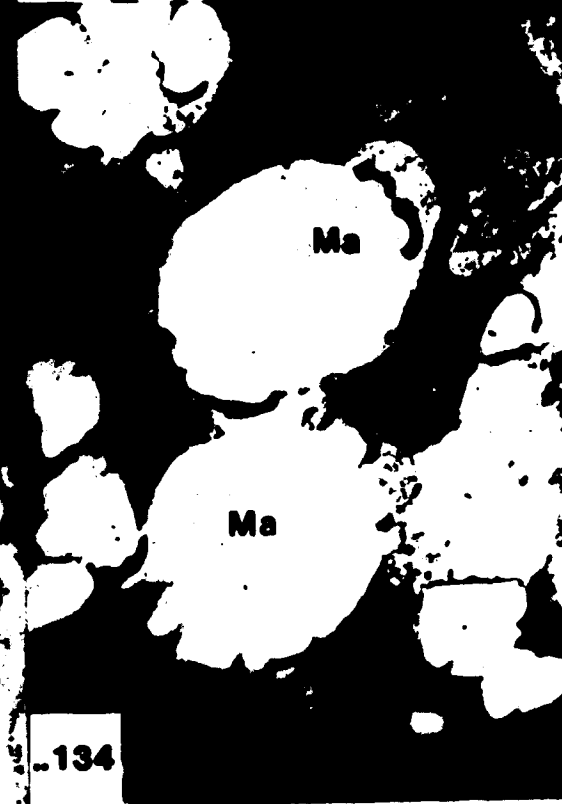
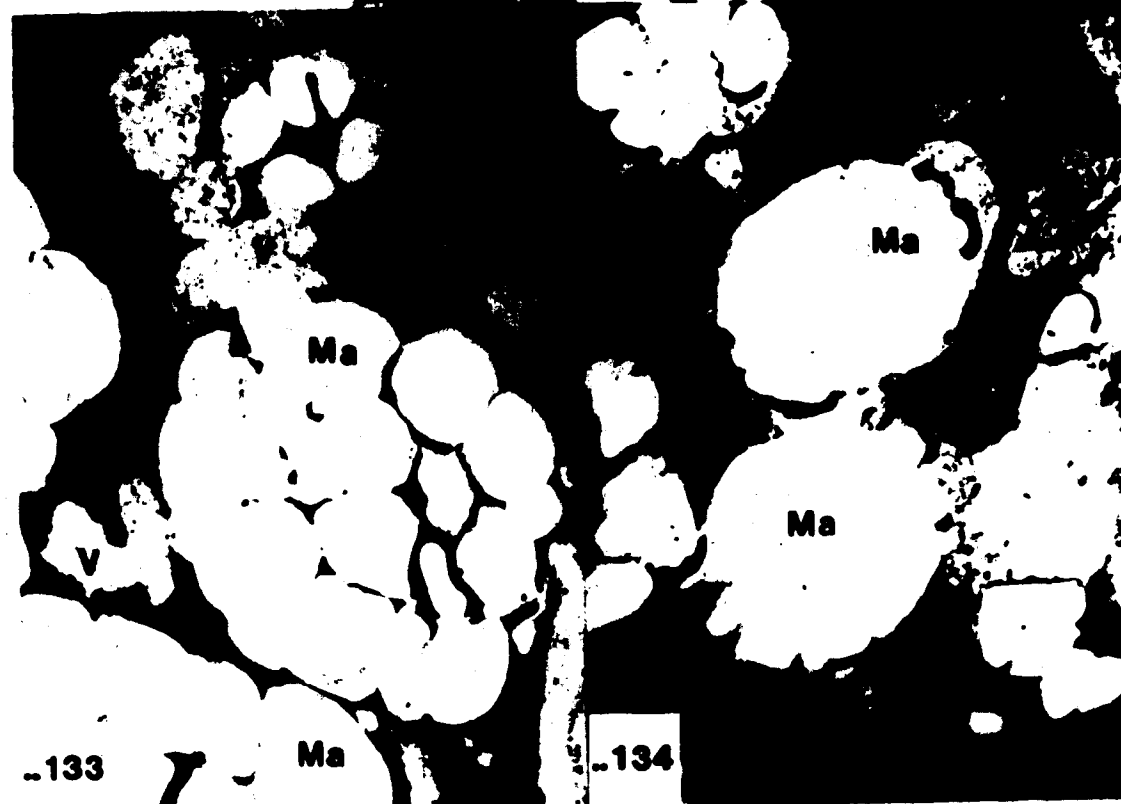
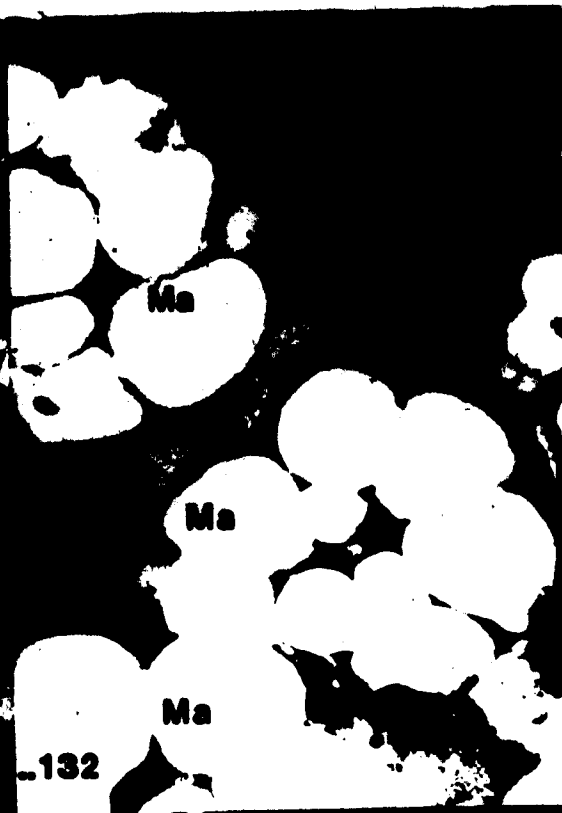
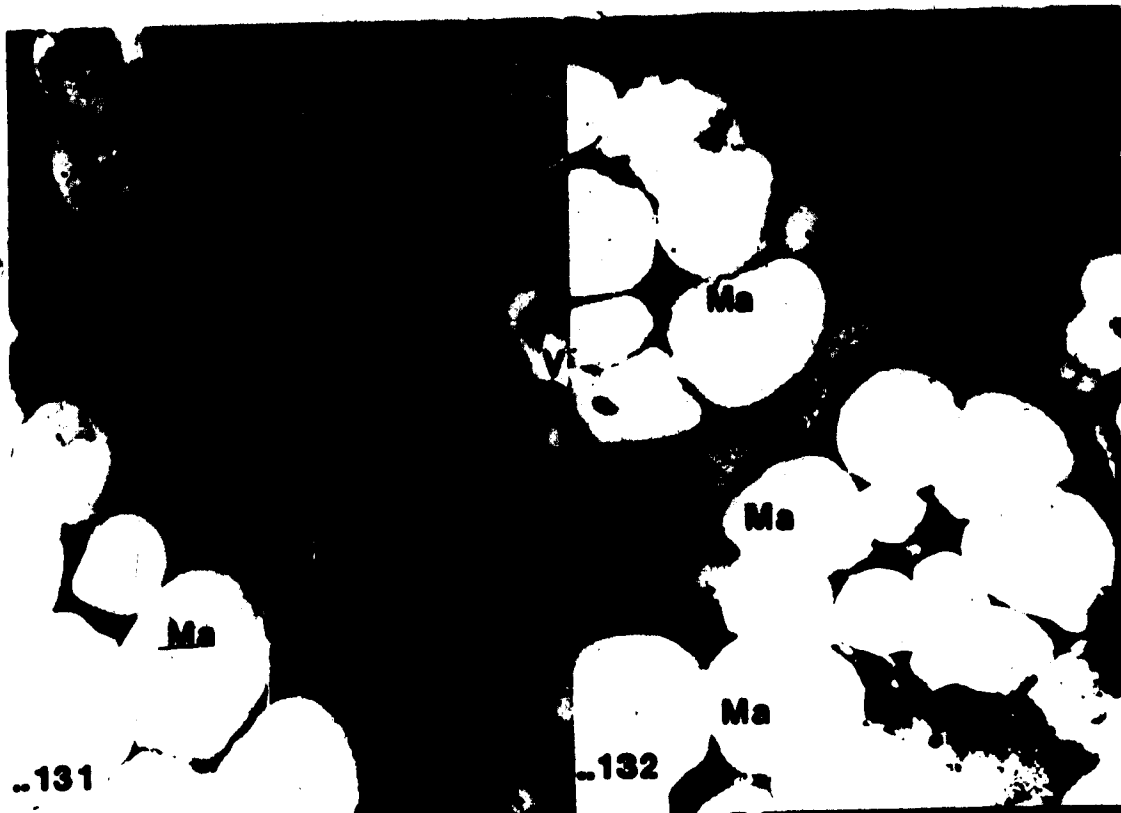
**Fig. 131. Cytoplasm showing ER (arrow) and dilated rough endoplasmic reticulum. E.M. x22,720.**

**Fig. 132. Vesicular golgi body in central cell cytoplasm. E.M. x26,000.**

**Fig. 133. Vacuole fusing with both multigrain amyloplasts and protein bodies. E.M. x15,200.**

**Fig. 134. Vacuoles fusing to form a network through the soybean central cell. E.M. x9,200.**

**Key to Abbreviations: G, golgi body; Ma, multigrain amyloplast; Pb, protein body; Rer, rough endoplasmic reticulum; V, vacuole.**



Soybean central cell and antipodal apparatus.

Fig. 135. Coomassie Brilliant Blue staining shows protein deposition around multigrain amyloplasts in the central cell (arrows). L.M. x710.

Fig. 136. Young antipodal apparatus showing all 3 cells. Two of the cells are chalazal to the third. E.M. x5,200.

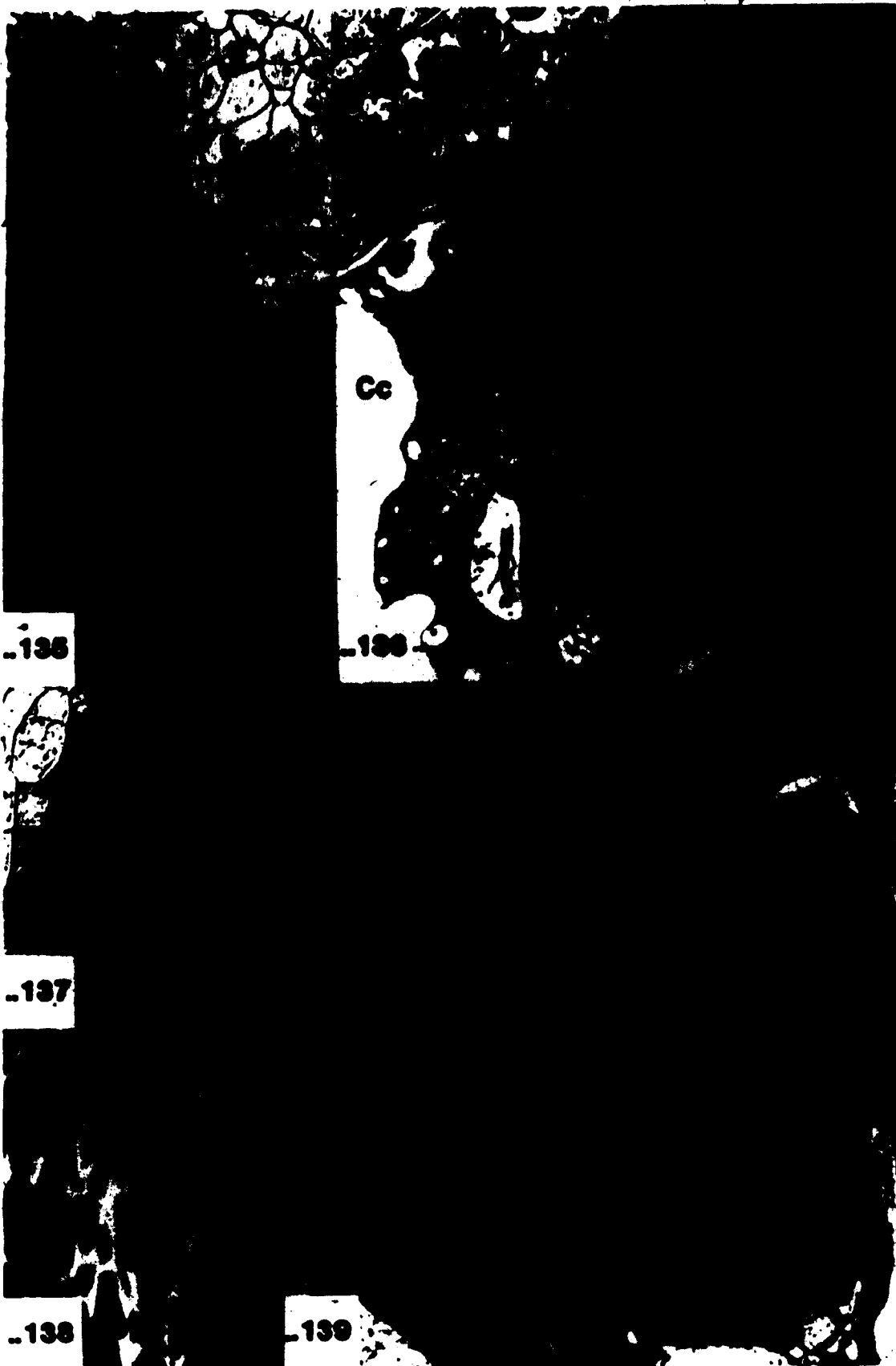
Fig. 137. Oblique section showing an antipodal apparatus cell wall (arrows). Nomarski. L.M. x870.

Fig. 138. Section in Fig. 137 stained with Calcofluor White showing presence of cellulose in the antipodal apparatus wall (arrow). L.M. x870.

Fig. 139. Antipodal apparatus with the third cell chalazal to the other 2. Note presence of plasmodesmata in the embryo sac wall and all walls common to the antipodals and central cell. E.M. x8,250.

Key to Abbreviations: A, antipodal cell; Cc, central cell; M, mitochondria; N, nucleus; P, plasmodesmata; Pl, plastid; V, vacuole.





Cc

-135

-136

-137

-138

-139

### The antipodals:

In soybean the 3 antipodal cells are ephemeral. They form as a result of cellularization and disappear well before fertilization. The arrangement of these cells reflects both position of chalazal nuclei and shape of the late 4-nucleate embryo sac (Fig. 47). The antipodals are organized into 2 tiers with the micropylar layer usually consisting of 2 cells and the chalazal one being 1-celled (Figs. 69 - 71). However this configuration does not appear to be fixed since the opposite type of arrangement can often be seen (Fig. 136). Staining of an oblique section of the antipodals with Calcofluor White shows fluorescence of a wall which separates these cells (Figs. 137 & 138). Plasmodesmata, also occur in the embryo sac wall connecting antipodal cells to inner nucellar cells, in the common walls of antipodals and in walls separating the antipodals from the central cell (Fig. 139). Walls of the young antipodal cells, like those of the egg apparatus, do not appear to contain a middle lamella (Figs. 69 & 70). However, later in development the antipodal walls appear to form a more electron dense area which may be a middle lamella (Fig. 139). The cytoplasm of antipodal cells consists of a prominent nucleus, strands of RER, mitochondria, undifferentiated plastids, and vacuoles (Figs. 136 & 139).

### The embryo sac after pollen tube discharge:

After pollen tube penetration of the embryo sac, discharge into a synergid, and sperm target cell syngamy many changes are evident in the soybean embryo sac. The egg containing a sperm nucleus has a dense cytoplasm filled with an elevated number of amyloplasts, a large basal vacuole and is covered on its chalazal end with a discontinuous layer of osmiophilic material (Figs. 140 & 141). The rest of the egg apparatus contains one persistent and one degenerate synergid (Figs. 141 & 142). The darkly staining degenerate synergid has walls that are structurally abnormal, lacking the nucleus and large vacuole present in earlier developmental stages (Figs. 141 - 143). The only recognizable features of the degenerate synergid are the filiform apparatus in its micropylar base (Fig. 142). The pollen tube has

**Egg apparatus of soybean at the approximate time of fertilization.**

**Fig. 140. Egg cell showing breakup of the micropylar vacuole. E.M. x2,080.**

**Fig. 141. Egg apparatus with persistent and degenerate synergids and egg cell containing a sperm nucleus. Note the presence of an osmophilic layer enclosing the egg cell that is continuous with the degenerate synergid and the breakup of the persistent synergid's chalazal vacuole. E.M. x4,400.**

**Fig. 142. Scattered small vacuoles in the egg and persistent synergid cytoplasm. E.M. x2,080.**

**Fig. 143. Wall separating the egg from persistent and degenerate synergids (arrows). Note degenerate nature of the wall between the degenerate synergid and egg cell when compared to that between the persistent synergid and egg. E.M. x17,600.**

**Key to Abbreviations: Cc, central cell; Ds, degenerate synergid; E, egg; Fa, filiform apparatus; N, nucleus; Ps, persistent synergid; S, sperm nucleus; V, vacuole; Wi, wall ingrowth.**

-140

V

-141

E

-142

-143

**Pollen tube in the embryo sac.**

- Fig. 144.** Route of pollen tube into a synergid. E.M. x14,000.  
**Fig. 145.** Terminal pore of the pollen tube (arrow). E.M. x17,600.  
**Fig. 146.** Egg and polar nucleus before sperm nucleus fusion. L.M. x625.  
**Fig. 147.** Sperm nucleus in central cell cytoplasm. E.M. x2,080.  
**Fig. 148.** Lobe of the polar nucleus containing a small nucleolus. E.M. x11,200.

**Key to Abbreviations:** Ds, degenerate synergid; E, egg; Es, embryo sac wall; Fa, filiform apparatus; N, nucleoli; Pn, polar nuclei; Ps, persistent synergid; Pt, pollen tube; Pv, pollen tube vesicle; S, sperm nucleus; Scw, synergid common wall.



grown up through the center of the wall separating the synergids and bent immediately adjacent and chalazal to the filiform apparatus to enter the cell (Fig. 144). Once inside the cell the pollen tube is contorted in various directions before ending in a terminal pore (Fig. 145). The region of degenerate synergid immediately adjacent to the pore contains the pollen tube discharge and has a somewhat lighter density than the rest of the cell. This discharge contains many polysaccharide vesicles. These vesicles are also found in the pollen tube and its terminal pore (Fig. 145). The persistent synergid also shows changes in structure from that found previously. The large chalazal vacuole has begun to fragment (Fig. 141) and many smaller vacuoles occur throughout the synergid cytoplasm (Fig. 142). Also, Golgi activity has increased and a polarity appears to have developed in the distribution of organelles with the smaller vacuoles and Golgi bodies located in the micropylar two-thirds of the cell (Figs. 141 & 142). The central cell still contains many multigrain amyloplasts along with the fused polar nuclei and a sperm nucleus (Figs. 146 & 147). The polar nucleus is lobed with several "arms" extending between the starch packets and contains a number of nucleoli (Figs. 146 - 148).

When serial sections of the soybean egg apparatus are examined the layer of darkly staining material that covers the egg can be seen connected to the degenerate synergid (Figs. 141 & 142). This layer develops between the plasmalemmae of the egg and central cell and extends over the chalazal end of the egg terminating near the persistent synergid (Figs. 141 & 142). It is composed of osmiophilic material that appears to have been extruded from the degenerate synergid and is interrupted by clear areas (Figs. 149 & 150). Vacuoles containing an electron dense flocculent material were seen fused with the plasmalemma in both the egg and central cells. Such fusion occurred only in the area where the degenerate synergid cytoplasm had separated the plasma membranes of the egg and central cells (Figs. 149 & 150). The remainder of the egg cell wall is fairly continuous interspersed with occasional regions of membrane contact (Fig. 151). The proportion of wall to membrane area in the egg is higher now than during earlier developmental stages (compare Figs. 83 & 151).

The wall previously found around the degenerate synergid has also undergone massive changes in structure. When this wall is compared to the wall of the persistent synergid that of

The egg cell wall.

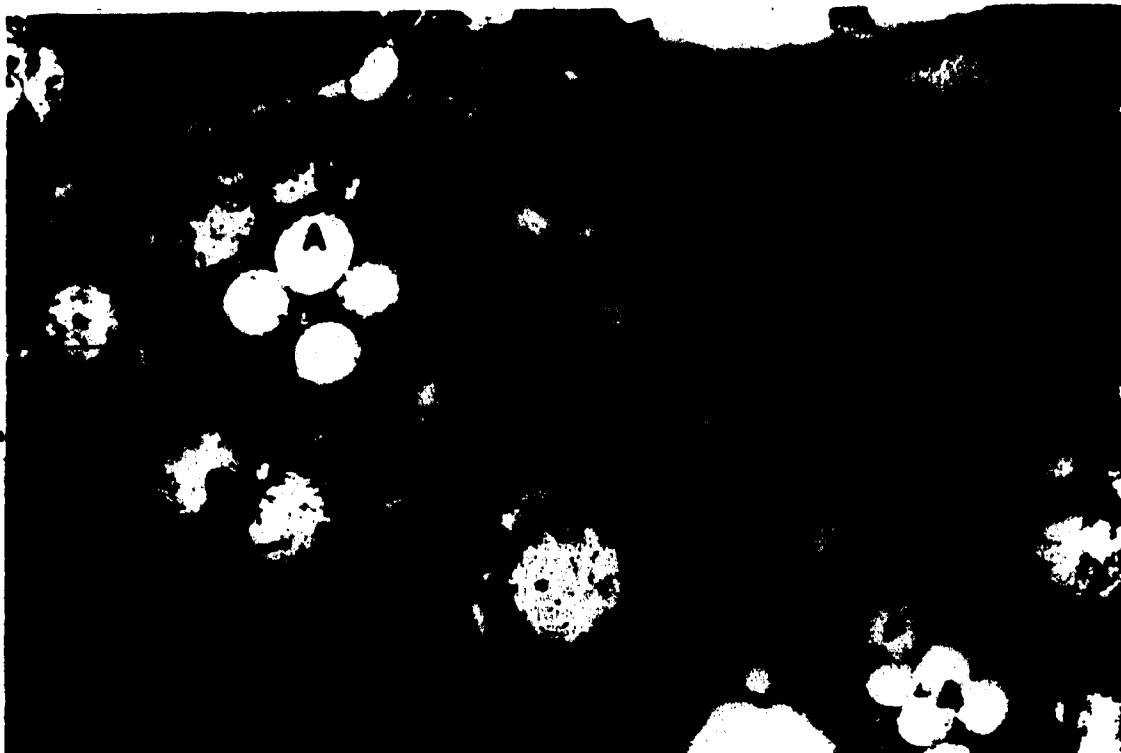
Fig. 149. Plasmalemma of egg and central cell (arrows) separated by osmiophilic material assumed to be from the degenerate synergid. Note vacuoles fused with the central cell plasmalemma (asterisk). E.M. x16,800.

Fig. 150. Plasmalemma of egg and central cell (arrows) separated by osmiophilic material. Same tissue and area as in Fig. 199 but shows vesicle fused with egg cell plasmalemma (asterisk). E.M. x14,000.

Fig. 151. Part of wall enclosing the egg toward the persistent synergid. Note continuous nature of the wall (arrows). E.M. x14,000.

Key to Abbreviations: A, amyloplast; Cc, central cell; E, egg; N, nucleus; Om, osmiophilic material; Pb, protein body; V, vacuole.





-149



-150


-151

the degenerate synergid appears broken down (Fig. 143). Examination of these two cells shows that an intact plasma membrane lines the wall of the persistent synergid while in the degenerate synergid no plasmalemma could be found (Fig. 143).

#### Early embryogenesis:

As fusion of egg and sperm nuclei occurs and development proceeds the large vacuole previously found in the egg breaks down to an assemblage of smaller vacuoles (Fig. 152). Besides these small vacuoles the zygote cytoplasm also contains multigrain amyloplasts, protein bodies, mitochondria and strands of RER (Fig. 153). The process of zygotic shrinkage results in a decrease in the cell's length by approximately 38%. The wall that encloses the zygote is now much more developed, lacks a middle lamella and in some areas appears continuous without any areas of membrane contact (Figs. 152 & 153). Division of the zygote results in a 2-celled proembryo. The newly formed cell wall is perpendicular to the long axis of the embryo (Figs. 154 & 155), possesses a middle lamella and plasmodesmata along its entire length (Fig. 156). Both the terminal and basal cell of the embryo contain amyloplasts, protein bodies, mitochondria, strands of RER and vacuoles (Figs. 155 & 156). The main difference in the two cells is the higher level of vacuolation in the basal versus the terminal cell (Fig. 155).

The wall that separates terminal and basal cells of the proembryo from the central cell is continuous showing a distinct middle lamella and plasmodesmata (Figs. 157 - 159). Distribution of plasmodesmata is not uniform, the few present between the basal and central cells are found near remains of the persistent synergid (Fig. 157). Plasmodesmata are occasionally seen in the chalazal region of the wall between terminal and central cells (Fig. 159). At this developmental stage remnants of both synergids can still be seen (Figs. 154, 155, 157, 158 & 160). Remains of the two synergids differ, with that of the degenerate being osmiophilic (Fig. 158) and that of the persistent synergid being represented by a translucent area containing electron dense dots (Figs. 157 & 160).



Zygote and 2-celled embryo of soybean.

Fig. 152. Zygote after shrinkage. E.M. x2,800.

Fig. 153. Amyloplasts in the zygote. E.M. x15,200.

Fig. 154. A 2-celled proembryo showing terminal, basal cells and also a degenerate synergid cell. The central cell is highly vacuolate with scattered multigrain amyloplasts along its lateral walls and patches of free nuclear endosperm. Arrows indicate micropylar extent of nucellus. L.M. x550.

Key to Abbreviations: A, amyloplast; Bc, basal cell; Cc, central cell; Cr, chalazal region of the central cell; Ds, degenerate synergid; Esw, embryo sac wall; F, free nuclear endosperm; Ii, inner integument; Ma, multigrain amyloplast; N, nucellus; Pb, protein body; Tc, terminal cell; V, vacuole; Wi, wall ingrowth; Z, zygote.



Two-celled embryo in soybean.

Fig. 155. Two-celled embryo in soybean showing a basal cell that is more vacuolate than the terminal cell. E.M. x2,080.

Fig. 156. Wall separating the 2 cells of the embryo. Note presence of plasmodesmata along its length (arrows). E.M. x6,600.

Fig. 157. Plasmodesmata in the wall between basal and central cells near remains of the persistent synergid. E.M. x8,320.

Fig. 158. Osmiophilic remains of the degenerate synergid in the wall between basal and central cells and also enclosed in a projection of the degenerate synergid wall into the basal cell (arrow). E.M. x6,600.

Key to Abbreviations: A, amyloplast; Bc, basal cell; Cc, central cell; F, free nuclear endosperm nucleus; M, mitochondria; N, nucellus; P, plasmodesmata; Pb, protein body; Ps, persistent synergid; Tc, terminal cell; Wi, wall ingrowth.

Cc



**Soybean embryo sac after fertilization.**

**Fig. 159.** Plasmodesmata in the wall between the central and terminal cells (arrow). E.M. x24,500.

**Fig. 160.** Translucent remains of the persistent synergid. E.M. x8,400.

**Fig. 161.** Central cell after fertilization. Note presence of the large micropylar vacuole. Nomarski. L.M. x750.

**Fig. 162.** Break-up of multigrain amyloplast in the central cell after fertilization. E.M. x4,000.

**Key to Abbreviations:** Bc, basal cell; Cc, central cell; Ma, multigrain amyloplast; Pn, polar nucleus; Ps, persistent synergid; Tc, terminal cell; V, vacuole; Wi, wall ingrowth.



Cc

Tc

-159

-160

V

PN

-161

-162



After fertilization the large central cell is filled with multigrain amyloplasts and contains the 1<sup>st</sup> endosperm nucleus (Fig. 161). The process of vacuolar fusion and multigrain amyloplast breakdown into individual grains which began well before fertilization continues (Fig. 162). Not all multigrain amyloplasts are completely destroyed, however, and some line the embryo sac wall during early stages of embryogenesis (Fig. 154). The 1<sup>st</sup> endosperm nucleus undergoes a series of mitoses resulting in a number of free nuclei that are found near the young embryo and along the lateral walls of the embryo sac (Figs. 154 & 155).

#### Development of transfer cells in the ovule after fertilization:

Before division of the zygote to form a 2-celled embryo the nucellus that surrounds the embryo sac comprises two distinct zones (Figs. 163 - 165). The first zone consists of cells containing a large vacuole and occurs both in the chalazal region of the nucellus and surrounding the lateral walls of the embryo sac. This is the larger of the two regions and constitutes almost all of the nucellus except for a few cells found in the second zone that surround the micropylar end of the embryo sac (Fig. 163). The cells which are found in the second zone have much smaller vacuoles and are more cytoplasmic (Figs. 164 & 165). Some of these nucellar cells along the lateral walls of the embryo sac can be classified as transfer cells since they contain wall ingrowths. Such ingrowths occur predominately on their tangential walls (Figs. 163 - 165). Other characteristics of these transfer cells is that they may contain many single or multigrain amyloplasts (Fig. 165) and are connected by plasmodesmata to the more vacuolate nucellar cells (Figs. 164 & 165). The symplast that terminates in these transfer cells extends through the nucellus as plasmodesmata are also seen in common walls of vacuolate nucellar cells (Figs. 164 & 165). However, this symplast does not reach the embryo sac as no plasmodesmata were seen in the embryo sac wall after the destruction of the antipodal cells. Examination of multiple sections from the same ovule reveals that the development of wall ingrowths is sporadic and that not all nucellar cells in the region possess them. These nucellar transfer cells develop shortly after fertilization and persist

Transfer cell development in the soybean embryo sac after fertilization.

Fig. 163. Nomarski micrograph of a zygote showing two different regions of the nucellus, the vacuolate and more cytoplasmic nucellar cells some of which are transfer cells. Central cell is filled with multigrain amyloplasts and an area of wall ingrowths (arrows) is visible in the micropylar end of this cell. x980.

Fig. 164. Wall ingrowths (arrows) in cytoplasmic nucellar cells and on the embryo sac wall near the micropylar base of the central cell. E.M. x2,600.

Fig. 165. Cytoplasmic nucellar cells and central cell showing wall ingrowths (arrows) and plasmodesmatal connections between cytoplasmic and vacuolate nucellar cells. E.M. x3,440.

Fig. 166. Two-celled proembryo after expansion of the embryo sac base. Note embryo sac wall is adnate to the inner integument. Arrows indicate micropylar extent of nucellus. L.M. x470.

Key to Abbreviations: A, amyloplast; Cn, cytoplasmic nucellar cell; Cr, chalazal region of the central cell; Esw, embryo sac wall; Ii, inner integument; Ma, multigrain amyloplast; N, nucellar cell; P, plasmodesmata; Pe, proembryo; T, transfer cell; Vn, vacuolar nucellar cell.

-100

100

Pe

-105

-105

until they are destroyed by embryo sac expansion. This expansion occurs during the transition from a zygote to a 2-celled embryo and results in the embryo sac wall becoming adnate to the inner integument (compare Figs. 154, 163 & 166).

As development proceeds from zygote to multicellular embryo, wall ingrowths form in two other areas. The first is a proliferation of embryonic basal cell wall, in the area common with the degenerate synergid, and projecting into the basal cell of the embryo (Figs. 158, 167 & 168). The second occurs on the chalazal embryo sac wall extending into the central cell (Figs. 169 & 170). Wall ingrowths of the chalazal region of the embryo sac are not formed in the numbers or density of those that develop in the base of this cell (Figs. 106, 108, 155, 163 & 164) but develop singly or in small groups along the embryo sac wall (Figs. 169 & 170). Wall ingrowths between the degenerate synergid and the basal cell of the young embryo are initially poorly defined (Fig. 167) but later expand (Fig. 168) and more closely resemble the papillate type of wall ingrowths that occur in the central cell (Figs. 106, 108, 164, 169 & 170).

In later stages of development, when there is a multicellular proembryo (Fig. 171), the basal cell not only possesses original wall ingrowths on its boundary with the degenerated synergid (Fig. 172), but also exhibits wall ingrowths on its most micropylar boundary, the embryo sac wall (Fig. 173). At this stage these wall ingrowths are fairly well developed, intricate structures that appear to have some degree of fusion between the projections (Fig. 173). Wall ingrowths also extend along the walls which separate the basal suspensor cell from other suspensor cells (Fig. 174) as well as on common walls between suspensor cells (Fig. 175). Absent at earlier stages of development wall ingrowths now occur in cells at the micropylar end of the inner integuments bordering the embryo sac wall (Fig. 171).

Wall ingrowths (arrows) in the embryonic basal and central cell of soybean. For relative positions of cells see Fig. 154.

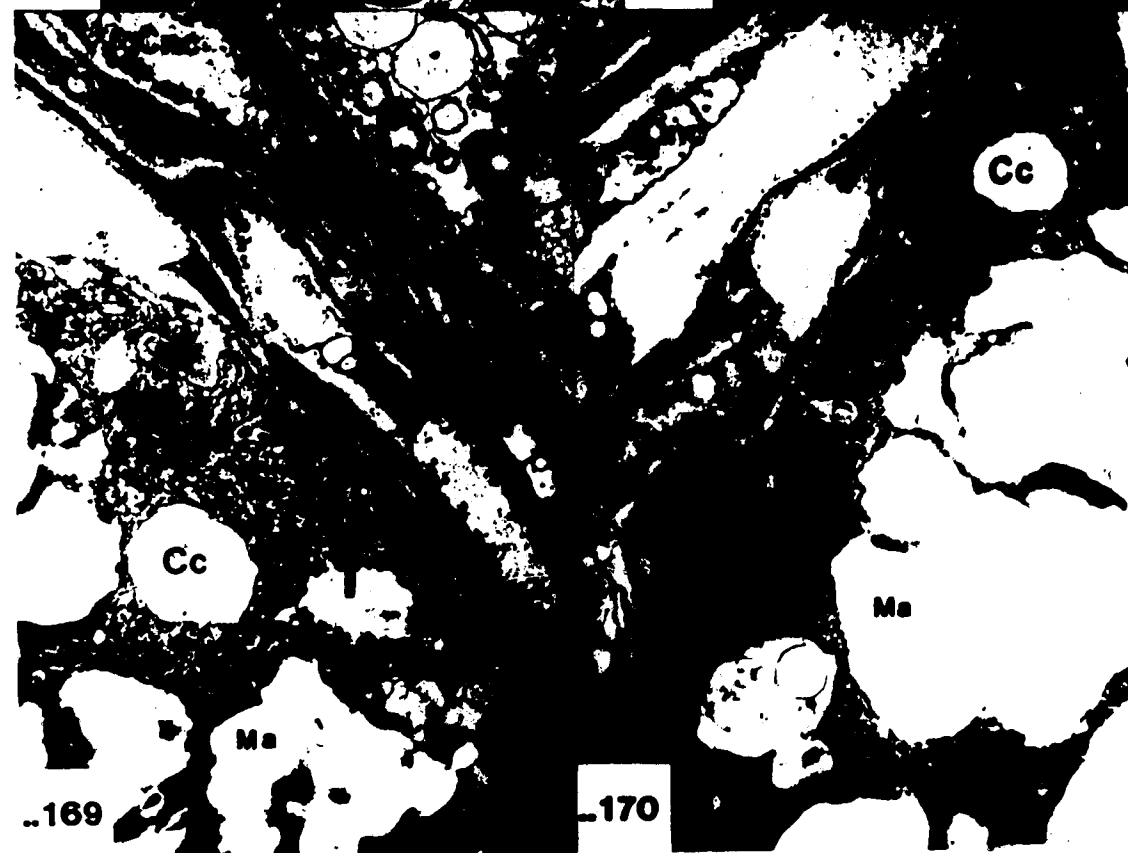
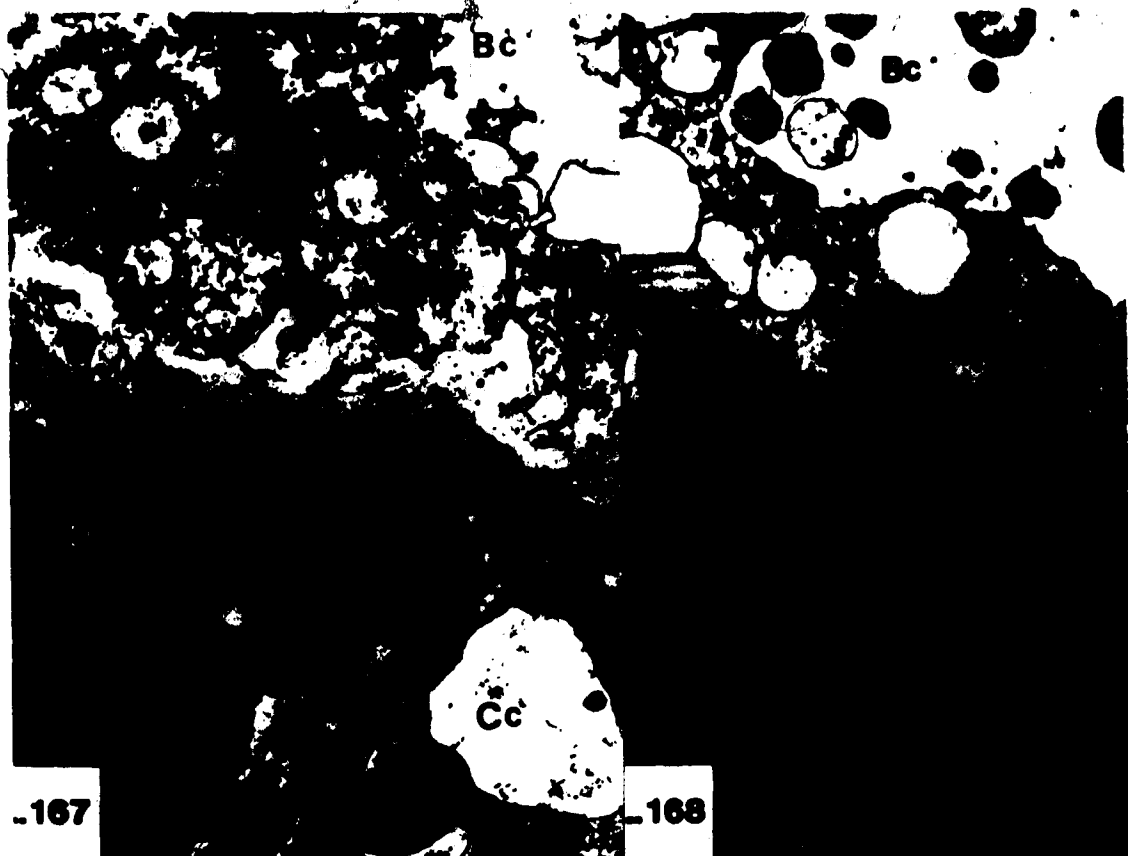
Fig. 167. Wall ingrowths in the embryonic basal cell from the wall bordering the degenerate synergid. E.M. x14,080.

Fig. 168. Wall ingrowths in the embryonic basal cell on its wall bordering the degenerate synergid in a slightly older embryo sac than that shown in Fig. 167. E.M. x11,200.

Fig. 169. Wall ingrowths in the chalazal end of the central cell adjacent to crushed nucellar cells. E.M. x11,200.

Fig. 170. Wall ingrowths scattered along the embryo sac wall in the chalazal region of the central cell. E.M. x11,200.

**Key to Abbreviations:** Bc, basal cell; Cc, central cell; Cnc, crushed nucellar cell; Ds, degenerate synergid; Esw, embryo sac wall.



Wall ingrowths (arrows) in various areas of the embryo sac, shown in Fig. 171.

Fig. 171. Multicellular proembryo showing suspensor, degenerate synergid and associated free nuclear endosperm. Transfer cells exhibiting wall ingrowths in the inner integument adjacent to micropylar base of the embryo sac. L.M. x625.

Fig. 172. Wall ingrowths from embryonic basal cell wall bordering both the degenerate synergid and embryo sac wall. E.M. x14,000.

Fig. 173. Wall ingrowths in the basal cell. E.M. x17,600.

Fig. 174. Wall ingrowths in the basal cell and along adjacent walls of suspensor cells. Micropylar base of the embryo sac is toward left of the micrograph. E.M. x14,000.

Fig. 175. Wall ingrowth on a common wall of a micropylar suspensor cells. E.M. x20,800.

Key to Abbreviations: Bc, basal cell; Cc, central cell; Ds, degenerate synergid; Esw, embryo sac wall; F, free nuclear endosperm nucleus; P, plasmodesmata; Pe, proembryo; S, suspensor cell; T, transfer cell.





#### IV. Discussion

The purpose of the present study is to describe the processes of megasporogenesis, megagametogenesis, aspects of fertilization, early embryogenesis and nutrition of the soybean embryo sac. Although much work has been done at an ultrastructural level, describing the mature megagametophyte prior to fertilization, the process of fertilization and selected stages of early embryogenesis, there are only a few accounts which concern the development and nutrition of the embryo sac. Descriptions of the megasporocyte or processes of megasporogenesis and megagametogenesis at an ultrastructural level have only been provided in *Capsella* (Schulz & Jensen, 1981, 1986), *Dendrobium* (Sagawa & Isreal, 1964; Isreal & Sagawa, 1964, 1965), *Helianthus* (Newcomb, 1973a), *Hordeum* (Cass et al., 1985), *Myosurus* (Woodcock & Bell, 1968) and *Zea* (Russell, 1979). Information on routes by which nutrients enter the embryo sac consists of studies describing the occurrence of wall ingrowths, patterns of starch accumulation (Buell, 1952), tracer localization (Coe, 1954; Mogensen, 1981b), and enzyme histochemistry (Mogensen, 1981a).

The embryo sac of soybean has been shown to be monosporic and to undergo *Polygonum*-type development resulting in a 7-celled, 8-nucleate megagametophyte (George et al., 1979; Kennell & Horner, 1985; Pamplin, 1963; Prakash & Chan, 1976). According to Maheshwari (1950) approximately 70% of all angiosperms that have been objects of embryological investigation exhibit this developmental pattern. Therefore the general aspects of megasporogenesis, megagametogenesis and fertilization in soybean are similar to the majority of angiosperms.

##### Megasporogenesis:

In angiosperms an archesporium develops in the hypodermal layer of the young ovule. Although the archesporium usually consists of a single cell, multicellular archesporia have been reported. Archesporial cells are large with dense cytoplasm and have a large nucleus when compared to the other cells of the nucellus (Maheshwari, 1950; McLean & Ivimey-Cook, 1956). In the archesporium a single cell divides to form a primary sporogenous

cell toward the chalaza of the ovule and a primary parietal cell toward the micropylar region of tissue. It is the sporogenous cell which develops into the megasporocyte. Alternately the archesporial cell can function directly as the megaspore mother cell (Maheshwari, 1950).

There appears to be some controversy in the literature with regard to the number of archesporial cells formed in soybean before the differentiation of the megasporocyte. While Pamplin (1963), Kennell and Horner (1985) and George et al., (1979) state that a multicellular archesporium develops in soybean, Prakash and Chan (1976) and Rembert (1969) show only one archesporial cell present in the nucellus before the formation of the megasporocyte. I found no evidence, in the form of large nucellar cells containing a dense cytoplasm associated with the megasporocyte, which would support the presence of a multicellular archesporium in Gnome soybean. However, as Pritchard (1964) showed in *Stellaria* after megasporocyte differentiation the remaining archesporial cells become morphologically and cytochemically indistinguishable from other nucellar cells. Therefore the presence of a multicellular archesporium in soybean, if formed, would be difficult to detect since the remaining archesporial cells could de-differentiate before the expansion of the megasporocyte.

The youngest soybean megaspore mother cell observed in this study is a large cell with a centrally placed nucleus and sparse cytoplasm containing randomly distributed organelles and plasmodesmata scattered in its walls. During development the megaspore mother cell expands. This expansion is correlated with development of numerous small vacuoles. These vacuoles appear to be distributed equally at both the chalazal and micropylar ends of the cell and may be formed in part by pinocytotic activity of the plasma membrane.

As the occurrence of plasmodesmata implies the possibility of symplastic transport (Robards, 1975) their presence and distribution have been noted in the megasporocyte of *Dendrobium* (Isreal & Sagawa, 1964), *Lilium* (Dickinson & Potter, 1978) and *Myosurus* (Woodcock & Bell, 1968). In *Zea* (Russell, 1979), certain orchids (Rodkiewicz & Bednara, 1976) and in *Capsella* (Schulz & Jensen, 1981) the plasmodesmata are mainly limited to the chalazal wall of the megasporocyte. After expansion of the megaspore mother cell the

plasmodesmata are reported to be lost in *Dendrobium* (Isreal & Sagawa, 1964) and *Lilium* (Dickinson & Potter, 1978). Soybean differs in that it possesses plasmodesmata in all regions of its wall both before and after expansion of the megaspore mother cell.

The pattern of callose deposition is another factor which could affect metabolite flow into the developing megasporocyte. Heslop-Harrison and Mackenzie (1967) proposed that callose special walls could act as macromolecular sieves during the process of microsporogenesis. Callose walls have been shown to act as a barrier to molecules such as thymidine (Southworth, 1971) and phenylalanine (Heslop-Harrison & Mackenzie, 1967) while allowing passage of both glucose and acetate (Southworth, 1971) during pollen development. Although there is some question as to the level of specificity of commercially available aniline blue it has often been used as a stain for callose (Smith & McCully, 1978). If callose has a similar function during megasporogenesis the presence of callose walls could effectively limit the types of molecules that enter the developing megasporocyte. Callose appears transiently in the megasporocytes of many monosporic plants and its rapid appearance and disappearance could be correlated with the ability of the polysaccharide to polymerize and depolymerize quickly (Kuran, 1972).

Callose can be shown to be deposited along portions of the megaspore mother cell wall of soybean. Examination of sections from the same embryo sac show consistent localization only along the micropylar half with sporadic deposition along the chalazal wall of the cell. Patterns of callose deposition and depolymerization have been reported in many different plants during various stages of megasporogenesis (Kuran, 1972; Noher de Halac, 1980; Noher de Halac & Harte, 1977; Rodkiewicz, 1968, 1970; Rodkiewicz & Bednara, 1976; Russell, 1979; Schulz & Jensen, 1981; Willemse & Bednara, 1979). It has been demonstrated that the first sign of callose in the megaspore mother cell occurs adjacent to the walls at the pole where persistent megaspore will form followed by a generalized deposition along the rest of the cell wall in *Polygonum*-type embryo sacs (Kuran, 1972). The chalazal pole is also where the callose staining first becomes faint in such embryo sacs (Rodkiewicz, 1970). Since soybean has the *Polygonum*-type of embryo sac the observations of a megasporocyte with a continuous

callose layer at the micropylar pole and only sporadic callose staining at its chalazal end suggests that it is the chalazal pole where the persistent megaspore will form.

Once the megasporocyte in soybean has expanded callose was not seen lining any of its walls. The disappearance of callose in the megasporocyte of soybean before meiosis occurs does not correlate with any of the plants discussed by Kuran (1972). According to Kuran (1972) callose appears to be present through meiosis although its distribution in megaspore mother cells may vary during different stages of development. The fate of callose formed in the young megasporocyte of soybean is not known. However, it has been proposed that the polysaccharide can act as a reserve material during megasporogenesis in other plants (Noher de Halac, 1980).

Although there is some evidence of transient polarity in the soybean megaspore mother cell as reflected by the chalazal breakdown of callose none of the cellular organelles exhibit any polarity of distribution. This differs from *Zea* where megaspore mother cell cytoplasmic components, except for vacuoles, are all displaced toward the chalazal end (Russell, 1979).

The term cytoplasmic density is used as a synonym for the concentration of cellular organelles and is believed to be suggestive of the level of physiological activity in the cell. Observations that the megasporocyte was denser than the surrounding nucellar cells have been made in *Capsella* (Schulz & Jensen, 1981), *Dendrobium* (Sagawa & Iwano, 1964; real & Sagawa, 1964, 1965), *Helianthus* (Newcomb, 1973a), *Lilium* (Dickinson & Potter, 1977; Dickinson & Potter, 1978; Rodkiewicz & Mikulska, 1965), *Myosurus* (Sagawa & Iwano, 1968), *Stellaria* (Pritchard, 1964) and *Zea* (Russell, 1979). The density of the megaspore mother cell in soybean is, however, similar to the cells of the nucellus. At this developmental stage the megasporocyte contains undifferentiated plastids, mitochondria and only a small amount of ER. Like *Zea* (Russell, 1979) amyloplasts are absent in soybean megasporocytes. This situation differs from *Lilium* (Dickinson & Potter, 1978) where plastids containing starch grains were seen early in development of the megaspore mother cell.

During the expansion of the megasporocyte an increase in cytoplasmic density occurs. The increase in density as revealed by toluidine blue oxide staining and in the electron microscope appears to be caused by an increased ribosome concentration in the megaspore mother cell. The observation that density increases in the megasporocyte of soybean prior to meiosis differs from the situation described in *Dendrobium* (Sagawa & Isreal, 1964; Isreal & Sagawa, 1964, 1965), *Lilium* (Dickinson & Andrews, 1977; Dickinson & Potter, 1978; Rodkiewicz & Mikulska, 1965) and *Stellaria* (Pritchard, 1964) where the megaspore mother cell is initially denser than the nucellus but decreases in density prior to meiosis. However, the processes that causes the megasporocytes of *Dendrobium*, *Lilium* and *Stellaria* to undergo this change in density differs. Cytoplasmic purging has been shown to occur during megasporogenesis in both *Lilium* (Dickinson & Potter, 1978; Heslop-Harrison, 1972) and *Dendrobium* (Sagawa & Isreal, 1964; Isreal & Sagawa, 1964, 1965). In *Lilium* the preprophase megasporocyte appears to undergo intense protein synthesis based on quantities of polysomes, RER and free ribosomes (Dickinson & Andrews, 1977). Its cytoplasm also contains mitochondria with prominent cristae and amyloplasts (Dickinson & Potter, 1978). During callose deposition at the beginning of prophase in *Lilium* the ER is reorganized into whorls that enclose areas of cytoplasm and isolate cellular organelles. During zygotene free ribosomes disappear from the cytoplasm and only those enclosed in membrane whorls persist. The ER remains in this whorled configuration until the early megaspore stage. Dickinson and Andrews (1977) suggest that these membrane whorls function to protect ribosomes from cytoplasmic degradation. Heslop-Harrison (1972) proposed that the process of organelle degradation or cytoplasmic purging is involved in rearranging cytoplasm for development of the gametophyte generation. In *Stellaria* (Pritchard, 1964) it was suggested that the decrease in density of the megaspore mother cell was caused by a lag in the rate of RNA synthesis during expansion of the megasporocyte. Lower ribosomal concentration could explain the decreased staining intensity.

Dickinson and Potter (1978) acknowledge that the formation of persistent callose special walls results in cytoplasmic isolation but suggest that the formation of these walls was

not the cause of cytoplasmic purging. Admittedly there have not been enough ultrastructural studies of megasporogenesis to draw conclusions on how widespread the process of cytoplasmic purging is and to what extent cytoplasmic isolation and possession of nutritional reserves affect the occurrence of this process. Since cytoplasmic purging does not occur in soybean, a plant that maintains plasmodesmata in the embryo sac wall during development, it seems clear that the process is not universal in flowering plants and that more studies are needed on the possible relationship between cytoplasmic isolation and purging.

During expansion of the soybean megaspore mother cell it becomes totally surrounded by a tissue layer, the inner nucellus, which does not appear similar to any of the nucellar modifications listed by Maheshwari (1950). Initially the inner nucellus totally encloses the megasporocyte but during subsequent development inner nucellar cells are crushed by expansion of the acellular embryo sac starting at the micropylar end and proceeding chalazally. The cells of the soybean inner nucellus contain dense cytoplasm and are enclosed in thick walls. Aniline blue and Calcofluor staining indicates that their walls are similar to outer nucellar cell walls in terms of containing callose and cellulose. As with the megasporocyte, cells of the inner nucellus stain intensely with toluidine blue oxide and their density, seen with the electron microscope, is granular suggesting a high concentration of ribosomes. As the inner nucellus is not present in earlier stages of megaspore mother cell differentiation it is assumed that nucellar cells are induced to take on the characteristics of inner nucellar cells by some factor(s) produced by the megasporocyte. Support for the concept that inner nucellar cells are induced also comes from the observation that certain cells on the boundary between the inner and outer nucellus show thick walls similar to those of the inner nucellus while containing cytoplasm intermediate in density.

Among the various types of nucellar modifications cited by Maheshwari (1950), the hypostase is the most similar to the inner nucellus. A hypostase has never been reported to develop before fertilization in soybean (George et al., 1979; Kennell & Horner, 1985; Pamplin, 1963; Prakash & Chan, 1976) or in other members of the family (Banerji, 1938; Bharathi & Murty, 1984; Brown, 1917; Cooper, 1933, 1935b; Farley & Hutchinson, 1941;

Hindmarsh, 1964; Martin, 1914; Reed, 1924; Reeves, 1930; Rembert, 1967, 1969, 1977a, b; Roy, 1933; Smith, 1956; Weinstein, 1926). However, Pamplin (1963) and George et al. (1979) both report that after fertilization a hypostase develops between the chalazal vascular strand and the nucellus but that the structure does not extend through the nucellus to the embryo sac. In other plants it has been proposed that the hypostase is involved in nutrition of the megagametophyte and embryo (Malik & Vermani, 1975; Masand & Kapil, 1966; Tilton, 1980; Tilton & Mogensen, 1979), controlling the water relations of the ovule or that it limits the chalazal growth of the embryo (Johansen, 1928). However, work by Coe (1954) on *Zephyranthes* and by Tiwari (1983) on *Torenia* has questioned a nutritional role for the hypostase. Coe (1954) fed radioactive  $CO_2$  to *Zephyranthes* and showed that during ovule development the hypostase never contained any  $C^{14}$  suggesting that metabolites pass around the hypostase while moving through the nucellus to the embryo sac. Tiwari (1983) and others (Kapil & Tiwari, 1978) have demonstrated that the walls of the hypostase contain callose and have proposed that its presence would limit the movement of metabolites through these cells to the embryo sac.

Since inner nucellar cells of soybean are not limited to the chalazal region of the ovule, do not have elevated levels of callose in their walls, occur only in the nucellus and do not extend near the chalazal vascular trace of the ovule it would appear that the inner nucellus is not merely another form of a hypostase. As the megasporocyte, megaspores, persistent megaspore, 2- and 4-nucleate embryo sacs and the chalazal end of the cellular megagametophyte are all enclosed and connected to the inner nucellus with plasmodesmata it appears likely that these cells are involved in megagametophyte nutrition. The exact nature of inner nucellar involvement in megagametophyte nutrition has yet to be resolved. Certainly the increased cell wall thickness in the inner nucellus could be involved in facilitating apoplastic transport while the higher ribosomal concentration may provide a pool of both nucleic and amino acids to be utilized by the megagametophyte as the inner nucellar cells are crushed during embryo sac expansion.

After development of the inner nucellus and expansion of the megasporocyte, the process of meiosis in soybean results in the formation of a linear tetrad of megaspores. Except for the chalazal megaspore being the largest of the four they are all similar in distribution of cytoplasmic organelles. During meiosis three aniline blue positive, Calcofluor negative walls are laid down separating the 4 megaspores. These walls are perpendicular to the long axis of the former megasporocyte and are structurally amorphous, lacking an electron opaque middle lamella when compared with walls of nucellar cells. These staining characteristics suggest that the walls formed during meiosis are callosic (Hughes & McCully, 1975; Wood, 1980; Yeung, 1984). The presence of round electron dense areas in the callosic walls may represent vestiges of plasmodesmata that could have been formed during wall formation.

The pattern of soybean megaspore formation has been discussed previously. Although only linear meiotic tetrads were seen during the course of this research or by Pamplin (1963) George et al. (1979) and Kennell and Horner (1985) report both linear and T-shaped tetrads. Maheshwari (1950), citing examples where both linear and T-shaped tetrads occur in different ovules of the same ovary, states that the plane of division of the micropylar dyad often varies within a taxon and suggests that this type of variation may be of little importance.

Callose walls separating megaspores have been reported in many plants (Kennell & Horner, 1985; Kuran, 1972; Noher de Halac, 1980; Noher de Halac & Harte, 1977; Rodkiewicz, 1968, 1970; Rodkiewicz & Bednara, 1974, 1976; Russell, 1979; Willemse & Bednara, 1976). To date Tilton (1981a) is the only worker to report that a monosporic plant (*Ornithogalum*) does not appear to produce callose during meiosis. In most other reports the polysaccharide callose not only composes most of the wall that separates megaspores from each other but also lines other walls of the megaspore cell. In soybean, however, the only detectable callose occurs in walls that separate megaspores from each other and none was seen lining the other walls of megaspores. Soybean like *Zea* (Russell, 1979) exhibits plasmodesmata connecting the persistent megaspore to the nucellus.



The chalazal megaspore in soybean expands and becomes the functional megaspore. This is in agreement with all the other reports on soybean (George et al., 1979; Kennell & Horner, 1985; Pamplin, 1963; Prakash & Chan, 1976) and apparently is typical for monosporic plants undergoing *Polygonum*-type embryo sac development (Maheshwari, 1950). Expansion of the chalazal megaspore is accompanied by senescence of the other three. Aniline blue staining shows that the callose walls are displaced toward the micropyle as the persistent megaspore expands to occupy the space previously occupied by the other 3 megaspores. Staining with Calcofluor demonstrates that cellulose is present at this stage in the micropylar wall of the persistent megaspore.

#### Megagametogenesis:

In soybean the process of megagametogenesis involves a series of 3 mitotic divisions and subsequent wall formation. During the first mitotic division the metaphase plate is perpendicular to the long axis of the embryo sac. At this stage the megagametophyte shows a polarity in the distribution of vacuoles with most of them being found and, as evidenced by activity of the plasma membrane, formed in the micropylar region of the embryo sac. A different type of polarity was seen in *Holdeum* where, at a similar stage of development, the megagametophyte contains a diffuse assemblage of small vacuoles with most of the remaining cellular organelles located at its micropylar end. In this case polarity was shown to develop in the functional megaspore and persist until the 4-nucleate stage (Cass et al., 1985). However, polarity in soybean appears to be more transient and was not seen before or after the 1-nucleate stage of development. In soybean the polar formation of vacuoles may represent a mechanism by which the embryo sac is expanded micropylarly during the transition from the 1- to 2-nucleate stage.

The smaller vacuoles found in the 1-nucleate embryo sac coalesce after separation of the chromatids and form the large central vacuole characteristic of the 2- and 4-nucleate embryo sac and the central cell of the young megagametophyte. Expansion of the major vacuole is seen to occur through fusion of smaller vacuoles. Additionally, Golgi vesicles are

seen fusing with the major vacuole in 2- and 4-nucleate embryo sacs. These Golgi vesicles could act to add osmotically active substances to the vacuole (Matile, 1969, 1976; Matile & Moor, 1968). This activity of the Golgi apparatus may well be important in creating or maintaining the osmotic pressure necessary for embryo sac expansion.

The large vacuole characteristic of the 2- and 4-nucleate embryo sacs may have another function besides involvement in a lytic complex (Russell, 1979) or maintenance of turgor in the embryo sac. The timing of its formation could be critical to the developmental pattern occurring in embryo sacs. Coalescence of small vacuoles in the center of the megagametophyte to form the larger vacuole only occurs after the first mitotic division in soybean. This is also true for other plants that are monosporic and have *Polygonum*-type embryo sacs (Maheshwari, 1950). The effect of formation and expansion of a vacuole at this stage is to isolate nuclei at opposite ends of the embryo sac. In contrast to this the major vacuole of the megagametophyte in other monosporic plants having *Oenothera*-type embryo sac development forms before the first nuclear division. In these plants the mitotic products are all found in the micropylar end of the embryo sac (Johansen, 1929; Khan, 1942) supporting the concept that this vacuole acts to isolate nuclei at opposite ends of the embryo sac. As there are only 4 nuclei produced in the embryo sac of plants with *Oenothera*-type embryo sacs it seems clear that these plants undergo one less mitotic division than plants similar to soybean. Based on observations of vacuolar activity the difference between the two groups of plants should be considered as loss of the first nuclear division and not the last as Maheshwari (1950) has suggested. Battaglia (1951) recognized this and suggested that the main difference between these two types of embryo sacs is the presence of a mitotic division before the process of polarization. He suggested (1951) that there are only 4 nuclei formed in plants with the *Oenothera*-type embryo sac development because the two mitotic divisions which occur at the micropylar end of the embryo sac act independently from the one which occurs before polarization. Therefore, the stimulus for wall formation may come from the second micropylar mitotic division and the presence or absence of nuclei in the chalazal region of the embryo sac has no real effect on this process (Battaglia, 1951).

After the embryo sac has become polarized the second mitotic division occurs resulting in formation of a 4-nucleate embryo sac. In the micropylar region this division is perpendicular to the preceeding one while in the chalazal region the division plane appears to vary. The cytoplasm of the 2- and early 4-nucleate embryo sacs are similar in distribution and concentration of organelles. Late in the 4-nucleate stage of embryo sac development changes occur in the shape of the chalazal end of the embryo sac, in the position of the nuclei in both micropylar and chalazal ends of embryo sacs and in the production of osmiophilic bodies throughout the cytoplasm. The apparent movement of nuclei in the 4-nucleate embryo sac of soybean has been noted before (George et al., 1979); however, the fact that this separation not only involves a lateral movement of the two nuclei but also the displacement of one of the nuclei toward the chalazal end of the embryo sac has not been reported. The two nuclei in the chalazal end of the embryo sac assume an orientation parallel to its long axis. This may be in response to the change in the originally dome shaped chalazal end of the embryo sac to a more conical structure during development. As the cytoplasm and nuclei move into this conical region the two nuclei change position relative to one another. Osmiophilic bodies form in the cytoplasm and become associated with the tonoplast of the large central vacuole and can be resolved as myelin-like bodies composed of whorls of membranes (Bowes, 1969; Thomas & Isaac, 1967).

The final mitotic division during megagametogenesis in soybean results in the formation of the egg, synergids, antipodals and central cell. In other plants it has been observed that one of the two micropylar nuclei divides to form two synergid nuclei and the other forms the egg and micropylar polar nucleus while the two chalazal nuclei, if present, divide to form the chalazal polar nucleus and three antipodal nuclei (Brown, 1909; Brown & Sharp, 1911; Cooper, 1937, 1939; Howe, 1975; Ishikawa, 1918; Johansen, 1929; Langlet, 1927; Pace, 1909; Palser et al., 1971; Schaffner, 1901; Weatherwax, 1919). Summing up the evidence that synergid nuclei are sister nuclei and that egg and micropylar polar nuclei are products of the same division Schnarf (1936) stated:

"We can regard it as probable that the synergids on the one hand, and the egg-cell

and the upper polar nucleus on the other hand, represent sister-nuclei; at least this is definitely shown in certain cases while no reliable observations are at hand to substantiate the idea of any other origin."

Work on megagametogenesis in *Epipactis* (Brown & Sharp, 1911, fig. 8), *Erythronium* (Schaffner, 1901, fig. 71), *Euchlaena* (Cooper, 1937 fig. 25), *Grindelia squarrosa* (Howe, 1926, figs. 13-15), *Grindelia stricta* (Howe, 1975 fig. 7), *Habenaria* (Brown, 1909 fig. 4), *Hartmannia* (Johansen, 1929 figs. 4a & 4), *Oenothera* (Ishikawa, 1918 fig. 8) and *Rhododendron* (Palser et al., 1971, figs. 35 & 36) has shown that the more micropylar of the two nuclei divides to form the synergids while the more chalazal forms the egg and micropylar polar nuclei. Likewise observations on the two chalazal polar nuclei have shown that the more micropylar nucleus divides to form the chalazal polar nucleus and an antipodal nucleus while the other nucleus divides to form two additional antipodal nuclei (Brown, 1909; Cooper, 1937).

The proposal that the position of the micropylar nuclei in soybean prior to the final mitotic division in megagametogenesis influences which nucleus is involved in the formation of synergid, egg or micropylar polar nucleus is also supported by examination of the relative positions of egg apparatus nuclei in the cellular embryo sac of soybean. In the mature embryo sac of soybean key features which differentiate the egg from synergid, other than the presence of a filiform apparatus in synergids, are the relative positions of the nuclei and the major vacuole. The egg most frequently has a chalazal nucleus and a micropylar vacuole while in synergids the reverse is true (Folsom & Peterson, 1984). This also holds true for virtually all angiosperms so far described (Jensen, 1963; Willemse & Van Wieren, 1984). When very young cells of the egg apparatus of soybean are studied, they are found to contain neither a filiform apparatus nor a large vacuole but still can be distinguished by nuclear position. The young egg cell contains a chalazal nucleus when compared to the position of the nuclei in the two synergids. Not only is there a difference in relative height of young synergid and egg nuclei but when serial sections are examined it is found that these two groups of nuclei are spatially separated with those of the synergids being very close to one another. As there is an apparently uniform relationship, shown in a number of different plants, between nuclear

position and the products of the final mitotic division in megagametogenesis it is assumed that a similar situation occurs in soybean. Therefore, the apparent movement of micropylar nuclei in the late 4-nucleate embryo sac of soybean may represent the initial stage of differentiation that predicts which nucleus will divide to form the two synergids and which will form the egg and one of the central cell nuclei.

During cellularization walls usually develop in both chalazal and micropylar ends of the embryo sac with those of the antipodals often being formed first (Davis, 1966). From reports on megagametogenesis in *Habenaria* and *Epipactus* it seems clear that the cells at both ends of the embryo sac are formed in a similar manner (Brown, 1909; Brown & Sharp, 1911). Plants such as *Eschscholzia* (Sachar & Mohan Ram, 1958) and *Rudbeckia* (Maheshwari & Srinivasan, 1944) possess antipodal cells that closely resemble those of the egg apparatus. However, a difference in the morphology of the cells at both poles is readily apparent after comparing the size and shape of the antipodals and cells of the egg apparatus of soybean. This difference in structure between the antipodal and egg apparatus cells has been noted before in many plants and shape of the respective ends of the embryo sac during cellularization implicated as the cause (McLean & Ivimey-Cook, 1956).

The result of the final karyokinesis and cytokinesis in soybean is a 7-celled, 8-nucleate embryo sac composed of three micropylar cells of the egg apparatus, three antipodals at the chalazal end and a large vacuolate central cell with nuclei at opposite poles occupying the rest of the megagametophyte. Embryo sac cellularization has not been described in soybean and only discussed in a limited sense in other plants. Observations on events surrounding cellularization include work on *Calopogon* (Pace, 1909), *Camassia* (Smith, 1942), *Clintonia* (Smith, 1943), *Crepis* (Langlet, 1927), *Epipactus* (Brown and Sharp, 1911), *Erythronium* (Cooper, 1939; Schaffner, 1901), *Euchlaena* (Cooper, 1937), *Grindelia* (Howe, 1975), *Habenaria* (Brown, 1909), *Hartmannia* (Johansen, 1929), *Hordeum* (Cass et al., 1985), *Juglans* (Bowillot, 1969), *Lilium henryi* (Cooper, 1935a), *Lilium martagon* (Langlet, 1927), *Lycopersicon* (Cooper, 1931), *Medicago* (Cooper, 1935b), *Phryma* (Cooper, 1941), *Solanum* (Rees-Leonard, 1935) and *Zea* (Cooper, 1937). Some of these workers did not deal with

development of cell plates but only discussed the occurrence of spindles during the last mitotic division before cellularization. However, as cell plate and wall formation are closely tied to the development of a spindle (Hepler, 1976), all of these papers may provide some information on the process of cellularization.

In soybean the structure of egg and antipodal apparatus cells immediately after cellularization and before expansion may also provide some information about the process of cytokinesis in the embryo sac. Essentially, the egg apparatus and antipodals in soybean are each seen to be segmented by 3 walls. The number of cell plates formed in the embryo sac of different plants has been discussed before. Cooper (1935a) in his study of *Lilium henryi* states that 3 cell plates develop in both ends of the embryo sac during cellularization. A similar situation has been seen in *Camassia* (Smith, 1942), *Clintonia* (Smith, 1943), *Erythronium* (Cooper, 1939; Schaffner, 1901), *Euchlaena* (Cooper, 1937), *Medicago* (Cooper, 1935b), *Solanum* (Rees-Leonard, 1935), and *Zea* (Cooper, 1937). However in other reports only one (Johansen, 1929) or two (Brown, 1909; Brown & Sharp, 1911; Howe, 1975) persistent cell plates per end were viewed during cytokinesis of the megagametophyte. As all studies of this type have to contend with timing to view various phases of development it may be that the observation of a third spindle and cell plate by Cooper (1935a) and others represents a rare encounter with a short-lived developmental phenomenon.

If the process of cellularization is reasonably uniform within structurally similar types of embryo sacs the presence or absence of a third spindle along with the corresponding cell plate could be critical in understanding how cells of the egg apparatus and antipodals are formed. Information provided by Cooper (1935a) and Rees-Leonard (1935) on spindle and cell plate formation and orientation along with the observations of Brown (1909) on the relationship of nuclei in the egg apparatus provide an explanation for the process of cellularization in many plants including soybean. Based on this information it could be proposed that the cell plate formed on the spindle involved in the mitotic division producing the synergid nuclei segments the micropylar base of embryo sac into two roughly equal halves. In soybean this wall is parallel to the long axis of the embryo sac. The cell plate that develops

on the spindle involved in formation of the egg and micropylar polar nuclei is roughly perpendicular to the long axis of the embryo sac and forms the top wall of the egg apparatus. The activity of these 2 cell plates would result in the micropylar base of the megagametophyte being segmented into two halves enclosed by walls on all sides. Since, in soybean, the young micropylar megagametophyte base consists of two halves one of which contains a synergid cell while the other an egg and second synergid cell it is possible to conclude that these 2 cell plates are also involved in soybean embryo sac cellularization. At an early developmental stage the third wall of the soybean egg apparatus is oblique to the other two walls and separates the egg from the second synergid cell (see Figs. 62 - 68). If the third wall in soybean is in fact the wall formed by the third spindle seen by Cooper (1935a) in *Lilium* and Rees-Leonard (1935) in *Solanum* or if it is produced by another mechanism can only be the subject of speculation at this time.

The antipodals of soybean also possess 3 clearly defined walls just after cellularization 2 of which are perpendicular and the third parallel to the long axis of the embryo sac. Observations on *Grindelia* have shown that the more micropylar of the nuclei, in the chalazal region of the 4-nucleate embryo sac, divides to form antipodal and the chalazal polar nucleus while the other nucleus divides to form 2 more antipodal nuclei (Howe, 1975). If a similar system holds true for soybean the formation of 2 walls perpendicular to the long axis of the embryo sac can be seen to occur by spindle and cell plate formation. The third wall serves to segment one of the areas created by the two parallel walls in the antipodals into 2 cells. In this regard it is interesting to note that in many members of the Asteraceae only 2 antipodals are normally formed during megagametophyte cellularization one of which is binucleate (Davis, 1964a, 1964b; Howe, 1969, 1975; Langlet, 1925; Newcomb, 1973a; Norris, 1892). As 3 spindles were observed by Cooper (1935a) and Rees-Leonard (1935) in both ends of the embryo sac and since it has been proposed that cellularization occurs in a similar manner in both ends of the embryo sac (Brown, 1909; Brown & Sharp, 1911) it may be that the development of binucleate antipodal cells in many plants is the result of a failure of the plant to form a third wall during cellularization of the megagametophyte.

### Expansion of the egg apparatus:

During expansion and maturation there are many changes in the morphology of egg apparatus cells. Few reports dealing with the development of the egg apparatus exist. The work by Wilms (1981) on spinach and brief references in other papers (Brown, 1917; Cass, 1972; Cass et al., 1985; Cooper, 1931, 1933, 1935b; Davis, 1964a, 1964b; Haskell & Postlewait, 1971; Hindmarsh, 1964; Rees-Leonard, 1935; Smith, 1942; Woodland, 1964) represents most of the literature which deals with this topic. Mature soybean egg apparatus cells are approximately equal in length and width. The key differences between mature synergids and egg are the relative location of the major vacuole and nucleus, development of a filiform apparatus in synergids and size and density of wall packets covering the chalazal end of egg apparatus cells. After cellularization neither the immature egg nor synergids show the large vacuole characteristic of mature soybean egg apparatus cells nor do the synergids possess a filiform apparatus. Also it is impossible to discern any structural differences in walls surrounding the egg apparatus cells. The soybean egg and synergid cells are formed in the same cytoplasmic milieu with the only apparent difference between the two cell types being the position of their nuclei after cellularization has occurred. It, therefore, seems reasonable to conclude that most of the process of differentiation in the soybean egg apparatus occurs during cellular expansion.

Expansion of soybean egg apparatus cells, as in spinach (Wilms, 1981) and *Solanum* (Rees-Leonard, 1935), appears to be caused by development of large vacuoles chalazal to the nucleus in synergids and micropylar to the nucleus in the egg. The expansion of soybean egg apparatus cells can be correlated with a decrease in cytoplasmic density and in thickness of the walls surrounding the cells. The cytoplasm of newly formed egg apparatus cells appears extremely dense as it is tightly packed with ribosomes and other organelles. During egg and synergid expansion cytoplasmic density decreases markedly. This trend continues until near maturity when some density is re-established. As the major component of this density appears to be cytoplasmic ribosomes a situation analogous to the expanding megasporocyte in *Stellaria* (Pritchard, 1964) may well be envisaged where it was proposed that the decrease in cellular



density which occurred during the expansion of the megaspore mother cell was a result of a lag in RNA synthesis. Also, activity of the Golgi apparatus appears to be low during expansion of egg apparatus cells. In young cells Golgi bodies were only seen in a few cases. As these Golgi bodies were usually associated with vacuoles it is assumed that they function in adding osmotically active substances to the vacuome in a manner similar to that proposed for dictyosomes in the 2- and 4-nucleate embryo sac (Matile, 1969, 1976; Matile & Moor, 1968). In association with egg apparatus vacuoles, myelin-like bodies were observed scattered in the cytoplasm during cellular expansion.

As the soybean egg apparatus cells expand they extend into the central cell achieving their characteristic bulbous chalazal ends. Bending of the central cell and egg apparatus common wall in the region where it attaches to the embryo sac wall forms synergid and egg cell hooks. In soybean this also appears to be the developmental period when wall segmentation occurs. In the top wall and chalazal region of the common wall segmentation results in the formation of mature egg apparatus cell walls. This wall is seen to consist of expanded areas containing wall material interspersed between regions of membrane contact. A similar situation has been reported to occur in the chalazal wall of the egg apparatus cells of *Capsella* (Schulz & Jensen, 1968b).

The walls that initially enclose the soybean egg apparatus cells are thick, lack a middle lamella and appear to be heavily dissected by electron dense bands. Absence of a discernible middle lamella in the young soybean egg apparatus walls is similar to *Hartmannia* (Johansen, 1929) and suggests that these walls are structurally unique. These electron dense bands may be remnants of microtubules formed during the wall building process. Throughout egg apparatus expansion in soybean walls become segmented presumably along lines previously established by the electron dense bands and decrease in thickness by at least 50%. As areas of wall separate they form the wall packets characteristic of the mature egg and synergid cells of soybean. These areas were shown to contain an insoluble carbohydrate in another variety of soybean (Folsom & Peterson, 1984). As walls of young soybean egg apparatus cells fluoresce after staining with Calcofluor White it is probable that the expanded areas or wall packets covering

the chalazal ends of egg and synergid cells contain cellulose. Since little Golgi activity is associated with walls during cellular expansion it seems reasonable to assume that large amounts of new wall materials are not being deposited during this period. However, Golgi bodies were often seen associated with individual wall packets of the egg apparatus cells after expansion and segmentation had occurred suggesting that these wall packets can later expand. Therefore, increases in cell wall length which occur during cellular expansion may well result in both segmentation and a decrease in wall thickness. All regions of the egg apparatus walls undergo segmentation except the micropylar portion of the egg and synergid cells common wall. This results in common walls of the soybean egg apparatus cells being thicker at their micropylar base than at their chalazal end. A similar progressive thinning of walls separating the mature egg and synergid cells from one another has also been noted in another variety of soybean (Folsom & Peterson, 1984) and in *Capsella* (Schulz & Jensen, 1968a, 1968b), cotton (Jensen, 1965a), *Petunia* (van Went, 1970a), *Torenia* (van der Pluijm, 1964) and *Zea* (Diboll & Larson, 1966).

The filiform apparatus does not develop until the cells have expanded and can be shown to be a proliferation of the cell wall common to the synergids. The filiform apparatus is attached to the wall in a restricted area and its projections radiate out into the cytoplasm of both synergids. By Calcofluor White staining the filiform apparatus, as well as all of the walls of the egg apparatus of soybean are shown to contain a cellulosic component. This supports previous work in *Aquilegia* (Vijayaraghavan et al., 1972), *Bellis* (Engell & Petersen, 1976), cotton (Jensen, 1963), *Papaver* (Olson & Cass, 1981) and *Scilla* (Bhandari & Sachdeva, 1983) where it has been shown that the filiform apparatus and all of the walls that surround egg and synergid cells contain an insoluble carbohydrate.

According to the terminology of Gunning, Pate & Briarty (1968), later modified by Pate and Gunning (1972), any cell which contains a region of wall ingrowths and is thought to be involved in a transport function can be termed a "transfer cell". Thus, because of the presence of a filiform apparatus, the synergids can be considered transfer cells (Gunning et al., 1970). Exactly what the filiform apparatus transports is a subject of some controversy.

While van der Pluijm (1964) discussed the function of the filiform apparatus only in terms of secretion of chemotropic substances involved in directing the growth of the pollen tube, Jensen (1965a) saw a much broader role for the filiform apparatus and the synergid. In cotton Jensen (1965a) proposed that the filiform apparatus functions both in releasing chemotropic substances and transport of nutrients into the embryo sac. In later work Mogensen (1981a, 1981b) and Tilton (1981b) rejected Jensen's (1965a) proposal and concluded that the filiform apparatus is only involved in secretion of substances out of the synergid.

The attachment of the filiform apparatus to the synergids' common wall in Gnome, the variety studied in this research, differs from that of another soybean variety, Bragg (Folsom & Peterson, 1984). In Bragg the filiform apparatus was found attached to both the embryo sac wall and the common wall of the synergids. This type of variability between the attachment of the filiform apparatus in different varieties of the same species has not been noted before. In a broader comparison of different species there appears to be a similar type of variability as evidenced by the fact that the filiform apparatus ranges from vase shaped profiles on the common wall of the synergids in *Nicotiana* (Mogensen & Suthar, 1979), *Petunia* (van Went, 1970a), *Proboscidea* (Mogensen, 1978a) and *Helianthus* (Newcomb, 1973a) to massive proliferations of wall material from the basal region of the synergids in *Agave* (Tilton & Mogensen, 1979), *Capsella* (Schulz & Jensen, 1968a), cotton (Jensen, 1965a), *Petunia* (Wilms, 1981) and *Stipa* (Maze & Lin, 1975).

During this research other differences were seen between the megagametophyte cells of Bragg (Folsom & Peterson, 1984) and Gnome. These concern the presence of concentric layers of rough endoplasmic reticulum (RER) chalazal to the egg nucleus in Bragg (Folsom & Peterson, 1984) but not seen in Gnome and observations that the Bragg egg lacks amyloplasts (Folsom & Peterson, 1984) while several starch containing plastids were observed in the egg of Gnome. With respect to the presence of starch in the egg cell the situation in the two varieties of soybean mirrors the difference between *Capsella*, cotton and spinach. In *Capsella* (Schulz & Jensen, 1968b) and spinach (Wilms, 1981) the egg was shown to contain starch

while amyloplasts were not seen in the egg of cotton (Jensen, 1965b). Although variations in structure and organelle content between similar cells in different species could be based on some major differences between plants involved the presence of similar levels of variability in two soybean varieties suggests that no one variety may be entirely typical for a species as intraspecific variation can exist. The presence of a natural amount of variability serves to bring into question the importance of both the position and presence or absence of certain structures and organelles to the overall function of the cells of the egg apparatus.

#### Development of the central cell:

The morphology of the mature soybean central cell differs greatly from that immediately after cellularization. The 3 most obvious features of the mature central cell are the region of wall ingrowths at the micropylar base of the cell, the paired polar nuclei and large numbers of multigrain amyloplasts. With embryo sac cellularization the central cell is delimited at its poles by the chalazal wall of the egg apparatus and micropylar wall of the antipodal apparatus. The central cell consists of 2 polar nuclei located at the micropylar and chalazal poles, a large central vacuole and a layer of cytoplasm lining all of its walls. As cells of the egg and antipodal apparatus of soybean expand a number of changes begin to occur in the central cell. Initially these changes involve development of wall ingrowths in the cell's micropylar base on the embryo sac wall, differentiation of multigrain amyloplasts from a population of undifferentiated plastids and fragmentation of the large vacuole. Subsequent to the onset of these developmental changes the chalazal polar nucleus moves toward the egg apparatus and becomes associated with the micropylar polar nucleus. In soybean like *Capsella* (Schulz & Jensen, 1973) nuclear fusion probably begins soon after pairing of polar nuclei.

Proliferations of embryo sac wall known as wall ingrowths have been reported in the basal region of the central cell of soybean both before (Folsom & Peterson, 1984) and after fertilization (Tilton et al., 1984) and have been shown to occur in the central cell of *Euphorbia* (Gori, 1977), spinach (Wilms, 1981) and *Helianthus* (Newcomb, 1973a; Newcomb & Steeves, 1971). The location and time of wall ingrowth formation varies among plants. In

*Nicotiana* (Mogensen & Suthar, 1979) and *Proboscidea* (Mogensen, 1978a) wall ingrowths also occur in the central cell but develop from the synergid wall. In *Capsella* wall ingrowths develop in both micropylar and chalazal ends of the central cell but form only after fertilization has occurred, originating from both the suspensor and embryo sac wall (Schulz & Jensen, 1969, 1971, 1974). Wall ingrowths have been purported to augment metabolite flow by increasing plasma membrane surface area (Gunning & Pate, 1969, 1974; Pate & Gunning, 1972) and it has been concluded that they have a similar function in the central cells of angiosperms (Tilton et al., 1984).

The observation in soybean that both amyloplasts and ingrowths develop soon after cellularization suggests that their formation may be related. In pea stems development of wall ingrowths in cells between the vascular tissue (source) and centers of growth (sink) was negatively affected by slowing the movement of the transpiration stream (Pate et al., 1970). Pate, Gunning and Milliken (1970) further suggest that metabolite movement may be involved in induction of wall ingrowth formation. The situation between the central cell (sink) of soybean and surrounding nucellar tissue (source) could be considered analogous to that of pea as the development of central cell wall ingrowths either precedes or is simultaneous with the development of starch grains in plastids. Further support for a relationship between amyloplast development and wall ingrowth formation could come from more developmental studies in angiosperms with large amounts of starch in their central cell to see when and in what region of wall ingrowths develops.

After the initial appearance of multigrain amyloplasts the individual starch grains expand ultimately filling the plastid envelope making it difficult to discern the presence of a plastid membrane. It is these large multigrain amyloplasts that Pamplin (1963) called "starch packets". Maheshwari (1950) considered that the development of nutritional reserves in the central cell or any cell of the egg apparatus to be atypical in the angiosperms. However Dahlgren (1927, 1939) listed many plants where starch has been found in the embryo sac and suggests that the situation is more common than once believed. The formation of starch has been reported in the central cells of *Arachis* (Banerji, 1938; Reed, 1924), barley (Cass &

Jensen, 1970), *Euchlaena*, *Euchlaena* x *Zea* (Cooper, 1937), *Medicago* (Cooper, 1935b; Farley & Hutchinson, 1941; Reeves, 1930), *Nicotiana* (Mogensen & Suthar, 1979), *Penstemon* (Evans, 1919), *Petunia* (Cooper, 1946; van Went, 1970b), *Plantago* (Cooper, 1942) and *Rhododendron* (Palser et al., 1971). A rosette arrangement of the starch packets is fairly uniform in the soybean central cell. No evidence for the proposal of Kennell and Horner (1985) that small grains fuse to produce larger ones was found in this research. Rather from ultrastructural observations on multigrain amyloplast development in the soybean central cell each packet or rosette of starch grains develops from the activity of a single multigrain amyloplast.

Concomitant with the development of large multigrain amyloplasts is a decrease in the volume of the central cell vacuome until it is represented by a population of small scattered vacuoles. Segmentation of the initially large central cell vacuole in soybean appears to involve the production and expansion of myelin-like bodies. Organelles structurally similar to myelin-like bodies have also been referred to as lamellar bodies (Bowes, 1969; Mollenhauer et al., 1978), membranous whorls (Bowes, 1969) and in certain cases inclusion bodies (Fineran, 1971). It has been proposed that myelin-like bodies are not naturally occurring structures but artifacts induced by fixation (Curgy, 1968; Palade & Claude, 1949a, 1949b). However, it has recently been shown by the use of various fixation protocols and the process of freeze etching that myelin-like bodies are present in living tissue and not formed during the process of fixation (Bowes, 1969; Fineran, 1971; Mollenhauer et al., 1978; Thomas & Issac, 1967; Yamada et al., 1983). Myelin-like bodies have been proposed to develop from the tonoplast (Fineran, 1971) or by joint activity of protein and lipid bodies (Mollenhauer et al., 1978). The function of these bodies is unknown but in one instance it has been suggested that they are involved in the biogenesis of endoplasmic reticulum (Mollenhauer et al., 1978). As myelin-like bodies in soybean are often associated with dark osmiophilic structures it seems that here too their development at least partially involves lipid bodies in the embryo sac. Based on observations of the soybean embryo sac before and after cellularization it appears that myelin-like bodies develop in the cytoplasm, fuse with the large central vacuole and

expand forming a network of membranes in the vacuole. It is these membranes that allow for the subdivision of the large central cell vacuole. Evidence for this type of segmentation before vacuolar shrinkage comes from observations of soybean central cell maturation. During this developmental phase numerous cases of vacuolar invaginations occur where the tonoplast forms a sharp thin point ending in a membrane associated with a myelin-like body. This is observed repeatedly around the periphery of the vacuole, with the invaginations exhibiting various lengths and widths.

In soybean the highest activity of rough endoplasmic reticulum (RER) and Golgi apparatus activity occurs when the vacuome is reduced to the greatest extent. In rice (Bechtel & Juliano, 1980) and to a lesser extent wheat endosperm (Bechtel et al., 1982a, 1982b) protein bodies appear to be formed by activity of both RER and the Golgi apparatus. Because of the high number of Golgi bodies and elevated level of dilated RER early in the development of the central cell soybean may be similar to these plants. In the central cell no evidence was found for a process that occurs in soybean cotyledons (Yoo & Chrispeels, 1980) involving the pinching off of protein bodies by subdivision of a vacuole containing reserve proteins. Rather in the central cell of soybean it is with the small vacuoles that the protein bodies and multigrain amyloplasts fuse. Except for observations that both protein bodies and multigrain amyloplasts fuse with vacuoles and not with one another the order of fusion appears random. As the vacuoles are much smaller than the multigrain amyloplasts many vacuoles attach to each starch packet. All of these small vacuoles eventually fuse with one another to enclose each starch packet in a continuous vacuole. Ultimately, all vacuoles coalesce creating a vacuome that extends throughout the cell containing most of the multigrain amyloplasts and protein bodies of the central cell. Once fusion has occurred protein bodies and starch packets begin to break down. The breakdown of multigrain amyloplasts not only involves the separation of constituent grains but also a reduction in grain size. Protein body degradation involves a loss in their condensed state forming flocculent material in the vacuole. Staining of sections with Coomassie Brilliant Blue shows that, in later stages of development before fertilization, proteins can be detected throughout the soybean central cell in the

vacuoles enclosing multigrain amyloplasts.

The possession of large amounts of protein and carbohydrate in the soybean central cell suggests that it may be involved in sequestering nutritional reserves. The overall process of development of nutrient reserves (amyloplasts and protein bodies), vacuolar fusion and breakdown in soybean is roughly similar to that observed in endosperm of wheat (Bechtel et al., 1982a, 1982b), *Oryza* (Bechtel & Pomeranz, 1978, 1980; Harris & Juliano, 1977; Saigo et al., 1983) and oats (Bechtel & Pomeranz, 1981; Saigo et al., 1983) and also the cotyledons of pea (Craig et al., 1980; Goodchild & Craig, 1982) and cowpea (Harris & Boulter, 1976). This has important consequences for the future development of the egg, zygote, embryo and endosperm as the embryo sac has already acquired large amounts of nutritional reserves and begun the process of breaking them down in the central cell vacuome before fertilization many of the metabolites needed for growth and development are present in the embryo sac to be drawn upon after gametic fusion.

#### The antipodals:

With cellularization of the soybean embryo sac 3 irregularly shaped antipodals are formed at its chalazal end. Antipodal cells in soybean are said to either degenerate at some point before fertilization (George et al., 1979; Kennell & Horner, 1985; Pamplin, 1963) or to persist until fertilization occurs (Prakash & Chan, 1976). In the variety of soybean used in this research, Gnome, the antipodals were seen to degenerate well before embryo sac maturity.

As the antipodals show a great deal of variability in both longevity and structure it is difficult to draw any conclusions about their function (Willemse & van Went, 1984). Perhaps, because of their ephemeral nature ultrastructural reports have only been provided in *Gasteria* (Willemse & Kapil, 1981), spinach (Wilms, 1981), *Helianthus* (Newcomb, 1973a) and *Zea* (Diboll & Larson, 1966). Antipodals in different angiosperms exhibit structural features that suggest an absorptive function. Masand and Kapil (1966) list many angiosperms that form antipodal haustoria and wall ingrowths have been shown to develop in antipodals of *Papavera*



(Olson & Cass, 1981), *Stipa* (Maze & Lin, 1975), *Helianthus* (Newcomb, 1973a) and *Zea* (Diboll & Larson, 1966). Support for a nutritive function does not appear to be universal. Coe (1954) followed the movement of  $C^{14}$  through the ovule of a plant with a hypostase. He was not able to demonstrate  $C^{14}$  in the hypostase and since it encloses the chalazal end of the embryo sac postulated that nutrients would not enter the embryo sac by way of the antipodals.

Like the egg and synergids the antipodal apparatus walls initially lack an observable middle lamella. However the antipodal walls develop an electron dense region, which may be a middle lamella, before senescence while those of the egg apparatus do not. The observation that walls of both the egg and antipodal apparatus do not initially possess middle lamellae tends to support statements by Brown (1909) and Brown and Sharp (1911) that cellularization occurs in a similar manner at both ends of the embryo sac. In soybean, plasmodesmata are present in the embryo sac wall connecting the inner nucellus to the antipodals, in all walls of the antipodals and in the antipodal/central cell wall. In both *Helianthus* (Newcomb, 1973a) and *Gasteria* (Willemse & Kapil, 1981) plasmodesmata exhibit a similar pattern leading Willemse and Kapil (1981) to propose that the antipodals provide a symplastic route between the nucellus and the central cell. Although a similar proposal could be made for soybean the period of activity for the pathway is limited as the plasmodesmata appear to be lost after degeneration of the antipodals. Since the antipodals degenerate during multigrain amyloplast expansion the pathway provided by these cells cannot be the only one responsible for central cell nutrition and growth of the starch grains.

#### The central cell and egg apparatus after pollen tube entry:

The observation that the pollen tube of soybean has grown into a synergid and is closely associated with the filiform apparatus agrees with reports on barley (Cass & Jensen, 1970), *Capsella* (Schulz & Jensen, 1968a), cotton (Jensen & Fisher, 1968), *Epidendrum* (Cocucci & Jensen, 1969), *Nicotiana* (Mogensen & Suthar, 1979), *Petunia* (van Went, 1970c), *Proboscidea* (Mogensen, 1978b), *Quercus* (Mogensen, 1972) and *Torenia* (van der Pluijm,

1964). The relationship between the point of pollen tube entry into the embryo sac and the possession and position of a filiform apparatus appears quite strong. Even in *Plumbago*, a synergidless plant, a modification of the egg cell micropylar wall forms a filiform apparatus (Cass, 1972, Cass & Karas, 1975). Here, as in other plants, it is near the filiform apparatus that the pollen tube enters the embryo sac (Russell, 1982; Russell & Cass, 1981).

The synergids ultrastructural appearance immediately before pollen tube entry appears to vary from degenerate to normal (van Went & Willemse, 1984). In cotton (Jensen & Fisher, 1968) and *Nicotiana* (Mogensen & Suthar, 1979) synergid degeneration begins before pollen tube entry while in *Capsella* (Schulz & Jensen, 1968a) and *Helianthus* (Newcomb, 1973b) the process does not appear to start until after pollen tube penetration. It has been proposed that this type of degeneration aids in directing pollen tube growth into the synergid (Jensen & Fisher, 1968; Mogensen, 1978a). In soybean two conflicting views have been proposed about the physiological state of the synergids before pollen tube entry. Kennell and Horner (1985) reported that the synergid which received the pollen tube persists after entry while Tilton et al. (1983) stated that the pollen tube enters a degenerate synergid. Evidence from the present research suggests that whatever the physiological state at the time of pollen tube entry the synergid of *Gnome* becomes degenerate soon afterwards.

Free sperm nuclei were seen in both the egg and central cell of soybean. Based on the presence of chromatin bands the soybean sperm nuclei appear similar to those in barley (Cass, 1973; Cass & Karas, 1975) and rye (Karas & Cass, 1976). The lack of nucleoli in sperms present in target cells of soybean is different from reports in cotton (Jensen & Fisher, 1967) and *Plumbago* (Russell & Cass, 1981). Changes begin to occur in the soybean egg after sperm entry. Besides formation of additional wall material and development of numerous amyloplasts the cell's major vacuole begins to fragment. Also, the persistent synergid exhibits changes. At this developmental stage the large chalazal vacuole begins to break up, numerous small vacuoles are formed and a higher level of Golgi activity is observed in the persistent synergid of soybean. A new polarity is also seen in this cell with most of the cellular organelles now located in the micropylar two-thirds of the synergid. Although it is not known

whether these changes represent the beginning of persistent synergid degeneration, it seems likely that the production of many small vacuoles and Golgi bodies in the cell may represent the beginning of an elevated level of lytic activity.

Cells of the soybean egg apparatus undergo marked changes after fertilization. The large central vacuole of the zygote breaks up, the cell decreases in volume and now possesses a large amount of starch. This reduction of egg/zygote volume is referred to as zygotic shrinkage and has also been reported in cotton (Jensen, 1968) and *Hibiscus* (Ashley, 1972). Ashley (1972), after studying hybrids in *Hibiscus*, proposed that zygotic shrinkage was a usual occurrence and necessary for "normal embryonic differentiation". In soybean, prior to karyogamy, vacuoles were observed fused with the plasmalemma of both the egg and central cell. This fusion was restricted to areas where the degenerate synergid cytoplasm had separated the egg and central cell plasma membranes and may be involved in the process of zygotic shrinkage in soybean.

An elevation of nutritional reserves in the zygote over levels in the egg has been noted in a number of plants either in the form of starch (Jensen, 1968) or lipids (Schulz & Jensen, 1968b). In soybean the zygote also possesses a greater amount of starch than the mature egg, however, the increase in this type of reserve begins before sperm and egg nuclear fusion occurs. There are also changes in the nature of the zygote wall. Before fertilization the wall that encloses the chalazal end of the egg is composed of packets of wall material separated by areas of plasma membrane contact. After fertilization the amount of wall enclosing the early zygote increases forming a complete wall around the cell. This is apparently a common occurrence and has been seen in all plants whose zygote has been investigated at an ultrastructural level (Mogensen, 1972). However, in soybean, the formation of a complete wall begins before fertilization is complete and, along with the increase in nutritional reserves, may be more a response to egg/sperm cell plasmogamy than karyogamy.

After fusion of the polar nucleus with a sperm cell to form the 1' endosperm nucleus the central cell become highly vacuolate. Development of the vacuome and corresponding destruction of the multiple amyloplasts actually begins well before fertilization and

ultimately results in only a few multigrain amyloplasts remaining along the walls of the cell with the remainder occupied by a large vacuole. Numerous mitotic divisions of the soybean 1' endosperm nucleus occur to form the initially free nuclear endosperm.

The first mitotic division in the young proembryo of soybean is perpendicular to its long axis and establishes the terminal and more vacuolate basal cell. Maheshwari (1950) reported that this type of division is normal for dicots and Pamplin (1963) has classified soybean embryo development as of the Onograd type. In a situation similar to *Capsella* (Schulz & Jensen, 1968b) and *Helianthus* (Newcomb, 1973b) plasmodesmata were seen in the newly formed wall between terminal and basal cells. Soybean, however, differs that it has plasmodesmata not only in the wall separating the basal cell from the central cell but also in the wall between the terminal and central cell. The wall separating the terminal and basal cells from the central cell can be seen as an elaboration of the egg and zygote walls. During the development of the 2-celled proembryo a middle lamella develops in this wall. The lack of a middle lamella in the young egg apparatus cell walls of *Hartmannia* has been reported before (Johansen, 1929); however, the development of a middle lamella has not been discussed previously: As the middle lamella is the first wall layer laid down during wall formation its differentiation in existing cell walls is problematical and suggests that these walls may be structurally unique.

#### Involvement of transfer cells in embryo nutrition:

Throughout the development of the gametophyte and sporophyte generations the soybean embryo sac and ovule forms wall ingrowths. According to Pate and Gunning (1972) any cell which contains wall ingrowths and is thought to be involved in short distance transport of solutes can be termed transfer cells. This means not only the embryonic basal cell, distal cells of the suspensor, some of the cells of the micropylar end of the nucellus and inner integuments are transfer cells, but also the central cell of the embryo sac of soybean.

Although direct evidence of a transport function for transfer cells is lacking there are reports linking development of wall ingrowths to initiation of metabolite transport. Some of

this evidence is provided by tracer studies (Gunning et al., 1968), metabolite uptake experiments (Browning & Gunning, 1979b, 1979c) and enzyme histochemistry (Brentwood & Cronshaw, 1978). It has been reported that the movement of sugars into sieve tube members is an energy consuming process and that the hydrolysis of adenosine triphosphate by an adenosine triphosphatase (ATPase) could play an important role in supplying the necessary energy (Gilder & Crownshaw, 1973). Brentwood and Crownshaw (1978) established a linkage between the development of ingrowths and ATPase activity by showing that in *Pisum* the plasmalemma of phloem transfer cells was positive for this enzyme only after wall ingrowths were formed. A correlation between ingrowth appearance and transport was also demonstrated by Gunning, Pate and Briarty (1968) who used labeled  $CO_2$  to study the phloem of *Pisum* and showed that development of wall ingrowths in its phloem transfer cells occurred only when export of metabolites from the leaf began. Additional proof for transfer cells having a transport function comes from a series of papers by Browning & Gunning (1979a, 1979b, 1979c) on the structure and function of transfer cells in the sporophyte haustoria of *Funaria hygrometrica* was discussed. This involved determining rates of uptake of both glucose and sucrose into transfer cells that develop at the base of *Funaria* sporophytes. Flux rates for absorption of glucose, expressed in terms of amount of uptake per unit tissue weight, were 50 times greater in the sporophyte haustoria of *Funaria* than in typical plant tissue. Only when these rates were adjusted to compensate for the surface amplification caused by wall ingrowths did the value for the transfer cells of *Funaria* become similar to that determined for other plants (Browning & Gunning, 1979b). All these findings tend to support the conclusion that wall ingrowths appear in a cell only at times of active transport and augment metabolite flow by increasing membrane area (Gunning & Pate, 1969). Although factors causing development of wall ingrowths have not been firmly established, it has been suggested that they develop because of a deficiency in the transport system between metabolite source and sink (Pate et al., 1970).

There is good circumstantial evidence that wall ingrowths play a part in facilitating solute movement and that their appearance signifies the beginning or intensification of this

type of activity. Therefore the sequential development of transfer cells in different areas of the soybean ovule could provide information about which parts of the structure are involved in elevated levels of transport thus aiding our understanding of the nutritional environment of the embryo and developing endosperm of soybean. These observations however, cannot tell us anything about the specific nature of metabolites that might be undergoing importation into the embryo sac.

The small collection of nucellar transfer cells found around the micropylar region of the post-fertilization embryo sac could well serve as a mechanism for metabolites to be "exported" from the nucellus to the developing embryo sac. Pate and Gunning (1972) reported that the possession of plasmodesmata connecting transfer cells to surrounding cells was a common occurrence and that these plasmodesmata would allow the transfer cells to draw upon the rest of the symplast for metabolites. In a similar manner the presence of plasmodesmata in walls common with the vacuolate cells may facilitate movement of metabolites from the soybean nucellus to the transfer cells for exportation to the embryo sac. The collection of transfer cells formed, in later stages of development, at the base of the inner integuments could function in much the same way as nucellar transfer cells.

Wall ingrowths found in the chalazal region of the central cell suggest that this area is involved in solute flux. It is interesting to note that these wall ingrowths develop at the micropylar base of the central cell at a time when starch packet formation is occurring. This temporal association between starch packet formation and central cell wall ingrowth development suggest that these micropylar wall ingrowths are also formed in response to metabolite flux. It is possible that the appearance of the second set of wall ingrowths in the chalazal region of the central cell of soybean is similar in that it signals the beginning of an elevated level of metabolite flux into this region of the central cell. Such a flux in the embryo sac of soybean might be important in the energy requiring process of free nuclear endosperm formation. Besides wheat (Fineran et al., 1982) wall ingrowths have been observed in the chalazal region of the central cell of *Capsella* where it has been proposed that they function in the absorption of nutrients from crushed nucellar cells (Schulz & Jensen, 1974).

In soybean the embryonic basal cell and degenerated synergid walls are in contact. In this region ingrowths from the basal cell wall are directed into the basal cell of the suspensor. Although wall ingrowths have been reported to be associated with the degenerate synergid of cotton (Schulz & Jensen, 1977), they were directed into the base of the central cell. Schulz and Jensen (1977) proposed that the synergid's contents were being used by the developing endosperm and that the function of wall ingrowths was to facilitate this process. A similar activity can be envisaged in soybean although the developing embryo appears to be the recipient.

The occurrence of wall ingrowths in the basal and suspensor cells of angiosperm embryos has been noted before. Wall ingrowths have been reported in the basal cell of *Capsella* (Schulz & Jensen, 1968b, 1969), *Stellaria* (Newcomb & Fowke, 1974) and soybean (Dute & Peterson, 1984) also in the suspensor of *Phaseolus* (Clutter & Sussex, 1968; Yeung & Clutter, 1979). Experiments with the suspensor of *Phaseolus* have shown that it is the main site of labeled sucrose uptake during early embryo development (Yeung, 1980). A similar pathway for embryo nutrition can be envisaged in soybean with the wall ingrowths in the basal and more micropylar cells of the suspensor aiding in absorption of metabolites.

#### Embryo sac wall as a common apoplast in soybean:

The question of embryo nutrition has long been of interest. Haberlandt (1914) expressed the opinion that all young flowering plant embryos were parasitic organisms. It has since been realized that the developing embryo is not only parasitic on but cytoplasmically isolated from maternal tissue (Pate & Gunning, 1972). Therefore materials must move from surrounding tissue through the embryo sac wall to the developing embryo and endosperm. In soybean the wall enclosing the embryo sac is continuous, lacks plasmodesmata and can be considered a common apoplast despite regional variations in thickness. It has been shown that transport in a wall is a passive process regulated by size of pores in the cellulose framework and the ionic charges of groups attached to the matrix material (Lüttge & Higinbotham, 1979). The work of Brentwood & Crownshaw (1978) established that ATPase activity in

*Pisum* phloem transfer cells occurred along the entire length of the plasmalemma and was not localized near areas of wall ingrowths. Since there is no evidence that the embryo sac wall or the plasmalemma of the cells connected to it differ regionally in their ability to allow for transport of metabolites it is probable that solutes diffuse through this wall in all directions according to their individual potentials and enter embryo sac cells along the entirety of their plasma membranes.

The question arises, by what route do the developing embryo and central cell obtain metabolites? I have presented structural evidence that the embryo and central cell of soybean can only be absorbing materials from the embryo sac wall. It seems reasonable to assume that the embryo sac wall, as a common apoplast, be considered as both a sink and a source for solutes *en route* to the developing embryo sac and that the point of entry of a metabolite from the nucellus and the point of exit of that same molecule to cells of the embryo sac cannot be simply considered as "across the embryo sac wall".

This concept may be important in understanding the significance of transfer cells associated with the embryo sac wall both before and after fertilization. It seems probable that transfer cells, which occur in the micropylar nucellus and the base of the inner integuments of soybean, could function in supplying the embryo sac wall with metabolites. These transfer cells could develop either because these areas represent a deficiency in the transport pathway (Pate et al., 1970) or simply because there is heavier metabolite requirement in the micropylar region of the embryo sac. The development of wall ingrowths in the central cell, embryonic basal cell and suspensor cells of soybean could be seen as a means to facilitate uptake of soluble metabolites from the same embryo sac wall. The presence of wall ingrowths covering most of the micropylar base of the embryo sac during stages of development discussed in this thesis suggests that this region requires an elevated level of transport because it is metabolically dynamic. On this point my interpretation and that of Jensen (1972) are in agreement.



#### V. Literature cited

- Ashley, T. 1972. Zygote shrinkage and subsequent development in some *Hibiscus* hybrids. *Planta* 108:303-317.
- Banerji, I. 1938. A note on the embryology of the ground nut (*Arachis hypogaea* L.). *J. Bombay Nat. Hist. Soc.* 40:539-543.
- Battaglia, E. 1951. The male and female gametophyte of angiosperms an interpretation. *Phytomorph.* 1:87-116.
- Bechtel, D. B., R. L. Gaines, and Y. Pomeranz. 1982a. Early stages in wheat endosperm formation and protein body initiation. *Ann. Bot.* 50:507-518.
- Bechtel, D. B., R. L. Gaines, and Y. Pomeranz. 1982b. Protein secretion in wheat endosperm formation of the matrix protein. *Cereal Chem.* 59:336-343.
- Bechtel, D. B., and B. O. Juliano. 1980. Formation of protein bodies in the starchy endosperm of rice (*Oryza sativa* L.): A re-investigation. *Ann. Bot.* 45:503-509.
- Bechtel, D. B., and Y. Pomeranz. 1978. Ultrastructure of the mature ungerminated rice (*Oryza sativa*) caryopsis. The starchy endosperm. *Amer. J. Bot.* 65:684-691.
- Bechtel, D. B., and Y. Pomeranz. 1980. Formation of protein bodies in the starch endosperm of rice (*Oryza sativa* L.): A re-investigation. *Ann. Bot.* 45:503-509.
- Bechtel, D. B., and Y. Pomeranz. 1981. Ultrastructure and cytochemistry of mature oat (*Avena sativa* L.) endosperm. The Aleurone layer and starchy endosperm. *Cereal Chem.* 58:61-69.
- Behnke, O., and T. Zelander. 1970. Preservation of intercellular substances by the cationic dye alcian blue in preparative procedures for electron microscopy. *J. Ultra. Res.* 31:424-438.
- Bhandari, N. N., and A. Sachdeva. 1983. Some aspects of organization and histochemistry of the embryo sac of *Scilla sibirica* Sato. *Protoplasma* 116:170-178.
- Bharathi, M. and U. R. Murty. 1984. Comparative embryology of wild and cultivated species of *Arachis*. *Phytomorph.* 34:48-56.
- Bouillot, J. 1969. Individualisation progressive des cellules du sac embryonnaire chez le

- Juglans regia* L. Rev. Cytol. Biol. Veg. 32:203-208.
- Bowes, B. G. 1969. Electron microscopic observations on myelin-like bodies and related membranous elements in *Glechoma hederacea* L. Z. Pflanzenphysiol. Bd. 60:414-417.
- Brentwood, B. J., and J. Cronshaw. 1978. Cytochemical localization of adenosine triphosphatase in the phloem of *Pisum sativum* and its relation to the function of transfer cells. Planta 140:111-120.
- Brown, M. M. 1917. The development of the embryo-sac and of the embryo in *Phaseolus vulgaris*. Bull. Torrey Bot. Club 44:535-544.
- Brown, W. H. 1909. The embryo sac of *Habenaria*. Bot. Gaz. 48:241-250.
- Brown, W. H., and L. W. Sharp. 1911. The embryo sac of *Epipactis*. Bot. Gaz. 52:439-452.
- Browning, A. J., and B. E. S. Gunning. 1979a. Structure and function of transfer cells in the sporophyte haustorium of *Funaria hygrometrica* Hedw. I. The development and ultrastructure of the haustorium, J. Exp. Bot. 30:1233-1246.
- Browning, A. J., and B. E. S. Gunning. 1979b. Structure and function of transfer cells in the sporophyte haustorium of *Funaria hygrometrica* Hedw. II. Kinetics of uptake of labelled sugars and localization of absorbed products by freeze-substitution and autoradiography. J. Exp. Bot. 30:1247-1264.
- Browning, A. J., and B. E. S. Gunning. 1979c. Structure and function of transfer cells in the sporophyte haustorium of *Funaria hygrometrica*. III. Translocation of assimilates into the attached sporophytes and along the seta of attached and excised sporophytes. J. Exp. Bot. 30:1265-1273.
- Buell, K. M. 1952. Developmental morphology in *Dianthus*. II. Starch accumulation in ovule and seed. Amer. J. Bot. 39:458-467.
- Carroll, T. W., and D. E. Mayhew. 1976. Anther and pollen infection in relation to the pollen and seed transmissibility of two strains of barley stripe mosaic virus in barley. Can. J. Bot. 54:1604-1621.
- Cass, D. D. 1972. Occurrence and development of a filiform apparatus in the egg of *Plumula capensis*. Amer. J. Bot. 59:279-283.

- Cass, D. D. 1973. An ultrastructural and Nomarski-interference study of the sperms of barley. *Can. J. Bot.* 51:601-605.
- Cass, D. D., and W. A. Jensen. 1970. Fertilization in barley. *Amer. J. Bot.* 57:62-70.
- Cass, D. D., and I. Karas. 1975. Development of sperm cells in barley. *Can. J. Bot.* 53:1051-1062.
- Cass, D. D., D. J. Peteya, and B. L. Robertson. 1985. Megagametophyte development in *Hordeum vulgare*. 1. Early megagametogenesis and the nature of cell wall formation. *Can. J. Bot.* 63:2164-2171.
- Clutter, M. E., and I. M. Sussex. 1968. Ultrastructural development of bean embryo cells containing polytene chromosomes. *J. Cell Biol.* 39:26a.
- Cocucci, A., and W. A. Jensen. 1969. Orchid embryology: Megagametophyte of *Epidendrum scutella* following fertilization. *Amer. J. Bot.* 56:629-640.
- Coe, G. E. 1954. Distribution of carbon 14 in ovules of *Zephyranthes drummondii*. *Bot. Gaz.* 115:342-346.
- Cole, M. B., Jr., and S. M. Sykes. 1974. Glycol methacrylate in light microscopy: A routine method for embedding and sectioning animal tissues. *Stain Tech.* 49:387-400.
- Cooper, D. C. 1931. Macrosporogenesis and the development of the macrogametophyte of *Lycopersicon esculentum*. *Amer. J. Bot.* 18:739-751.
- Cooper, D. C. 1933. Macrosporogenesis and embryology of *Melilotus*. *Bot. Gaz.* 95:143-155.
- Cooper, D. C. 1935a. Macrosporogenesis and development of the embryo sac of *Lilium henryi*. *Bot. Gaz.* 97:346-355.
- Cooper, D. C. 1935b. Macrosporogenesis and embryology of *Medicago*. *J. Agr. Res.* 51:471-477.
- Cooper, D. C. 1937. Macrosporogenesis and embryo-sac development in *Euchlaena mexicana* and *Zea mays*. *J. Agr. Res.* 55:539-551.
- Cooper, D. C. 1939. Development of megagametophyte in *Erythronium albidum*. *Bot. Gaz.* 100:862-867.
- Cooper, D. C. 1941. Macrosporogenesis and the development of the seed of *Phryma*

- Leptostachya*. Amer. J. Bot. 28:755-761.
- Cooper, D. C. 1946. Double fertilization in *Petunia*. Amer. J. Bot. 33:44-57.
- Cooper, G. O. 1942. Development of the ovule and the formation of the seed in *Plantago lanceolata*. Amer. J. Bot. 29:577-581.
- Craig, S., D. J. Goodchild, and A. R. Hardham. 1979. Structural aspects of protein accumulation in developing pea cotyledons. I. Qualitative and quantitative changes in parenchyma cell vacuoles. Aust. J. Plant Physiol. 6:81-98.
- Craig, S., D. J. Goodchild, and C. Miller. 1980. Structural aspects of protein accumulation in developing pea cotyledons. II. Three-dimensional reconstructions of vacuoles and protein bodies from serial sections. Aust. J. Plant Physiol. 7:329-337.
- Curgy, J. J. 1968. Influence du mode de fixation sur la possibilité d'observer les structures myéliniques des hépatocytes d'embryons de poulet. J. Microscopie 7:63-74.
- Daddow, L. Y. M. 1983. A double lead stain method for enhancing contrast of ultrathin sections in electron microscopy: a modified multiple staining technique. J. Microsc. 129:147-153.
- Dahlgren, K. V. O. 1927. Über das vorkommen von Stärke in den Embryosackchen der Angiosperms. Ber. Deutsch. Bot. Ges. 45:374-384.
- Dahlgren, K. V. O. 1939. Sur la présence d'amidon dans le sac embryonnaire chez les Angiosperms. Bot. Notiser 1939:221-231.
- Davis, G. L. 1964a. Embryological studies in the Compositae. IV. Sporogenesis, gametogenesis, and embryogeny in *Brachycome ciliaris* (Labill.) Less. Aust. J. Bot. 12:142-151.
- Davis, G. L. 1964b. Development of the female gametophyte of *Minuria cunninghamii* (DC.) Benth. (Compositae). Aust. J. Bot. 12:152-156.
- Davis, G. L. 1966. *Systematic embryology of the Angiosperms*. John Wiley & Sons, Inc., New York.
- Diboll, A. G., and D. A. Larson. 1966. An electron microscopic study of the mature megagametophyte in *Zea mays*. Amer. J. Bot. 53:391-402.

- Dickinson, H. G., and L. Andrews. 1977. The role of membrane-bound cytoplasmic inclusions during gametogenesis in *Lilium longiflorum* Thunb. *Planta* 134:229-240.
- Dickinson, H. G., and U. Potter. 1978. Cytoplasmic changes accompanying the female meiosis in *Lilium longiflorum* Thunb. *J. Cell Sci.* 29:147-169.
- Dute, R., and C. M. Peterson. 1984. Features of the proembryo and free nuclear endosperm of soybean, *Glycine max* (L.) Merr. *Amer. J. Bot.* 71(5) pt. 2:25.
- Engell, K., and G. B. Petersen. 1976. Integumentary and endothelial cells of *Bellis perennis*. *Bot. Tidsskrift* 71:237-244.
- Evans, A. T. 1919. Embryo sac and embryo of *Pentstemon secundiflorus*. *Bot. Gaz.* 67:427-437.
- Farley, H. M., and A. H. Hutchinson. 1941. Seed development in *Medicago* (alfalfa) hybrids. I. The normal ovule. *Can. J. Res. (sec. c)* 19:421-437.
- Feder, N., and T. P. O'Brien. 1968. Plant microtechnique: some principles and new methods. *Amer. J. Bot.* 55:123-142.
- Fineran, B. A. 1971. Ultrastructure of vacuolar inclusions in root tips. *Protoplasma* 73:1-18.
- Fineran, B. A., D. J. C. Wild, and M. Ingerfield. 1982. Initial wall formation in the endosperm of wheat, *Triticum aestivum*: a reevaluation. *Can. J. Bot.* 60:1773-1793.
- Folsom, M. W. 1981. An ultrastructure study of the embryo sac of soybean *Glycine max* (L.) Merr. M. Sc. Thesis, Auburn University.
- Folsom, M. W., and C. M. Peterson. 1984. Ultrastructural aspects of the mature embryo sac of soybean, *Glycine max* (L.) Merr. *Bot. Gaz.* 145:1-10.
- George, G. P., R. A. George, and J. M. Herr Jr. 1979. A comparative study of ovule and megagametophyte development in field-grown and greenhouse-grown plants of *Glycine max* and *Phaseolus aureus* (Papilionaceae). *Amer. J. Bot.* 66:1033-1043.
- Gilder, J., and J. Cronshaw. 1973. Adenosine triphosphatase in the phloem of *Cucurbita*. *Planta* 110:189-204.
- Goodchild, D. J., and S. Craig. 1982. Structural aspects of protein accumulation in developing pea cotyledons. IV. Effects of preparative procedures on ultrastructural

- integrity. *Aust. J. Plant Physiol.* 9:689-704.
- Gordon-Weeks, P. R., R. D. Burgoyne, and E. G. Gray. 1982. Presynaptic microtubules: Organisation and assembly/disassembly. *Neuroscience* 7:739-749.
- Gori, P. 1977. Wall ingrowths in the embryo sac of *Euphorbia helioscopia*. *Israel J. Bot.* 26:202-208.
- Gunning, B. E. S., and J. S. Pate. 1969. "Transfer Cells" Plant cells with wall ingrowths, specialized in relation to short distance transport of solutes - their occurrence, structure, and development. *Protoplasma* 68:107-133.
- Gunning, B. E. S., and J. S. Pate. 1974. Transfer cells. Pages 441-480. In: *Dynamic aspects of plant ultrastructure*. A. W. Robards, ed. McGraw-Hill Book Co. (U.K.) Limited, Maidenhead, England.
- Gunning, B. E. S., J. S. Pate, and L. G. Briarty. 1968. Specialized "transfer cells" in veins of leaves and their possible significance in phloem translocation. *J. Cell Biol.* 37:C7-12.
- Gunning, B. E. S., J. S. Pate, and L. W. Green. 1970. Transfer cells in the vascular system of stems: taxonomy, association with nodes, and structure. *Protoplasma* 71:147-171.
- Haberlandt, G. 1914. *Physiological plant anatomy*, 4th ed., Translated by M. Drummond, Macmillan & Co., London: Reprinted, 1965, Today & Tomorrow's Book Agency, New Delhi, India.
- Harris, N., and D. Boulter. 1976. Protein body formation in cotyledons of developing cowpea (*Vigna unguiculata*) seeds. *Ann. Bot.* 40:739-744.
- Harris, N., and B. O. Juliano. 1977. Ultrastructure of endosperm protein bodies in developing rice grains differing in protein content. *Ann. Bot.* 41:1-5.
- Haskell, D. A., and S. N. Postlethwait. 1971. Structure and histogenesis of the embryo of *Acer saccharinum*. I. Embryo sac and proembryo. *Amer. J. Bot.* 58:595-603.
- Hepler, P. K. 1976. Plant microtubules. pages 142-187. In: *Plant biochemistry*. Third Ed., J. Bonner and J. E. Varner, ed., Academic Press, New York.
- Hepler, P. K. 1981. The structure of the endoplasmic reticulum revealed by osmium tetroxide

- potassium ferricyanide staining. *Eur. J. Cell Biol.* 26:102-110.
- Heslop-Harrison, J. 1972. Sexuality in angiosperms. pages 133-289. In: *Plant Physiology a treatise. Vol. VIc: Physiology of Development: From seeds to sexuality*. F. C. Steward, ed. Academic Press, New York.
- Heslop-Harrison, J. 1979. Aspects of the structure, cytochemistry and germination of the pollen of rye (*Secale cereale* L.). *Ann. Bot.* 44:1-47 (supplement #1).
- Heslop-Harrison, J., and A. Mackenzie. 1967. Autoradiography of soluble [ $2\text{-}^{14}\text{C}$ ] thymidine derivatives during meiosis and microsporogenesis in *Lilium* anthers. *J. Cell Sci.* 2:387-400.
- Hindmarsh, G. J. 1964. Gametophyte development in *Trifolium pratense*. L. *Aust. J. Bot.* 12:1-14.
- Hoagland, D. R., and D. I. Arnon. 1950. The water culture method for growing plants without soil. *Calif. Agric. Exp. Sta. Circ.* #347, 32 pages.
- Howe, T. D. 1926. Development of embryo sac in *Grindelia squarrosa*. *Bot. Gaz.* 81:280-296.
- Howe, T. D. 1969. The female gametophyte of *Machaeranthera pattersonii* (*Aster pattersonii*) and of *M. macetifolia*. *Amer. J. Bot.* 56:641-645.
- Howe, T. D. 1975. The female gametophyte of three species of *Grindelia* and of *Prionopsis ciliata* (Compositae). *Amer. J. Bot.* 62:273-279.
- Hughes, J., and M. E. McCully. 1975. The use of an optical brightener in the study of plant structure. *Stain Tech.* 50:319-329.
- Ishikawa, R. M. 1918. Studies on the embryo sac and fertilization of *Oenothera*. *Ann. Bot.* 32:279-317.
- Isreal, H. W., and Y. Sagawa. 1964. Post-pollination ovule development in *Dendrobium* orchids. II. Fine structure of the nucellar and archesporial phases. *Caryologia* 17:301-316.
- Isreal, H. W., and Y. Sagawa. 1965. Post-pollination ovule development in *Dendrobium* orchids. III. Fine structure of meiotic prophase I. *Caryologia* 18:15-34.
- Jensen, W. A. 1962. *Botanical histochemistry: principles and practice*. W. H. Freeman and Co., San Francisco.

- Jensen, W. A. 1963. Cell development during plant embryogenesis. Brookhaven Symposium in Biology 16:179-202.
- Jensen, W. A. 1965a. The ultrastructure and histochemistry of the synergids of cotton. Amer. J. Bot. 52:238-256.
- Jensen, W. A. 1965b. The ultrastructure and composition of the egg and central cell of cotton. Amer. J. Bot. 52:781-797.
- Jensen, W. A. 1968. Cotton embryogenesis: the zygote. Planta 79:346-366.
- Jensen, W. A. 1972. The embryo sac and fertilization in angiosperms. Harold L. Lyon Arbor. Lect. 3:1-32.
- Jensen, W. A., and D. B. Fisher. 1967. Cotton embryogenesis: Double fertilization. Phytomorph. 17:261-269.
- Jensen, W. A., and D. B. Fisher. 1968. Cotton embryogenesis: The entrance and discharge of the pollen tube in the embryo sac. Planta 78:158-183.
- Johansen, D. A. 1928. The hypostase: its presence and function in the ovule of the Onagraceae. Proc. Nat. Acad. Sci. 14:710-713.
- Johansen, D. A. 1929. Studies on the morphology of Onagraceae. I. The megagametophyte of *Hartmannia tetraptera*. Bull. Torrey Bot. Club 56:285-299.
- Johansen, D. A. 1945. A critical survey of the present status of plant embryology. Bot. Rev. 11:87-107.
- Johansen, D. A. 1950. *Plant embryology*. Chronica Botanica Company, Waltham, Mass., U. S. A.
- Kapil, R. N., and S. C. Tiwari. 1978. Plant embryological investigations and fluorescence microscopy: an assessment of integration. Inter. Rev. Cytol. 53:291-331.
- Karas, I., and D. D. Cass. 1976. Ultrastructural aspects of sperm cell formation in rye: evidence for cell plate involvement in generative cell division. Phytomorph. 26:36-45.
- Kennell, J. C., and H. T. Horner. 1985. Megasporogenesis and megagametogenesis in soybean, *Glycine max*. Amer. J. Bot. 72:1553-1564.
- Khan, R. 1942. A contribution to the embryology of *Jussieua repens* Linn. J. Indian Bot. Soc.



21:267-282.

- Kuran, H. 1972. Callose localization in the walls of megasporocytes and megaspores in the course of development of monospore embryo sacs. *Acta Soc. Bot. Polon.* 41:519-539.
- Langlet, O. F. I. 1925. On the embryology of *Adenostyles*. *Sv. Bot. Tidskr.* 19:215-231.
- Langlet, O. 1927. Ueber die entwicklung des eiapparates in embryosack der Angiospermen. *Sv. Bot. Tidskr.* 21:478-485.
- Lillie, R. D., and H. M. Fullmer. 1976. *Histopathologic technique and practical histochemistry*. McGraw - Hill, Inc., New York.
- Luft, J. H. 1971. Ruthenium red and violet. I. Chemistry, purification, methods of use for electron microscopy and mechanism of action. *Anat. Rec.* 171:347-368.
- Lüttge, U., and N. Higinbotham. 1979. *Transport in Plants*. Springer-Verlag, New York.
- Maheshwari, P. 1950. *An introduction to the embryology of angiosperms*. McGraw - Hill, New York.
- Maheshwari, P., and A. R. Srinivasan. 1944. A contribution to the embryology of *Rudbeckia bicolor* Nutt. *New Phytol.* 43:135-142.
- Malik, C. P., and S. Vermani. 1975. Physiology of sexual reproduction I. A histochemical study of the embryo sac development in *Zephyranthes rosea* and *Lagenaria vulgaris*. *Acta Histochem.* 53:244-280.
- Martin, J. N. 1914. Comparative morphology of some Leguminosae. *Bot. Gaz.* 58:154-167.
- Masand, P., and R. N. Kapil. 1966. Nutrition of the embryo sac and embryo - a morphological approach. *Phytomorph.* 16:158-175.
- Matile, Ph. 1969. Plant lysosomes. pages 406-430. In: *Lysosomes in biology and pathology*. Vol. 1., J. T. Dingle and H. B. Fell, ed., North-Holland Publishing Co., London.
- Matile, Ph. 1976. Vacuoles. pages 189-224. In: *Plant biochemistry*. Third Ed., J. Bonner and J. E. Varner, ed., Academic Press, New York.
- Matile, Ph., and H. Moor. 1968. Vacuolation: origin and development of the lysosomal apparatus in root-tip cells. *Planta* 80:159-175.
- Maze, J., and Shu-Chang Lin. 1975. A study of the mature megagametophyte of *Stipa elmeri*.

- Can. J. Bot. 53:2958-2977.
- McLean, R. C., and W. R. Ivimey-Cook. 1956. *Textbook of theoretical botany* Vol. II., Longmans, Green & Co., New York.
- Mogensen, H. L. 1972. Fine structure and composition of the egg apparatus before and after fertilization in *Quercus gambelii*: The functional ovule. Amer. J. Bot. 59:931-941.
- Mogensen, H. L. 1978a. Synergids of *Proboscidea louisianica* (Martineaceae) before fertilization. Phytomorph. 28:114-122.
- Mogensen, H. L. 1978b. Pollen tube-synergid interactions in *Proboscidea louisianica* (Martineaceae). Amer. J. Bot. 65:953-964.
- Mogensen, H. L. 1981a. Ultrastructural localization of adenosine triphosphatase in the ovules of *Saintpaulia ionantha* (Gesneriaceae) and its relation to synergid function and embryo sac nutrition. Amer. J. Bot. 68:183-194.
- Mogensen, H. L. 1981b. Translocation of uranin within the living ovules of selected species. Amer. J. Bot. 68:195-199.
- Mogensen, H. L., and H. K. Suthar. 1979. Ultrastructure of the egg apparatus of *Nicotiana tabacum* (Solanaceae) before and after fertilization. Bot. Gaz. 140:168-179.
- Mollenhauer, H. H. 1964. Plastic embedding mixtures for use in electron microscopy. Stain Technol. 39:111-114.
- Mollenhauer, H. H., D. J. Mörré, and C. L. Jelsema. 1978. Lamellar bodies as intermediates in endoplasmic reticulum biogenesis in maize (*Zea mays* L.) embryo, bean (*Phaseolus vulgaris* L.) cotyledon, and pea (*Pisum sativum* L.) cotyledon. Bot. Gaz. 139:1-10.
- Newcomb, W. 1973a. The development of the embryo sac of sunflower *Helianthus annuus* before fertilization. Can. J. Bot. 51:863-878.
- Newcomb, W. 1973b. The development of the embryo sac of sunflower *Helianthus annuus* after fertilization. Can. J. Bot. 51:879-890.
- Newcomb, W., and L. C. Fowke. 1974. *Stellaria media* embryogenesis: the development and ultrastructure of the suspensor. Can. J. Bot. 52:607-614.
- Newcomb, W., and T. A. Steeves. 1971. *Helianthus annuus* embryogenesis: embryo sac wall

- projections before and after fertilization. *Bot. Gaz.* 132:367-371.
- Newcomer, E. H. 1953. A new cytological and histological fixing fluid. *Science* 118:161.
- Noher de Halac, I. 1980. Callose deposition during megagametogenesis in two species of *Oenothera*. *Ann. Bot.* 46:473-477.
- Noher de Halac, I., and C. Harte. 1977. Different patterns of callose wall formation during megasporogenesis in two species of *Oenothera* (*Onagraceae*). *Plant Syst. Evol.* 127:23-28.
- Norris, H. W. 1892. Development of the ovule in *Grindelia squarrosa*. *Amer. Nat.* 26:703-705. *pl.* 20.
- O'Brien, T. P., and M. E. McCully. 1981. *The study of plant structure: principles and selected methods*. Termarcaphi Pty, Ltd., Melbourne, Australia.
- Olson, R. A., and D. D. Cass. 1981. Changes in megagametophyte structure in *Papavera nudicaule* L. (*Papaveraceae*) following in vitro placental pollination. *Amer. J. Bot.* 68:1333-1341.
- Pace, L. 1909. The gametophytes of *Calopogon*. *Bot. Gaz.* 48:126-137.
- Palade, G. E., and A. Claude. 1949a. The nature of the golgi apparatus I. Parallelism between intercellular myelin figures and golgi apparatus in somatic cells. *J. Morphology* 85:35-69.
- Palade, G. E., and A. Claude. 1949b. The nature of the golgi apparatus II. Identification of the golgi apparatus with a complex of myelin figures. *J. Morphology* 85:71-111.
- Palser, B. F., W. R. Philipson, and M. N. Philipson. 1971. Embryology of *Rhododendron*. *J. Ind. Bot. Soc.* 50A:172-188.
- Pamplin, R. A. 1963. The anatomical development of the ovule and seed in the soybean. Ph.D. Thesis, University of Illinois (Diss. Abstr. 63-5128).
- Park, P., S. Yamamoto, K. Kohmoto, and H. Otani. 1982. Comparative effects of fixation methods using tannic acid on contrast of stained and unstained sections from Spurr-embedded plant leaves. *Can. J. Bot.* 60:1796-1804.
- Pate, J. S., and B. E. S. Gunning. 1972. Transfer cells. *Ann. Rev. Plant Physiol.* 23:173-196.
- Pate, J. S., B. E. S. Gunning, and F. F. Milliken. 1970. Function of transfer cells in the nodal regions of stems, particularly in relation to the nutrition of young seedlings.

- Protoplasma 71:313-334.
- Pettitt, J. M. 1977. The megaspore wall in gymnosperms: ultrastructure in some zooidogamous forms. Proc. R. Soc. Lond. B. 195:497-515.
- Prakash, N. 1979. Embryological studies on economic plants. New Zealand J. Bot. 17:525-534.
- Prakash, N., and Y. Y. Chan. 1976. Embryology of *Glycine max*. Phytomorphology 26:302-309.
- Pritchard, H. N. 1964. A cytochemical study of embryo sac development in *Stellaria media*. Amer. J. Bot. 51:371-378.
- Probst, A. H., and R. W. Judd. 1973. Origin, U.S. history and development, and world distribution. pages 1-16. In: *Soybeans: improvement, production, and uses*. B. E. Caldwell, ed., Agron. Monogr. 16, Amer. Soc. Agron., Madison, Wis.
- Reed, E. L. 1924. Anatomy, embryology, and ecology of *Arachis hypogaea*. Bot. Gaz. 78:289-310.
- Rees-Leonard, O. L. 1935. Macrosporogenesis and development of the megagametophyte of *Solanum tuberosum*. Bot. Gaz. 96:734-750. pl. 9-10.
- Reeves, R. G. 1930. Development of the ovule and embryo sac of alfalfa. Amer. J. Bot. 17:239-246.
- Rembert, D. H., Jr. 1967. Development of the ovule and megagametophyte in *Wisteria sinensis*. Bot. Gaz. 128:223-229.
- Rembert, D. H., Jr. 1969. Comparative megasporogenesis in Papilionaceae. Amer. J. Bot. 56:584-591.
- Rembert, D. H., Jr. 1977a. Ovule ontogeny, megasporogenesis, and early gametogenesis in *Trifolium repens* (Papilionaceae). Bot. 64:483-488.
- Rembert, D. H., Jr. 1977b. Contribution to ovule ontogeny in *Glycine max*. Phytomorph. 27:368-370.
- Robards, A. W. 1975. Plasmodesmata. Ann. Rev. Plant Physiol. 26:13-29.
- Rodkiewicz, B. 1968. Differences in the distribution pattern of callose in cell walls during

- megasporogenesis in some species of flowering plants. Bull. Acad. Polon. Sci., Ser. Sci. Biol. 16:663-665.
- Rodkiewicz, B. 1970. Callose in cell walls during megasporogenesis in Angiosperms. *Planta* 93:39-47.
- Rodkiewicz, B., and J. Bednara. 1974. Distribution of organelles and starch grains during megasporogenesis in *Epilobium*. pages 89-95. In: *Fertilization in Higher Plants*. H. F. Linskens, ed., North-Holland Publishing Co., Amsterdam.
- Rodkiewicz, B., and J. Bednara. 1976. Cell wall ingrowths and callose distribution in megaspores in some Orchidaceae. *Phytomorph.* 26:276-281.
- Rodkiewicz, B., and E. Mikulska. 1965. The development of cytoplasmic structures in the embryo sac of *Lilium candidum*, as observed with the electron microscope. *Planta* 67:297-304.
- Roland, J.-C. 1978. General preparation and staining of thin sections. In: J. L. Hall, ed., *Electron microscopy and cytochemistry of plant cells*. Elsevier/North-Holland Biomedical Press. New York.
- Roy, B. 1933. Studies in the development of the female gametophyte in some leguminous crop plants of India. *Indian J. Agric. Sci.* 3:1098-1107.
- Russell, S. D. 1979. Fine structure of megagametophyte development in *Zea mays*. *Can. J. Bot.* 57:1093-1110.
- Russell, S. D. 1982. Fertilization in *Plumbago zeylanica*: entry and discharge of the pollen tube in the embryo sac. *Can. J. Bot.* 60:2219-2230.
- Russell, S. D., and D. D. Cass. 1981. Ultrastructure of fertilization in *Plumbago zeylanica*. *Acta Soc. Bot. Poloniae* 50:185-189.
- Sachar, R. C., and H. Y. Mohan Ram. 1958. The embryology of *Plumbago zeylanica* Cham. *Phytomorph.* 8:114-124.
- Sagawa, Y., and H. W. Isreal. 1964. Post-pollination ovule development in *Dendrobium* orchids. I. Introduction. *Caryologia* 17:53-64.
- Saigo, R. H., D. M. Peterson, and J. Holy. 1983. Development of protein bodies in oat

- starchy endosperm. *Can. J. Bot.* 61:1206-1215.
- Schaffner, J. H. 1901. A contribution to the life history and cytology of *Erythronium*. *Bot. Gaz.* 31:369-387.
- Schnarf, K. 1936. Contemporary understanding of embryo-sac development among Angiosperms. *Bot. Rev.* 2:565-585.
- Schulz, P., and W. A. Jensen. 1971. *Capsella* embryogenesis: The chalazal proliferating tissue. *J. Cell Sci.* 8:201-227.
- Schulz, P., and W. A. Jensen. 1973. *Capsella* embryogenesis: the central cell. *J. Cell Sci.* 12:741-763.
- Schulz, P., and W. A. Jensen. 1974. *Capsella* embryogenesis: The development of the free nuclear endosperm. *Protoplasma* 80:183-205.
- Schulz, P., and W. A. Jensen. 1977. Cotton embryogenesis: the early development of the free nuclear endosperm. *Amer. J. Bot.* 64: 384-394.
- Schulz, P., and W. A. Jensen. 1981. Pre-fertilization ovule development in *Capsella*: Ultrastructure and ultracytochemical localization of acid phosphatase in the meiocyte. *Protoplasma* 107:27-45.
- Schulz, P., and W. A. Jensen. 1986. Pre-fertilization ovule development in *Capsella*: the dyad, tetrad, developing megaspore, and two-nucleate gametophyte. *Can. J. Bot.* 64:875-884.
- Schulz, S. R., and W. A. Jensen. 1968a. *Capsella* embryogenesis: the synergids before and after fertilization. *Amer. J. Bot.* 55:541-552.
- Schulz, S. R., and W. A. Jensen. 1968b. *Capsella* embryogenesis: The egg, zygote, and young embryo. *Amer. J. Bot.* 55:807-819.
- Schulz, S. R., and W. A. Jensen. 1969. *Capsella* embryogenesis: The suspensor and the basal cell. *Protoplasma* 67:139-163.
- Scott, J. E., and J. Dorling. 1965. Differential staining of acid glycosaminoglycans (mucopolysaccharides) by alcian blue in salt solutions. *Histochemie* 5:221-233.
- Simpson, B. B., and M. Conner-Ogorzaly. 1986. *Economic Botany: Plants in our world.*

McGraw-Hill, Inc. New York.

- Smith, B. W. 1956. *Arachis hypogaea*. Normal megasporogenesis and syngamy with occasional single fertilization. Amer. J. Bot. 43:81-89.
- Smith, F. H. 1942. Development of the gametophytes and fertilization in *Camassia*. Amer. J. Bot. 29:657-663.
- Smith, F. H. 1943. Megagametophyte development of *Clintonia*. Bot. Gaz. 105:263-267.
- Smith, M. M., and M. E. McCully. 1978. A critical evaluation of the specificity of aniline blue induced fluorescence. Protoplasma 95:229-254.
- Southworth, D. 1971. Incorporation of radioactive precursors into developing pollen walls. pages 115-120. In: *Pollen: development and physiology*. J. Heslop-Harrison, ed., Butterworth & Co., Ltd., London.
- Spurr, A. R. 1969. A low viscosity epoxy resin embedding medium for electron microscopy. J. Ultrastruct. Res. 26:31-43.
- Sutherland, J., and M. E. McCully. 1976. A note on the structural changes in the walls of pericycle cells initiating lateral root meristems in *Zea mays*. Can. J. Bot. 54:2083-2087.
- Thiery, J. P. 1967. Mise en evidence des polysaccharides sur coupes fines en microscopie electronique. J. Microscopie. 6:987-1018.
- Thomas, P. L., & P. K. Isaac. 1967. An electron microscope study of intravacuolar bodies in the uredia of wheat stem rust and in hyphae of other fungi. Can. J. Bot. 45:1473-1478.
- Tilton, V. R. 1980. Hypostase development in *Ornithogalum caudatum* (Liliaceae) and notes on other types of modifications in the chalazae of angiosperm ovules. Can. J. Bot. 58:2059-2066.
- Tilton, V. R. 1981a. Ovule development in *Ornithogalum caudatum* (Liliaceae) with a review of selected papers on Angiosperm reproduction. II. Megasporogenesis. New Phytol. 88:459-476.
- Tilton, V. R. 1981b. Ovule development in *Ornithogalum caudatum* (Liliaceae) with a review of selected papers on Angiosperm reproduction. IV. Egg apparatus structure and function. New Phytol. 88:505-531.

- Tilton, V. R., and H. L. Mogensen. 1979. Ultrastructural aspects of the ovule of *Agave parryi* before fertilization. *Phytomorph.* 29:338-350.
- Tilton, V. R., R. G. Palmer, and L. E. Wilcox. 1983. The female reproductive system in soybeans *Glycine max.* (L.) Merr. (*Leguminosae*). pages 35-37. In: *Fertilization and embryogenesis in ovulated plants*. O. Erdelska, ed. Proceedings of the VII. International Cytoembryological Symposium. June, 1982.
- Tilton, V. R., L. E. Wilcox, and R. G. Palmer. 1984. Postfertilization wandlabrinthe formation and function in the central cell of soybean, *Glycine max* (L.) Merr. (*Leguminosae*). *Bot. Gaz.* 145:334-339.
- Tiwari, S. C. 1983. The hypostase in *Torenia fournieri* Lind.: a histochemical study of the cell walls. *Ann. Bot.* 51:17-26.
- van der Pluijm, J. E. 1964. An electron microscopic investigation of the filiform apparatus in the embryo sac of *Torenia fournieri*. pages 8-16. In: *Pollen physiology and fertilization*. H. F. Linskens, ed., North-Holland Publishing Co., Amsterdam.
- van Went, J. L. 1970a. The ultrastructure of the synergids of *Petunia*. *Acta. Bot. Neerl.* 19:121-132.
- van Went, J. L. 1970b. The ultrastructure of the egg and central cell of *Petunia*. *Acta Bot. Neerl.* 19:313-322.
- van Went, J. L. 1970c. The ultrastructure of the fertilized embryo sac of *Petunia*. *Acta Bot. Neerl.* 19:468-480.
- van Went, J. L., and M. T. M. Willemse. 1984. Fertilization. pages 273-317. In: *Embryology of Angiosperms*. B. M. Johri, ed., Springer-Verlag, New York.
- Venable, J. H., and R. Coggeshall. 1965. A simplified lead citrate stain for use in electron microscopy. *J. Cell Biol.* 25:407.
- Vijayaraghavan, M. R., W. A. Jensen, and M. F. Ashton. 1972. Synergids of *Aquilegia formosa* - their histochemistry and ultrastructure. *Phytomorphology* 22:144-159.
- Wardlaw, C. W. 1955. *Embryogenesis in plants*. Methuen & Co. Ltd., London.
- Weatherwax, P. 1919. Gametogenesis and fecundation in *Zea mays* as the basis of xenia and



- heredity in the endosperm. Bull. Torrey Bot. Club 46:73-90. pl. 6-7.
- Weinstein, A. I. 1926. Cytological studies of *Phaseolus vulgaris*. Amer. J. Bot. 13:248-263.
- Willemse, M. T. M., and J. Bednara. 1979. Polarity during megasporogenesis in *Gasteria verrucosa*. Phytomorph. 29:156-165.
- Willemse, M. T. M., and R. N. Kapil. 1981. Antipodals of *Gasteria verrucosa* (Liliaceae) - an ultrastructural study. Acta Bot. Neerl. 30:25-32.
- Willemse, M. T. M., and J. L. van Went. 1984. The female gametophyte. pages 159-196. In: *Embryology of Angiosperms*. B. M. Johri, ed., Springer-Verlag, New York.
- Wilms, H. J. 1981. Ultrastructure of the developing embryo sac of spinach. Acta Bot. Neerl. 30:75-99.
- Wood, P. J. 1980. Specificity in the interaction of direct dyes with polysaccharides. Carbohydrate Res. 85:271-287.
- Woodcock, C. L. F., and P. R. Bell. 1968. Features of the ultrastructure of the female gametophyte of *Myosurus minimus*. J. Ultra. Res. 22:546-563.
- Woodland, P. S. 1964. The floral morphology and embryology of *Themeda australis* (R.Br.) Stapf. Aust. J. Bot. 12:157-172.
- Yamada, N., M. Nagano, S. Murakami, M. Ikeuchi, E. Oho, N. Baba, K. Kanaya, and M. Osumi. 1983. Preparation for observation of fine structure of biological specimens by high-resolution SEM. J. Electron Microsc. 32:321-330.
- Yeung, E. C. 1980. Embryogeny of *Phaseolus*: the role of the suspensor. Z. Pflanzenphysiol. Bd. 96:17-28.
- Yeung, E. C. 1984. Histological and histochemical staining procedures. Pages 689-697. In: I. K. Vasil, ed., *Cell culture and somatic cell genetics of plants*, Vol. 1. Academic Press, Inc. New York.
- Yeung, E. C., and M. E. Clutter. 1978. Embryogeny of *Phaseolus coccineus*: growth and microanatomy. Protoplasma 94:19-40.
- Yeung, E. C., and M. E. Clutter. 1979. Embryogeny of *Phaseolus coccineus*: the ultrastructure and development of the suspensor. Can. J. Bot. 57:120-136.

Yoo, Y. B., and M. J. Chrispeels. 1980. The origin of protein bodies in developing soybean cotyledons: a proposal. *Protoplasma* 103:201-204.